The Optical Measurement of Acoustic Velocity Fields.

a thesis by

John P. Sharpe.

for the degree of

Doctor of Philosophy.

Physics Department,
Edinburgh University.

1988

To Ma and Da

and

Caroline.

Declaration.

I declare that this thesis is of my own composition and that the work described in it is, except where indicated by reference or acknowledgement, entirely my own.

John P. Sharpe.

Acknowledgements.

I would like to thank my project supervisor, Dr. C. A. Greated, for encouragement, advice and help at all stages of this project. I would further like to thank Dr. D. M. Campbell for keeping me on the acoustical straight and narrow and intimating the calculations given in appendix B.

Thanks must also go to Callum Gray for help with image analysis and some interesting collaborative work in Particle Image Velocimetry (see chapter 6) and to Frank Morris, the Fluid Dynamics technician, for technical assistance on some of the experimental work.

Contents.

CHAPTER 5: EXPERIMENTS. MEASUREMENT OF PERIODIC AND NOISY SOUND FIELDS.

CHAPTER 6: ACOUSTIC STREAMING AND PARTICLE IMAGE VELOCIMETRY.

CHAPTER 7: DISCUSSION AND CONCLUSIONS.

Abstract.

The application of two different optical techniques to the measurement of acoustic velocity fields is described. Firstly, (and forming the major part of the work) the application of laser Doppler anemometry to the measurement of the vibrational velocities associated with acoustic fields is described. Secondly, the technique of particle image velocimetry is introduced to measure the nonlinear, non-zero mean motions which arise when higher intensity sound fields are present.

For the first case consideration is given to the special requirements involved in measuring acoustic vibrational velocities: theory is then developed relating the photon correlation function to the sound field velocity distribution for the cases of periodic and noisy sound fields. A technique which can be used to measure the phase of the velocity with respect to the pressure is also described. Experiments are then described which test the technique and successful measurements are made of complex acoustic impedance.

These latter measurements lead us to consider acoustic streaming and to the realisation that it could be measured using particle image velocimetry. This technique is then applied to Rayleigh streaming and the measurements are shown to agree well with theory.

Chapter 1: Introduction.

Acoustics, which is defined in Kinsler *et. al.* (1982) as the generation, transmission and reception of energy in the form of vibrational waves in matter, covers an extremely large number of the topics open to physical investigation. For, not only does it include the regime (up to ~ 16 kHz) which mediates much of human communication but also embraces the areas of ultrasound, non-linear acoustics, underwater acoustics, molecular absorption phenomena etc..

In this thesis we shall be confining ourselves to sound fields of the order of 1 kHz and "moderate" intensity in air. We shall be demonstrating the use of optical techniques which permit measurements to be made of acoustic vibrational velocities and of the motions generated when, at higher intensities, non-linear effects start to become noticeable. At first sight this range of measurement may seem rather restricted, especially when compared to the list of topics given in the previous paragraph. However, this area covers much of the acoustics which interests those studying the sound fields which affect humans. This includes, for example, the assessment of acoustic absorption in building materials and the location of noise sources in industrial machinery. Indeed, since human pitch perception is dominated by the range 500 to 2000 Hz, the techniques introduced here could also be very useful in the study of, say, musical wind instruments [Campbell & Greated 1987].

In chapter 2 we shall briefly revise the basics of acoustics defining, for example, acoustic intensity and impedance and developing acoustic relationships which will be of use in later experimental work. Current methods of acoustic velocity measurement will be briefly reviewed, providing some indication for the motivation behind the work undertaken in this thesis. In

chapter 3, the Laser Doppler Anemometry (L.D.A.) technique is introduced and, after a brief resume of the technique, detailed consideration is given to the optical and signal processing requirements for acoustic measurement. This is followed in chapter 4 by a derivation of the correlation function for the laser Doppler signal from periodic and noisy acoustic velocity fields. A gating technique, which will be used to measure the phase difference between the acoustic pressure and velocity will also be described.

Chapter 5 describes the experimental work which confirms the theory of chapter 4 and goes on to describe the experimental determination of complex acoustic impedance in an open tube. This last piece of work leads us on to consider acoustic streaming, a non-linear phenomenon, and to realize that the technique of Particle Image Velocimetry (P.I.V.) could provide a means for its measurement. Accordingly, chapter 6 outlines the P.I.V. technique and experiments are described on Rayleigh Streaming and shown to give good agreement with theory. Difficulties and limitations of the technique are also discussed.

Finally in chapter 7 the two techniques of L.D.A. and P.I.V. are discussed and conclusions are drawn about their possible regimes of application and accuracy. It is also suggested where further developmental and applications work could be done.

Appendix A discusses the production of acoustic streaming by the sound field from a capillary and offers a qualitative explanation for the effect while appendix B details some calculations which have relevance to the measurement of complex acoustic impedance when the pressure and velocity are not measured on the same plane. Appendix C contains a list and copies of the reports and publications generated in the course of this work.

Chapter 2: Introductory Acoustics and Acoustic Measurement.

2.1. INTRODUCTION.

In this chapter we shall define the various acoustic quantities which are used to parametrise and describe sound fields. Expressions relating velocity and pressure are developed so that quantitative comparisons may be made in later experimental work. A theoretical expression is given for the input impedance of an open tube so that, again, quantitative comparison may be made with later work. Boundary layer effects in tubes are also discussed.

Current methods for measuring acoustic intensity and impedance are reviewed and it is observed how difficult it is to make direct measurement of acoustic velocity. This review also indicates the motivation for the work undertaken in this project.

2.2. INTRODUCTORY ACOUSTICS.

2.2.1. Intensity and impedance - relationship between acoustic velocity and pressure.

In order to completely define a sound field both the pressure, p, and the acoustic velocity, v, at any point must be determined. Here p is the difference between the instantaneous and the equilibrium (or hydrostatic) pressures while v is the particle velocity or instanteous velocity of a small element or particle of the fluid. These quantities are required for the evaluation of the acoustic impedance and intensity but, although the pressure is quite easily measured - small, cheap and accurate microphones being readily available - the measurement of acoustic velocity is much more difficult.

The acoustic intensity, which quantifies the transport of energy by the sound field, is defined as

$$I = \langle p . \vec{v} \rangle = \frac{1}{T} \int_0^T p . \vec{v} \, dt \qquad 2.2.1.$$

where the angled brackets indicate time averages and the integral is taken over one cycle of the acoustic disturbance. The intensity is useful in applications such as determining the location of noise sources or sinks in industrial machinery [Bruel & Kjaer 1982b].

Specific acoustic impedance, z, is defined as the ratio of pressure to acoustic particle velocity

$$z = p/v \qquad 2.2.2.$$

When dealing with sound in pipes or horns, however, it is more convenient to use the acoustic impedance which is defined, for a fluid acting on a surface of area S, as the complex quotient of the pressure at the surface divided by the volume velocity at the surface [Kinsler *et. al.* 1982]

$$Z = p/u \qquad 2.2.3.$$

where

$$u = Sv$$

U is known as the volume velocity. 2.2.3. can also be written as

$$Z = |Z| e^{i\phi} \qquad 2.2.4.$$

where $|Z|$ is the impedance amplitude and ϕ the phase difference between the velocity and pressure. Acoustic impedance is used when quantifying the coupling of sound fields in different media or in volumes of different dimensions. It is in fact closely analogous to electrical impedance, with pressure and volume velocity corresponding to voltage and current respectively. This analogy is quite useful and can be extended to cover areas where the sound field wavelength is much larger than the dimensions confining it (equivalent to discrete circuit elements like capacitors and inductors) and where the wavelength is much smaller (equivalent to waveguides). This latter analogy can be used in chapter 5 when computing the theoretical impedance for an open tube.

For a plane progressive wave the particle velocity and pressure are simply related through

$$p = \rho_0 c v \qquad 2.2.5.$$

where $\rho_0 c$ is the characteristic impedance of the medium and ρ_0 and c are the density of the medium and speed of sound in the medium respectively. For air at standard temperature and pressure $\rho_0 c$ takes the value 415 Pa.s/m. Acoustic pressure though is not usually given in pascals but in terms of sound pressure levels or intensities related to some arbitrary reference level (usually 10^{-12} W/m^2, equivalent to 20.4 μPa), which corresponds roughly to the lower limit of hearing at 1000 Hz.

For intensity levels measured in decibels

$$IL\,(dB) \equiv \text{INTENSITY LEVEL}$$

$$= 10 \log \left(I / I_{ref} \right) \qquad 2.2.6.$$

Then, since intensity and effective (r.m.s.) pressure for a plane progressive wave are related through [Kinsler *et. al* 1982]

$$I = p^2 / \rho_o c$$

we get

$$\text{SOUND PRESSURE LEVEL (SPL)} = 20 \log \left(p / p_{ref} \right)$$

2.2.7.

Rearranging 2.2.7. and using P_{ref}=20 μPa then gives the pressure in pascals as

$$p\,(P_a) = 10^{\left(\frac{SPL - 94}{20} \right)} \qquad 2.2.8.$$

Returning to 2.2.7. and remembering we are still dealing with plane progressive waves we also see, by writing the r.m.s. pressure as

$$P_{rms} = z\, V_{rms} \qquad X$$

where v_{rms} is the r.m.s. velocity and z=415 Pa.s/m that

$$SPL = 20 \log \left(\frac{z\, V_{rms}}{20 \times 10^{-6}} \right)$$

$$\therefore\ V_{rms} = \frac{20\times10^{-6}}{415}\ 10^{SPL/20}$$

Since the velocity amplitude a_m is related to v_{rms} through $a_m=\sqrt{2}v_{rms}$ we then get

$$a_m = 0.0694 \times 10^{(0.05\,SPL\,-\,6)} \qquad 2.2.9.$$

Although 2.2.9. was derived assuming that the sound field was a plane progressive wave, it can be applied to more complex fields provided one knows the phase relationship between the velocity and pressure. For example, for the first normal mode of a tube closed at both ends, the pressure starts as a maximum at one end, falls to a minimum at the tube centre and rises again to a maximum at the other end. The velocity however starts as a minimum, rises to a maximum at the centre and falls again to a minimum at the other end. We thus see that if the velocity is deduced from a pressure measurement at any point then this velocity is equal to the true velocity displaced by half a tube length, equivalent to a 90° phase shift. Equation 2.2.9. and arguments such as the above will be used extensively later on when making comparisons between acoustic pressures and velocities.

2.2.2. Input impedance for an open tube.

Consider a tube of length L and radius a, open at one end and closed at the other with acoustic excitation provided at the closed end. Then, if the

wavelength of the sound field is much greater than the tube radius, the tube can be thought of as a transmission line with distributed loss [Pratt, Elliot & Bowsher 1977]. The input impedance is thus given by [King 1943]

$$Z_i = Z_0 \left[\frac{Z_L \cosh \Gamma L + Z_0 \sinh \Gamma L}{Z_0 \cosh \Gamma L + Z_L \sinh \Gamma L} \right] \qquad 2.2.10.$$

Here Z_0 is the characteristic impedance, Z_L is the terminating or load impedance and Γ is the (generally complex) propagation constant; $\Gamma=k+i\alpha$ where α is the attenuation coefficient, k is the wavenumber and $i=\sqrt{-1}$. Then, following Pratt, Elliot and Bowsher it is possible to write Z_i as

$$Z_i = Z_0 \frac{\alpha L + j \tan kL'}{1 + j \alpha L \tan kL'} \qquad 2.2.11.$$

where $Z_0=\rho_0 c/\pi a^2$ and $L'=L+0.61a$. 0.61a is the end correction for an open tube [Kinsler *et. al.* 1982] i.e. the tube has an effective acoustic length a little greater than its geometrical length. Equation 2.2.11. can be used to compute theoretical expressions for the input impedance and phase (eqn. 2.2.4.) using the relationships $|Z_i|=\sqrt{Z_i Z_i^*}$ and $\phi=\arctan(\mathrm{Im}(Z_i)/\mathrm{Re}(Z_i))$ where * denotes complex conjugate and Re and Im the real and imaginary parts respectively. Equation 2.2.11. will be derived in appendix B by another method when we come to discuss the measurement of acoustic impedance in greater detail.

2.2.3. The acoustic boundary layer in a circular tube.

It is well known that flow past a solid boundary is slowed down due to viscous interaction between the fluid and the boundary [Batchelor 1970]. This naturally also applies to acoustic flows where the resulting boundary layer would, in the case of ducts or tubes, reduce the effective area of flow. This would then have to be taken into consideration when calculating, say, acoustic

impedance from point measurement of acoustic particle velocity (c.f. eqn. 2.2.3.).

For a cylindrical tube the ratio of mean particle velocity ($\bar{v}$) to the velocity at the tube centre (v(0)) is given by [Elliot, Bowsher & Watkinson 1982]

$$\bar{v}/v(0) = \left\{ 1 + \left(2/Ka \right) \left[J_1(Ka)/J_0(Ka) \right] \right\} \qquad 2.2.12.$$

where a is the tube radius and J_0 and J_1 are zero and first order Bessel functions respectively. K is equal to $(-i(\rho\omega/\eta))^{1/2}$ where ρ is the fluid density, ω the angular frequency and η the coefficient of viscosity. The effective boundary layer is usually quite small with effective thickness given by

$$t_e \simeq \left(\frac{\eta}{\rho\omega} \right)^{1/2} \qquad 2.2.13.$$

which, for air at standard temperature and pressure takes the value of 0.15mm at 100Hz and rapidly decreases at greater frequencies. Whether in any specific experiment the boundary layer need be considered depends on the size of the tube, the frequencies under investigation and the accuracy desired.

An area where the acoustic boundary layer becomes very important is in the regime of higher intensity sound fields. In this case the boundary layer causes dissipation of the acoustic wave and forces non-zero mean motions [Lighthill 1978a]. This effect is known as acoustic streaming and detailed consideration will be given later to its measurement (chapter 6).

2.3. ACOUSTIC IMPEDANCE AND INTENSITY MEASUREMENT.

Acoustic impedance and intensity measurements may be approached either directly by trying to measure the acoustic velocity or indirectly, by controlling the sound field so that a simple known relationship exists between the

pressure and velocity. Pressure measurements alone then become sufficient. Examples of indirect methods are constant volume velocity techniques and pressure gradient microphones while direct methods include Rayleigh Discs and Hot Wire Anemometers.

In the constant volume velocity technique (which was developed mainly for studying the input impedance of musical instruments) the acoustic excitation is fed into the system (instrument mouthpiece) via a high impedance series resistance (capillary tube) [Backus 1974, Salava 1980, Campbell 1987] (see figure 5.2.2.). The capillary tube maintains a constant volume velocity input over a wide frequency range and this input may be deduced either theoretically [Backus 1974, Keefe & Benade 1981, Kergomard & Caussé 1986] or by calibration using, say, a Helmholtz resonator [Campbell 1987]. The pressure, measured in the input plane, then suffices to deduce the impedance.

An equally ingenious approach to the measurement of acoustic intensity (which became feasible with the advent of cheap high speed digital signal processors) involves the use of two closely spaced microphones from which the pressure gradient is estimated and transformed to a velocity using the equations of motion for the sound field [Fahy 1977, Chung 1978, Bruel & Kjaer 1982a,b]. This technique can also be extended to direct measurement of impedance and absorption [Minten, Cops & Lauriks 1988].

Both these techniques however suffer from a variety of drawbacks ranging from calibration difficulties, need for empirical frequency corrections, directivity effects and assumptions needing to be made about the field under investigation. Probe devices such as the pressure gradient microphone can also upset the field under investigation [Bruel & Kjaer 1985].

Turning now to direct velocity measurement techniques, we see that the first of these was the Rayleigh Disc [Rayleigh 1896]. This takes the form of a thin

disc, typically made of mica or brass and of ~1cm diameter, suspended in the sound field. The acoustic velocity field acts on this disc to produce a measurable torque of magnitude proportional to the mean square velocity. Unfortunately such a device is rather difficult to use and a host of empirical correction factors and assumptions must be applied in order to take account of, for example, diffraction effects and flexural vibrations of the disc [Jensen & Saermark 1958, Rasmussen 1964]. Also, since the torque is proportional to the disc diameter, the disc cannot be made arbitrarily small and can hence produce significant distortion of the field under investigation.

The Hot Wire Anemometer (H.W.A.), a common fluid velocity measuring device which relies on the cooling effect of the flow on a thin electrically heated wire, has also been successfully applied to the measurement of acoustic velocities. Good results were obtained in measurements of brass instrument input impedances [Pratt, Elliot & Bowsher 1977, Elliot, Bowsher & Watkinson 1982]. In their experiments however there always seemed to be a steady flow in the instrument (due perhaps to acoustic streaming because high intensities were used to get reliable results from the H.W.A.) but it is not clear if such a device would work in a field without non-zero mean motions. For in this case the air would simply oscillate about the probe and would not be expected to have the same cooling effect as a non-zero mean flow. The H.W.A. also suffers from the drawbacks of calibration difficulties and, like other material probes, disturbance of the sound field.

Chapter 3: Considerations when using Laser Doppler Anemometry for Acoustic Velocity Measurement.

3.1. INTRODUCTION.

As was seen in chapter 2, conventional techniques for measuring acoustic velocity suffer from a variety of drawbacks. Consequently we now look to direct optical measurement techniques which will perhaps surmount some of these difficulties. The prime candidate for such a technique is Laser Doppler Anemometry (L.D.A.) which is absolute (requires no calibration) and is non - intrusive.

In this chapter the various configurations for L.D.A. will be examined to decide which of the various combinations of optics and signal processing most suit the requirements of acoustical measurement. That is, which system gives the best combination of measurement accuracy, speed, ease of operation etc. Such considerations will then allow us to go on and deduce how the velocity distribution in the sound field may be derived from the anemometer output signal.

3.2. PRINCIPLE OF THE L.D.A. TECHNIQUE.

The principle of L.D.A. is simple enough: laser light projected into the flow under investigation is scattered from small particles contained in and faithfully following the fluid. The Doppler shift imposed on the light is then analysed to reveal the flow velocity. Since the L.D.A. technique has been around since 1964 [Yeh & Cummins 1964] there has understandably been much progress in the fields of optical design and signal processing and the literature is vast. This literature now contains several books including Durst, Melling and Whitelaw (1976), Watrasiewicz and Rudd (1976), Durrani and Greated (1977) and Drain

(1980). All of these form excellent introductions to this work and Durrani and Greated will be referred to frequently.

L.D.A. systems fall into two general classes - reference beam heterodyne mode and crossed beam mode (Fig. 3.2.1.). In the heterodyne system the light scattered from the moving particles is mixed (heterodyned) with a reference beam and the resulting beat frequency analysed to deduce the flow velocity. In the crossed beam or differential Doppler mode the beating takes place between two beams scattered in different directions so that the beat frequency is equal to the difference between the Doppler shifts for the two angles of scattering. This system, for the purposes of visualization and calculation, can be imagined as an interference pattern of bright and dark sinusoidal fringes through which the particles pass scattering light (Fig. 3.2.1.(b)).

For the crossed beam system it can easily be shown that the separation of the fringes is given by

$$d = \frac{\lambda}{2 \sin\theta} \qquad 3.2.1.$$

where λ is the laser light wavelength and θ the half angle between the beams. If a particle in the flow then passes through the fringe pattern (perpendicular to the fringes) with velocity U, the angular frequency of the scattered light is

$$\omega = \frac{4\pi U \sin\theta}{\lambda} = DU \qquad 3.2.2.$$

where D is known as the velocity to frequency conversion factor. Thus the velocity can be deduced knowing only the wavelength of the light and intersection angle of the beams.

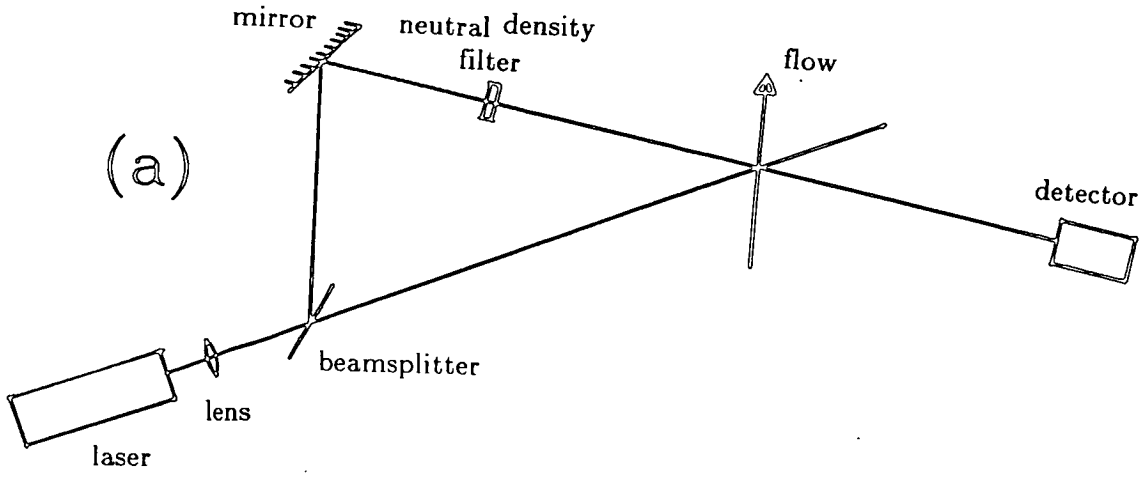

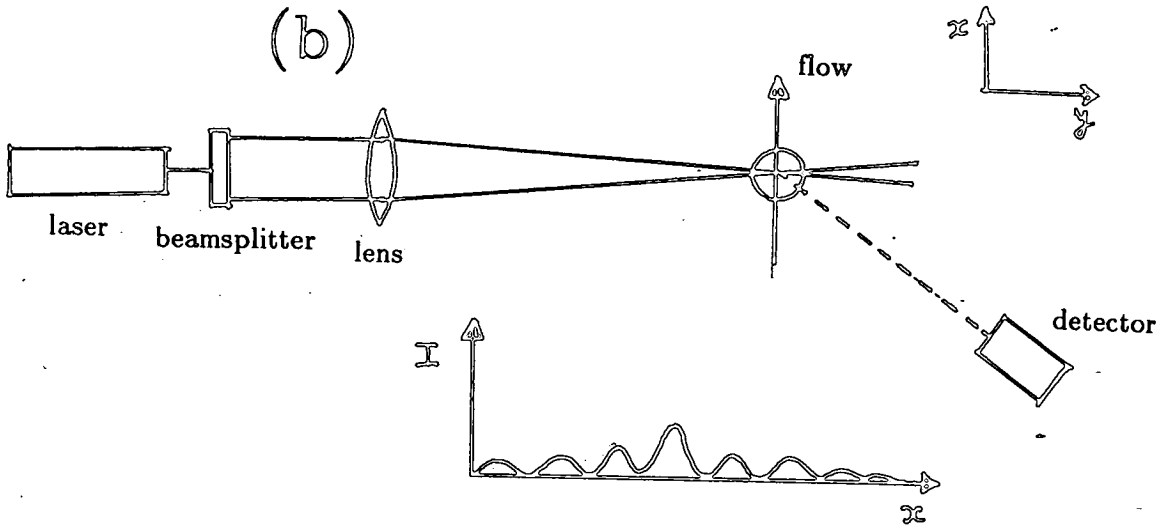

Figure 3.2.1. L.D.A. configurations. (a) Heterodyne mode. (b) Crossed beam mode showing variation in light intensity across the fringe pattern.

Before going on to give these L.D.A. systems more careful consideration we must first consider how faithfully typical seeding particles will track the motions of the acoustic field.

3.3. TRACKING OF PARTICLES SUSPENDED IN AN ACOUSTIC FIELD.

In air, the most commonly used artificial seeding particles are tobacco smoke or atomised vegetable or silicone oil. Tobacco smoke particles have diameters of roughly less than 1μm, depending on the smoke's age [Keith & Derrick 1960]. Atomised oil droplets can be obtained down to about 1μm using, for example, the Disa type 55L17 seeding generator. We note first that, taking the maximum field intensity we are likely to encounter as equivalent to a plane wave with sound pressure level of say 150 dB (re 20 μPa) then the maximum particle velocity will be ~2 m/s. Then, taking the average particle diameter as 1μm, we see that the characteristic Reynolds number for this flow is

$$R_e = \frac{U \cdot d \cdot \rho}{\mu_0} \simeq 0.07$$

where U is the velocity, d the particle diameter, μ_0 the air viscosity and ρ the density. Since this Reynolds number is less than unity, Stokes resistance law can be applied to the flow [Batchelor 1970] and, following Hinze (1959) the equation of motion for a seeding particle may be written

$$\frac{dV_p}{dt} + cV_p = cV_f \qquad 3.3.1.$$

where v_p and v_f are the particle and fluid velocities and

$$c = \frac{36\mu_0}{(2\rho_p + \rho_f)d^2} \qquad 3.3.2.$$

where ρ_p and ρ_f are the particle and fluid densities. In deriving 3.3.1. it has

been assumed that $\rho_p >> \rho_f$. Since $\rho_p/\rho_f \sim 1000$ for smoke or oil in air, this assumption is well justified.

Then, taking the fluid velocity magnitude as 1 and writing the fluid and particle velocities as

$$V_f = e^{j\omega_m t}$$

$$V_p = a_m e^{j\omega_m t}$$

where a_m is the (complex) particle amplitude and ω_m the frequency of the sound field, and substituting these into 3.3.1. yields, for the particle velocity amplitude

$$|a_m| = \frac{c}{\sqrt{c^2 + \omega^2}} \qquad 3.3.3.$$

If we wish the particles to follow the velocity of the fluid to within say 1% then 3.3.3. can be rearranged to yield

$$\omega_m^2 \leq \frac{c^2 - (0.99\,c)^2}{(0.99)^2} \qquad 3.3.4.$$

This gives the upper frequency limit for 1 µm particles of density 1000 kg/m^3 in air as approximately 8 kHz, which is well within the range of frequencies dealt with here. Even at 2 µm the particles will still follow the field to 5% up to 4 kHz. These calculations agree with the predictions of Taylor (1981) following the work of Brandt *et. al.* (1937).

Particles sizes below 1 µm can in fact be reasonably easily generated. For example, tobbacco smoke particles are on average < 0.4 µm if the smoke is

not less than about 4 minutes old [Keith and Derrick 1960]. Particles of this size would be required if oscillations much over 10 kHz were to be investigated. It must be born in mind of course that these estimates refer to sinusoidal oscillations: if the sound field were generated by say a square wave then the inertia of the tracking particles could cause filtering of the high frequency components. We will meet this observation again in connection with the measurement of noise fields.

It is also possible, when using the very sensitive photon counting correlation technique, to dispense entirely with artificial seeding and rely simply on naturally occuring "dust" particles in the air. This can be an advantage when carrying out measurements in systems where it is inconvenient or impossible to introduce artificial seeding particles and will be kept in mind when deciding on the optical system.

Finally, in this section, we will briefly touch on the contribution that Brownian motion might make to the output signal. As will be seen in the next chapter, the signal spectrum for an oscillating flow field will be expected to take the form of a series of narrow peaks separated by the frequency of the oscillation (typically 1 kHz for our sound fields). Brownian motion would contribute a broadening to the spectrum and, clearly, if this were too great, then the peaks would be unresolvable. The Brownian motion spectral broadening can be shown to have a Lorentzian shaped spectrum [Edwards *et. al.* 1971] with width at half intensity equal to $2K^2D_c$ where K is the magnitude of the scattering vector and D_c the diffusion coefficient of the particles. (K is equivalent to the frequency to velocity conversion factor defined in equation 3.2.2.). D_c can be calculated from

$$D_c = \frac{k_b T}{3\pi \mu_0 d} \qquad 3.3.5.$$

where k_b is Boltzmans constant and T the absolute temperature which gives, for 1 μm particles in air at 25°C, the spectral broadening to be ~50 Hz. Thus the technique should be able to handle sound fields well below 100 Hz.

3.4. OPTICAL CONSIDERATIONS.

As was seen in section 3.2. there are two basic types of laser Doppler setup - the heterodyne and crossed beam modes. We, in fact, will be using the crossed beam system - for the following reasons.

Firstly, this configuration is more suited to the lower particle concentrations generally found in air flows [See She & Wall (1975) for an excellent yet rarely cited treatment of signal to noise ratios in various L.D.A. systems]. In fact, in our experiments, we could usually have seeded as heavily as we liked, in which case the reference beam system would have been more effective. It was decided however to leave the system as flexible as possible.

Secondly, the cross beam system can use large collection optics unlike the reference beam system [She & Wall 1975] again increasing the sensitivity when only small seeding densities are available.

Finally, the optics of the crossed beam system are much easier to align and the Doppler signal is independent of the collection angle. This latter point is quite important because our experiments were usually made on narrow tubes (~1 cm radius) so it was useful to be able to to move the detector to avoid flare from the tube walls.

A factor that is usually quite critical when discussing L.D.A. systems is the

size of the measuring volume; that is, the spatial extent of the observed fringe pattern. It is important to know this for the estimation of transit time broadening when attempting to measure turbulence [Durrani & Greated 1977]. The size of the measuring volume also determines (in conjunction with the receiving optics) the "scale" over which the velocity field is measured. Neither of these considerations is critical to us however because, firstly, turbulence does not generally occur in the acoustic regimes we will be looking at and, secondly, in our experiments the velocity does not vary significantly over the measuring volume. This latter point would not hold if we were to make measurements near the boundary layer for then the velocity would vary (in the y direction of figure 3.2.1.(b)) significantly over the measuring volume. Careful consideration would then have to be given to the optical arrangement [Hanson 1973, Mullin & Greated 1978].

A very important consideration is the fringe spacing since it is this that determines the frequency output for a given velocity. One would expect, purely intuitively, that if there were only one or two particles in the fringe pattern, then the displacements of the particles should be of at least the order of the fringe spacing. Otherwise the particles would not properly "sample" the sinusoidal fringe variation. In the case of more particles we would expect their random distribution to more properly reflect all areas of the fringe pattern.

To get a feel for the quantities involved assume that the laser beams are focussed from a separation of 2 cm using a lens of focal length 20 cm. The fringe separation then becomes (eqn. 3.2.1.) 6.33 μm. If the particles are to have displacements say a half of this distance then, for a 1 kHz plane wave, we would expect a lower measurement limit of ~105 dB. We will see later (chapter 5) that this estimate is too high, but the above argument does give a useful rule of thumb estimate for the lower limit of the technique.

3.5. SIGNAL PROCESSING CONSIDERATIONS.

The signal from a laser Doppler anemometer can (like all temporal signals) be analysed in either the frequency (spectrum) or time (correlation function) domains. We have chosen to use the photon counting correlator which detects individual photons scattered from the fringe pattern and computes, digitally and directly, the correlation function. This type of analysis technique is more suited to low light levels and can deal with smaller SNRs than frequency techniques [She & Wall 1975, Durrani & Greated 1977]. We may note here that the photon count correlation function is proportional to the intensity correlation function [Durrani & Greated 1977].

As will become apparent later (chapters 4 and 5), the correlation method yields the sound field velocity amplitude in an easily invertible form and seems to be more robust than frequency techniques. As will also be seen, the output from the L.D.A. system when oscillating flows are observed, takes the form, in the frequency domain, of a series of narrow peaks whose relative heights are measured to deduce the velocity amplitude [Taylor 1976,1981]. Because of the stochastic nature of the scattering process it is easy to see that the measurement of these power spectrum peaks would present some difficulty. For example, if a swept frequency measuring device were used then there could be no particles in the fringe pattern when any particular frequency range was being observed.

The photon correlation technique does however suffer from the disadvantage that it is impossible to pre-filter the Doppler signal prior to processing thus eliminating low frequency terms. This makes the deduction of the correlation function a little more difficult.

Chapter 4: Theory. Derivation of correlation functions for time averaged and gated sound fields.

4.1. INTRODUCTION.

Having decided to use the crossed beam system with the photon correlation method of signal analysis, it now remains to deduce the form of the output signal and correlation function for the case of a sinusoidally oscillating velocity field.

This can be approached in several different ways. Firstly, one may apply directly the well known equations for frequency modulation as detailed in several texts e.g. [Betts 1970]. This was essentially the method adopted by Taylor (1976,1981) and Davis & Hews-Taylor (1986) who carried out the signal analysis in the frequency domain. This method however takes no account of the stochastic nature of the problem (e.g. random number of scattering particles, random scattering cross sections, arrival times etc.).

Another approach, adopted by Sharpe & Greated (1987a), involved the integration of the velocity probability density over the velocity dependent autocorrelation function for the fringe geometry under investigation. This method, a well known approach, following Durrani & Greated (1977) is however really only applicable for quasi - steady flows. That is, it is assumed that the velocity of each particle does not vary "too much" as the particle crosses the fringe pattern. How much is too much is considered at some length in the literature but the quasi - steady condition can often be achieved in practice by frequency shifting so that a large apparent mean motion is superimposed on the flow velocity. This technique was used in the work on oscillating flows by Durrani & Greated (1977) and Greated (1986) but it unfortunately makes the

deduction of the acoustic velocity very inaccurate because the contribution to the correlation function due to the sound field oscillations can become masked by the contribution due to the frequency shift (see section 4.5.).

It is also notable, for instance, in our earlier work [Sharpe & Greated 1987a] that the expression for the autocorrelation function did not show any dependence on the modulating frequency. Later studies however showed such a dependence [Sharpe & Greated 1987b]. This is perhaps intuitively consistent with the implicit assumption that, for any particle moving with velocity U, it travels a distance x=Ut rather than $x=\int_0^t U(s)ds$ in a time t.

The only really rigorous way to attack the problem is to write down the spatial autocorrelation function and deduce its time dependence. This would then be valid for any flow and provide a basis on which further development of the theory could be made. This approach should then yield up our earlier results [Sharpe & Greated 1987a] and the result for pure frequency modulation [Middleton 1960] as limiting cases. We will first look at the process in an idealised form and indicate areas of difficulty.

For a sinusoidal signal of frequency f_m modulating a carrier of frequency f_c, the resulting spectrum takes the form of a series of peaks with relative heights given by a series of Bessel functions and separated by the modulating frequency [Betts 1970] (Fig. 4.1.1.(a)). The number and relative sizes of the peaks depends on the strength of the modulation but, roughly, for large modulations (large particle velocity amplitudes) there are a large number of small peaks spread across the spectrum while for lower modulation strengths there are fewer but larger peaks. For $f_c >> f_m$ this is equivalent to the case of oscillating particles in a large mean flow (or, alternatively, with frequency shifting applied). For the case of zero carrier frequency the spectrum takes the form of figure 4.1.1.(b) where the components of the spectrum in the

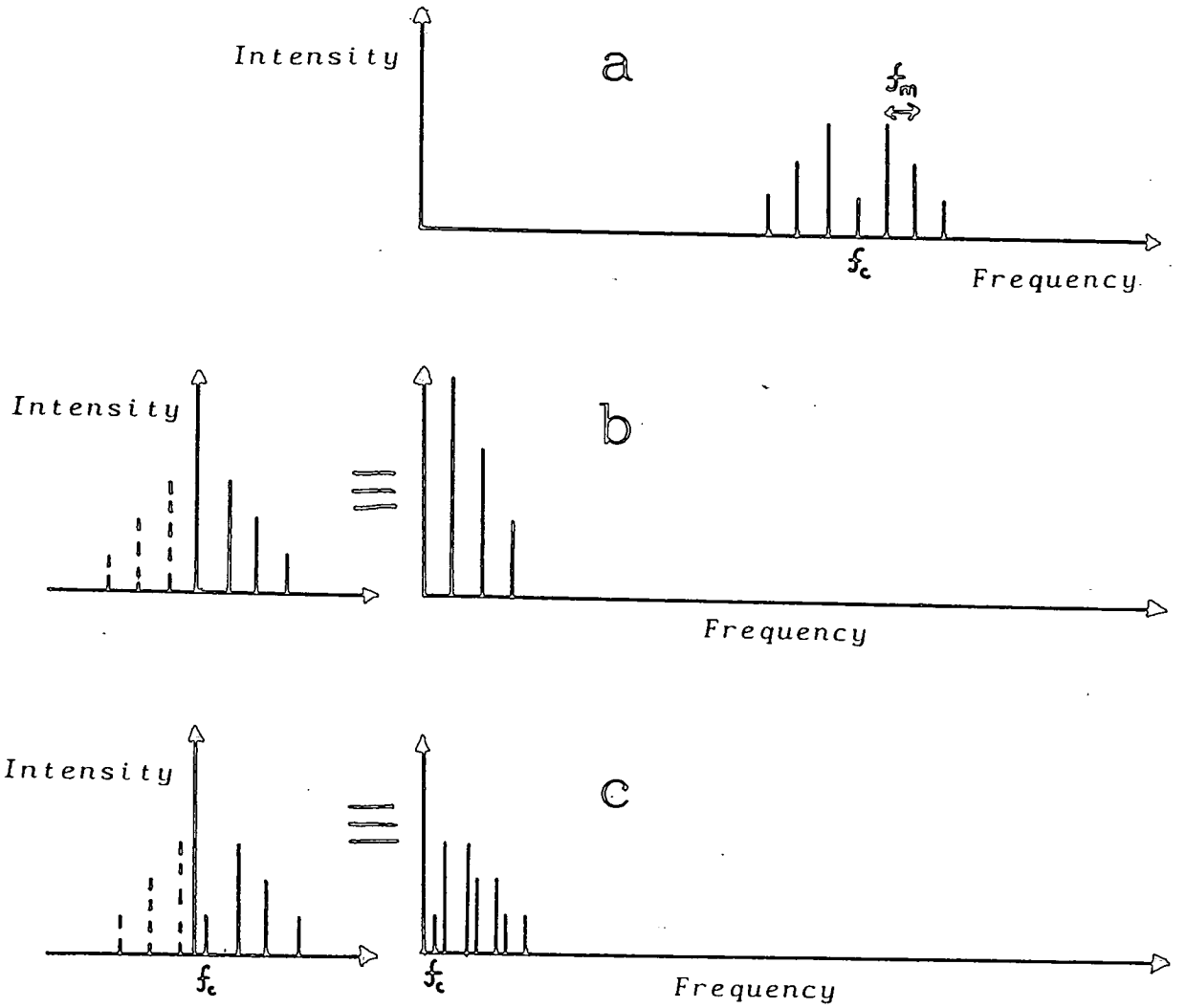

Figure 4.1.1. Form of output spectrum for sine wave frequency modulation of a sine wave. f_m is the modulating frequency and f_c the carrier frequency. (a) $f_c >> f_m$. (b) $f_c = 0$. (c) $f_c \sim f_m$.

negative frequency domain are folded back into the positive region. For the case however of the carrier frequency being roughly the same order as the modulating frequency the spectrum becomes rather more complicated (Fig. 4.1.1.(c)). The exact form of the spectrum would then depend critically on the value of the carrier frequency. We will not discuss this case in detail since it would be very difficult to obtain a general expression for the spectrum or correlation function.

We will now go on and deduce the form of the correlation function for a sinusoidal oscillation with no mean flow using the crossed beam Doppler setup. The case of a mean flow superimposed on the oscillation is simply an extension of this. We will follow the notation of Durrani & Greated (1977).

4.2. TIME AVERAGED CORRELATION FUNCTION FOR SINUSOIDAL OSCILLATIONS.

Let us write the voltage output associated with any pth particle in the observation volume as

$$x_p(t) = \kappa K_p W\left(\beta \xi_p(t)\right)\left[1 + \cos D \xi_p(t)\right] \qquad 4.2.1.$$

so that the total output is

$$x(t) = \kappa \sum_p K_p W\left(\beta \xi_p(t)\right)\left[1 + \cos D \xi_p(t)\right] \qquad 4.2.2.$$

where κ is a constant associated with the optical power and detector sensitivity, K_p characterises the scattering cross section of the particle, ξ_p is the particle position and D is the frequency to velocity conversion factor (see chapter 3). $W(\beta\xi_p(t))$ is the spatial weighting function which represents the envelope on the fringes due to the Gaussian cross section of the laser beams.

$$W(\beta \xi_p(t)) = \exp\left[-\beta^2 \xi_p^2(t)\right] \qquad 4.2.3.$$

with

$$\beta = \frac{\cos\theta}{r_0}$$

where θ is the laser beam intersection angle and r_0 the radius at the 1/e intensity points of the beam waist.

Note that in equation 4.2.1. low frequency terms have been retained (the constant term added to the cosinusoidal intensity variation). In standard analyses these are presumed to be filtered off but since this cannot be done in photon counting we will include them to see what their final effect will be. To determine the correlation function for x(t) we write ξ_p as the initial particle position (at time t=0) and ζ_p for its position a time τ later.

$$\zeta_p = \xi_p + \int_0^\tau V_p(z) = \xi_p + h_p(t) \qquad 4.2.4.$$

where $V_p(z)$ is the instantaneous velocity of the pth particle which in this case is

$$V_p(z) = a_m \sin(\omega_m z + \phi) \qquad 4.2.5.$$

We are ultimately interested in recovering the velocity amplitude, a_m.

Then, following the derivation of Durrani & Greated (1977) we find that the autocorrelation function for the output voltage is

$$R(\tau) = E\left[x(t)\,x(t+\tau)\right]$$

$$= \left[K\,C_0\,g_0 \int_{-\infty}^{\infty} W(\beta y)\left[1+\cos Dy\right] dy\right]^2$$

$$+ \frac{K^2 C_1 g_0}{2} \int_{-\infty}^{\infty} p_\eta(y;\tau)\, R_W(\beta y)\left[1+\cos Dy\right] dy \qquad 4.2.6.$$

where E[ ] is the expectation operator, $C_0 = E[K_p]$, $C_1 = E[K^2_p]$, g_0 represents the average number of particles per unit length of the measuring volume and $R_W(\beta y)$ is the autocorrelation of the spatial weighting function (see eqn. 4.2.3. and Gradshyteyn & Ryzhik 1965).

$$R_W(\beta y) = \sqrt{\frac{\pi}{2\beta^2}}\; e^{-\beta^2 y^2/2} \qquad 4.2.7.$$

$p_\eta(y;\tau)$ is the probability density function of the variable $\eta(\tau)$ which we must determine in order to evaluate the autocorrelation function. We will do this below but first we note that the first term on the r.h.s. of eqn. 4.2.6. is the squared mean value of the Doppler signal. We will ignore this term from now on since it is time independent, contains no velocity information and only contributes a constant or pedestal value to the correlation function.

From equations 4.2.4. and 4.2.5. we have

$$h_p(\tau) = a_m \int_0^{\tau} \sin\left(\omega_m z + \phi\right) dz$$

$$= \frac{2a_m}{\omega_m}\left[\sin\left(\frac{\omega_m \tau}{2}\right) \sin\left(\frac{\omega_m \tau}{2} + \phi\right)\right] \qquad 4.2.8.$$

where ϕ is a random variable uniformly distributed over the interval $0 - 2\pi$

$$p(\phi) = \frac{1}{2\pi} \qquad 0 < \phi < 2\pi \qquad 4.2.9.$$

We can now use the relationship for a function of a random variable [Bendat & Piersol 1966]

$$P_\eta(y;\tau) = 2p(\phi) \Big/ \frac{\partial \eta(\phi)}{\partial \phi} \qquad 4.2.10.$$

where the factor 2 on the r.h.s. occurs because η is a double valued function of ϕ over the interval 0 – 2π. We then get

$$P_\eta(y;\tau) = \frac{1}{\pi\sqrt{a_m'^2 - y^2}} \qquad -y \leq a_m' \leq y \qquad 4.2.11.$$

$$= 0 \qquad \text{elsewhere}$$

where

$$a_m' = \frac{2a_m}{\omega_m} \sin\left(\frac{\omega_m \tau}{2}\right) \qquad 4.2.12.$$

Equation 4.2.6. then takes the form

$$R(\tau) = \frac{k^2 C_1 g_0}{2}\sqrt{\frac{\pi}{2\beta^2}} \int_{-a_m'}^{a_m'} \frac{dy}{\pi\sqrt{a_m'^2 - y^2}} \exp\left[\frac{-\beta^2 y^2}{2}\right]\left[1 + \cos Dy\right] \qquad 4.2.13.$$

We proceed to evaluate 4.2.13. by substituting $y = a_m' \sin\alpha$ so that the integral becomes

$$\int_{-\pi/2}^{\pi/2} \frac{d\alpha}{\pi} \exp\left[\frac{-\beta^2 a_m'^2}{2} \sin^2\alpha\right]\left[1 + \cos D a_m' \sin\alpha\right] \qquad 4.2.14.$$

which we then split into two parts and make the substitution

$$\rho = \frac{\beta^2 a_m'^2}{2}$$

such that

$$R(\tau) = \frac{K^2 C_1 g_0}{2}\sqrt{\frac{\pi}{2\beta^2}}\left[F_1 + F_2\right]$$

where

$$F_1 = \int_{-\pi/2}^{\pi/2} \frac{1}{\pi} \exp\left[-\rho \sin^2\alpha\right] d\alpha$$

$$F_2 = \int_{-\pi/2}^{\pi/2} \frac{1}{\pi} \exp\left[-\rho^2 \sin^2\alpha\right]\left[\cos D a_m' \sin\alpha\right] d\alpha$$

First we evaluate F_1 by using the well known double angle formula to get

$$F_1 = \int_{-\pi/2}^{\pi/2} \frac{1}{\pi} \exp\left[\frac{-\rho}{2}\left(1 - \cos 2\alpha\right)\right] d\alpha$$

$$= \frac{1}{\pi} \exp\left[\frac{-\rho}{2}\right] \int_{-\pi/2}^{\pi/2} \exp\left[\rho/2 \cos 2\alpha\right] d\alpha$$

and letting $2\alpha = \phi$ gives

$$F_1 = \frac{1}{2\pi} \exp\left[\frac{-\rho}{2}\right] \int_{-\pi}^{\pi} \exp\left[\frac{\rho}{2} \cos\phi\right] d\phi$$

$$= \exp\left[-\rho/2\right] I_0(\rho/2) \qquad 4.2.15.$$

[McLachlan 1934] where $I_0(\ )$ is a zero order modified Bessel function of the first kind.

Turning then to F_2 and making the same substitution for y we get

$$F_2 = \frac{1}{\pi} \int_{-\pi/2}^{\pi/2} \exp\left[\frac{-\rho}{2}(1 - \cos 2\alpha)\right]$$

$$\times \left[J_0(Da'_m) + 2\sum_{n=1}^{\infty} J_{2n}(Da'_m)\cos(2n\alpha)\right] d\alpha$$

where this time we utilize the Bessel function expansion for cos(zsinθ). Making the substitution $2\alpha=\phi$ again and expanding then leads to

$$F_2 = \frac{1}{2\pi} \int_{-\pi}^{\pi} \exp\left[\frac{-\rho}{2}\right] \exp\left[\rho/2 \cos\phi\right]$$

$$\times \left[J_0(Da'_m) + 2\sum_{n=1}^{\infty} J_{2n}(Da'_m)\cos(n\phi)\right] d\phi$$

$$= \exp\left[\frac{-\rho}{2}\right]\left[I_0(\rho/2) J_0(Da'_m) + 2\sum_{n=1}^{\infty} J_n\left(\frac{\rho}{2}\right) J_{2n}(Da'_m)\right]$$

4.2.16.

where $J_{2n}(\ )$ and $I_n(\ )$ are Bessel and modified Bessel functions of the first kind and orders 2n and n respectively. So we finally obtain for 4.2.13.

$$R(\tau) = \frac{\kappa^2 C_1 g_0}{2}\sqrt{\frac{\pi}{2\beta^2}}\exp\left[-\frac{a_m'^2\beta^2}{4}\right]$$

$$\times\left[I_0\left(\frac{\beta^2 a_m'^2}{4}\right)\left(1+J_0(Da_m')\right)+2\sum_{n=1}^{\infty}I_n\left(\frac{\beta^2 a_m'^2}{4}\right)J_{2n}(Da_m')\right]$$

4.2.17.

This is the full expression for the time dependent part of the autocorrelation function. It can be simplified by considering typical magnitudes for β and a_m. For example, for laser beams of unfocussed e^{-1} width 0.5 mm focussed down from 2 cm separation using a 20 cm focal length lens, β takes the value 25000. Putting this into equation 4.2.17. along with typical acoustic magnitudes and considering the behaviour of $e^{-x}I_n(x)$ [Tranter 1968] reveals that we may write the time dependent periodic part of 4.2.17. as

$$R(\tau) \propto J_0(Da_m') = J_0\left(\frac{2Da_m}{\omega_m}\sin\left(\frac{\omega_m\tau}{2}\right)\right) \qquad 4.2.18.$$

to a very good approximation.

We can further simplify 4.2.18. by noting that for typical correlator lag times (see chapter 5)

$$\sin\frac{\omega_m\tau}{2} \simeq \frac{\omega_m\tau}{2}$$

so we may write

$$R(\tau) \propto J_0(Da_m\tau) \qquad 4.2.19.$$

Equation 4.2.19. was the expression derived in Sharpe and Greated (1987a).

This time however we can be sure that the expression 4.2.19. is valid for oscillatory flows and we are now more aware of its limits of applicability.

The acoustic velocity amplitude can thus be deduced by counting the lag time up to maxima or minima of the correlation function and using the tabulated values for the zero order Bessel function. For example, using the first minimum gives the velocity amplitude as

$$a_m = \frac{3.832}{D\tau} \qquad 4.2.20.$$

Finally, we can now compare the result we have obtained with that for pure frequency modulation. Middleton (1960) implies that the autocorrelation function for a sine wave frequency modulation of a zero frequency carrier is

$$R(\tau) \propto J_0\left(2\mu \sin\left(\frac{\omega_m \tau}{2}\right)\right)$$

where μ is the modulation index, defined as the ratio of the peak frequency deviation to the modulating frequency.

$$\mu = \frac{\Delta f}{f_m}$$

If we make the identification that the peak frequency deviation is the maximum particle velocity divided by the fringe separation

$$\Delta f = \frac{a_m}{d} = \frac{2 a_m \sin\theta}{\lambda} = \frac{D a_m}{2\pi}$$

then we see that

$$R(\tau) \propto J_0\left(2\frac{\Delta f}{f_m}\sin\left(\frac{\omega_m\tau}{2}\right)\right)$$

$$= J_0\left(\frac{2Da_m}{\omega_m}\sin\left(\frac{\omega_m\tau}{2}\right)\right)$$

which *is* 4.2.18.

4.3. TIME AVERAGED CORRELATION FUNCTION FOR BAND LIMITED NOISE FIELDS.

Having dealt with periodic sound fields we now turn to random or noisy fields. Greated (1986) had shown that the L.D.A. system responded to wide band noise with the correlogram becoming progressively more damped as the sound intensity increased. No theory was developed however and the measurements were all purely qualitative. We will now show how the correlation function is related to the mean velocity amplitude for narrow band noise. This type of sound field was chosen because it is then possible to make some form of quantitative comparison with pressure measurements. Also, if we can predict the form of the correlation function on the basis of our earlier work, then this will be a good check that our earlier theory is indeed correct.

Assume that the noise field is band limited white noise with zero mean and a gaussian velocity probability density. Also assume that no part of the noise spectrum is of greater frequency than that which can be tracked by the seeding particles (see chapter 3). For a sufficiently narrow bandwidth the velocity can be represented as a quasi-periodic sine wave with slowly varying amplitude and random phase uniformly distributed over 0 - 2π [Betts 1970] (see Figure 4.3.1.). The velocity amplitude, a_m, then assumes a Rayleigh probability density (Figure 4.3.1.(b)). $p(a_m)$ is given by

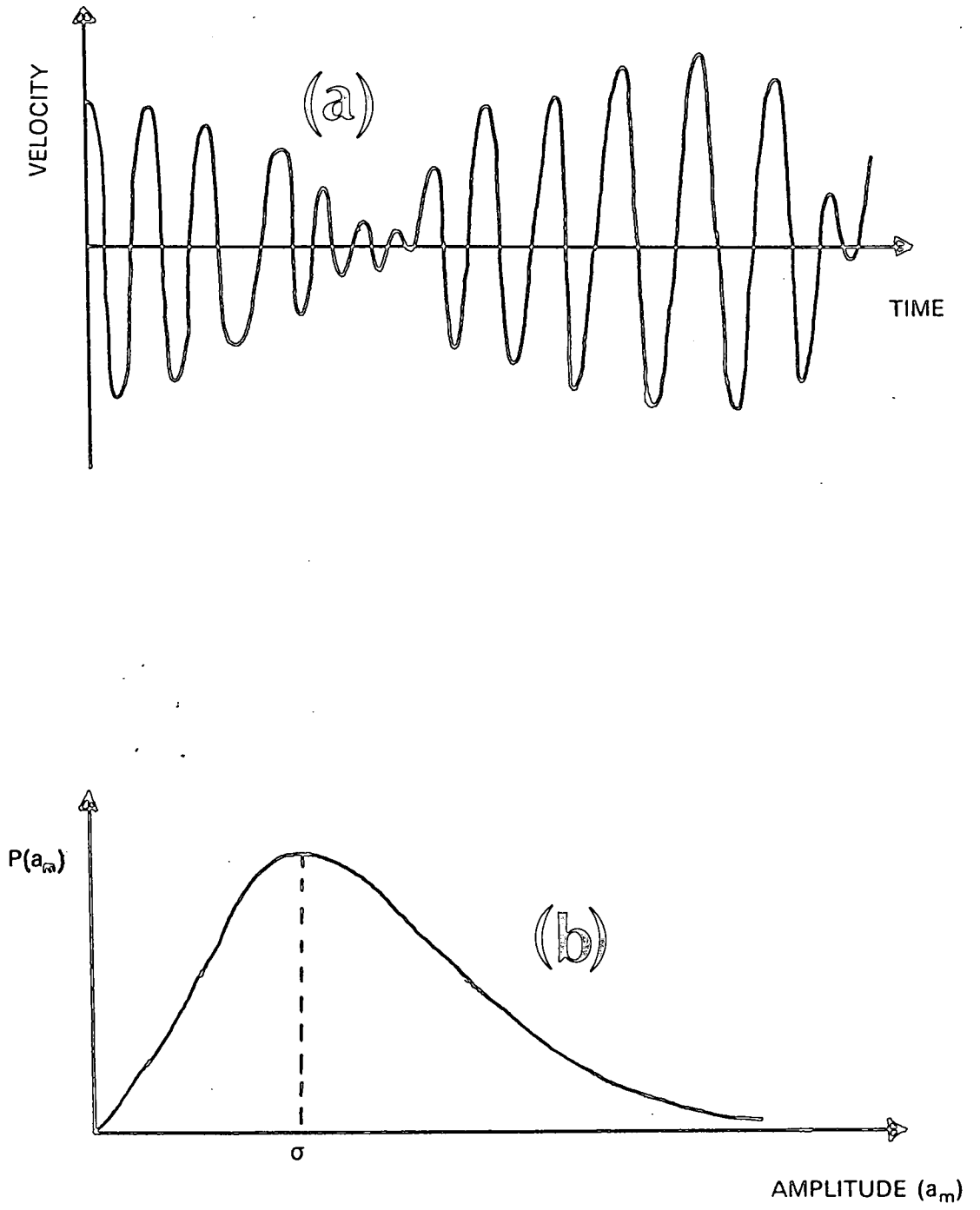

Figure 4.3.1. Narrow bandwidth noise. (a) Form of noise time history. (b) Probability density for amplitude of the signal illustrated in (a), σ = standard deviation.

$$p(a_m) = \frac{a_m}{\sigma^2} \exp\left[\frac{-a_m^2}{2\sigma^2}\right] \qquad 0 < a_m < \infty$$

where σ is the standard deviation of the velocity distribution. The mean velocity amplitude ($\bar{a}_m$) is related to the standard deviation through $\bar{a}_m = \sigma\sqrt{\pi/2}$. This can be plainly seen from

$$\bar{a}_m = E[a_m] = \int_{-\infty}^{\infty} a_m\, p(a_m)\, da_m$$

$$= \int_0^{\infty} \frac{a_m^2}{\sigma^2} \exp\left[\frac{-a_m^2}{2\sigma^2}\right] da_m$$

$$= \sigma\sqrt{\pi/2} \qquad 4.3.1.$$

[Gradshetyn & Ryzhik 1965]. To obtain the autocorrelation function for the noise field we then integrate the result for a single tone sound field (eqn. 4.2.19.) over the amplitude probability density.

$$R_{noise}(\tau) = B/\sigma^2 \int_0^{\infty} a_m \exp\left[\frac{-a_m^2}{2\sigma^2}\right] J_0(a_m D\tau)\, da_m \qquad 4.3.2.$$

where B is a constant. 4.3.2. evaluates to [Tranter 1968]

$$R_{noise}(\tau) = B \exp\left[-\frac{(D\tau\sigma)^2}{2}\right] \qquad 4.3.3.$$

Then, substituting for σ from 4.3.1. we can write

$$R_{noise}(\tau) = B \exp\left[-\frac{(D\tau\bar{a}_m)^2}{\pi}\right] \qquad 4.3.4.$$

This has a Gaussian form in τ with standard deviation of, say, σ_n. Hence we

can write

$$\bar{a}_m = \sqrt{\frac{\pi}{2(D\sigma_n)^2}} \qquad 4.3.5.$$

The mean velocity amplitude can thus be deduced by measuring the standard deviation of the correlogram.

4.4. THE GATING TECHNIQUE.

In chapter 2 we saw that to completely define a sound field the phase relationship between the velocity and pressure must be determined. We will do this using a gating technique which works in the following fashion.

The sinusoidal pressure signal from a microphone in the sound field is sent to a microcomputer which detects the positive going zero crossings of the signal and provides a pulse of a preset width and at a preset delay time from the zero crossing (Figure 4.4.1.) This pulse is then used to gate the photomultiplier so that the Doppler signal is only "seen" for the duration of the pulse. The velocity is thus being sampled at constant phase positions in its fluctuation. Clearly, if the pulse width is reasonably narrow, then the flow velocity will be approximately constant for the duration of the pulse and the autocorrelation function will be a cosine curve with period related to the velocity through equation 3.2.2. By incorporating a phase or frequency shifter into the optics the velocity direction as well as magnitude may be deduced from the correlogram period and, by selecting several different delay times so that at least one whole period is covered, it is then possible to reconstruct the velocity time history. If the microphone phase response is also known it is then possible to deduce the phase difference between the velocity and pressure.

The gating process can however distort the correlogram unless special

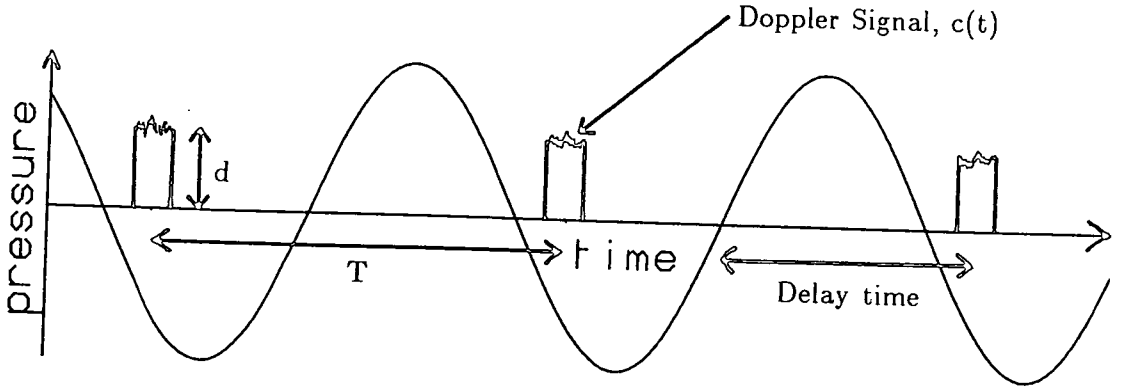

Figure 4.4.1. Pressure signal and gating pulses.

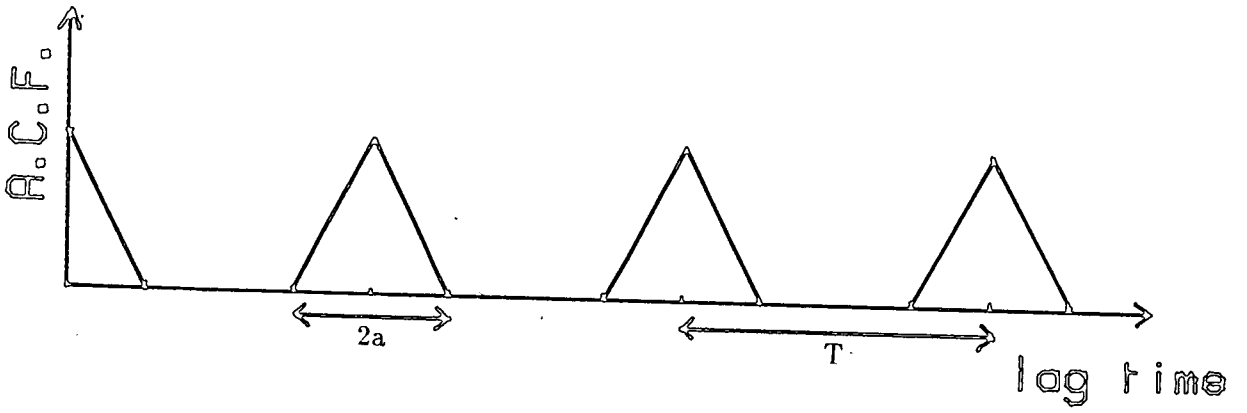

Figure 4.4.2. Autocorrelation function (A.C.F.) for a train of square pulses of width a and period T.

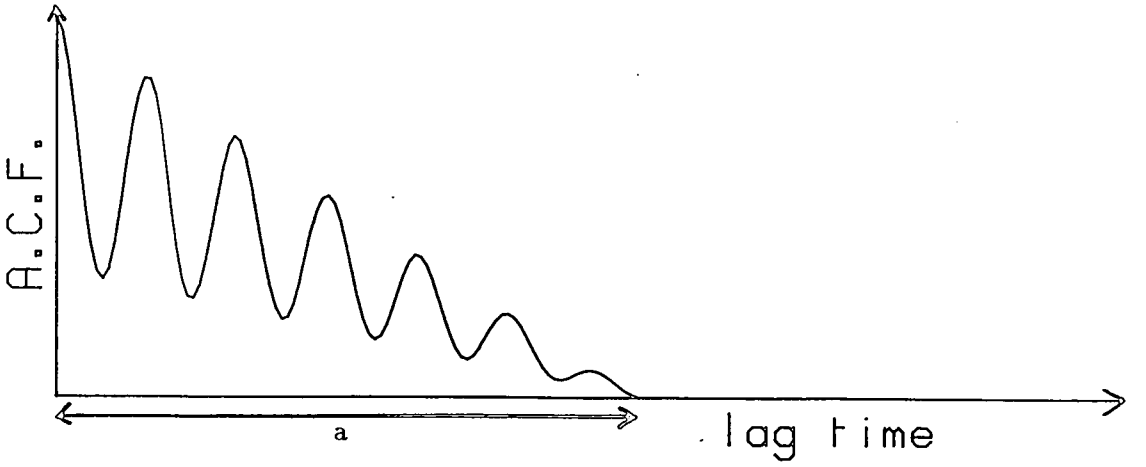

Figure 4.4.3. Autocorrelation of sampled velocity signal (c.f. eqn. 4.4.3.).

electronic circuitry is used; this is only available on certain types of correlator (see chapter 5). The form the correlation function takes when gated can be deduced as follows. The theoretical background can be found in, for example, Papoulis (1968).

For a continuous, wide sense stationary Doppler signal, c(t), riding on a pedestal d.c. current d and sampled by a square gating pulse p(t), the photodetector current is

$$I_p(t) = \left(c(t) + d \right) p(t) \qquad 4.4.1.$$

For our case (Fig. 4.4.1.) where there are many pulses, occuring with period T, p(t) is replaced by $\phi(t)$ where $\phi(t)$ is a single pulse convolved with a train of delta functions

$$\phi(t) = p(t) * \sum_{n=-\infty}^{\infty} \delta(t - nT) \qquad 4.4.2.$$

where

$$p(t) = 1 \qquad -a/2 < t < a/2$$

$$= 0 \qquad \text{elsewhere} \qquad 4.4.3.$$

δ is the well known delta function and * indicates convolution. The total photocurrent is then

$$I(t) = \left(c(t) + d \right) \phi(t) \qquad 4.4.4.$$

The autocorrelation of $I(t)$ then becomes

$$R_I(\tau) = E\left[I(t)\, I(t+\tau)\right]$$

$$= E\left[c(t)\, c(t+\tau)\, \phi(t)\, \phi(t+\tau)\right]$$

$$+ E\left[\rho^2 \phi(t)\, \phi(t+\tau)\right]$$

$$+ E\left[\rho\, \phi(t)\, \phi(t+\tau)\, c(t)\right]$$

$$+ E\left[\rho\, \phi(t)\, \phi(t+\tau)\, c(t+\tau)\right]$$

$$= R_c(\tau)\, R_\phi(\tau) + \rho^2 R_\phi(\tau) + 2\rho\, R_\phi(\tau)\, E[c(t)]$$

$$= R_c(\tau)\, R_\phi(\tau) + \rho^2 R_\phi(\tau) \qquad 4.4.5.$$

since E[c(t)] is, by definition, zero.

The autocorrelation of $\phi(t)$ is found in the following manner: taking the Fourier transform of both sides of 4.4.2. and using the convolution theorem gives

$$\mathcal{F}(\phi(t)) = \mathcal{F}(p(t)) \times \mathcal{F}\left(\sum_{n=-\infty}^{\infty} \delta(t - nT)\right)$$

$$= \frac{2 \sin a\omega}{\omega} \times \omega_0 \sum_{n=-\infty}^{\infty} \delta(\omega - n\omega_0) \qquad 4.4.6.$$

where $\omega_0 = 2\pi/T$. Since the r.h.s. of 4.4.6. is real the power spectrum of $\phi(t)$ becomes

$$\mathcal{F}^2(\phi(t)) = \frac{4K \sin^2 a\omega}{\omega^2} \times \omega_0^2 \sum_{n=-\infty}^{\infty} \delta(\omega - n\omega_0) \qquad 4.4.7.$$

where the constant K would be infinite if the train of delta functions were infinite. Most measurements however have a finite run time! The autocorrelation function for $\phi(t)$ is then given by the inverse transform of 4.4.7. (Wiener – Khinchine Theorem).

$$R_\phi(\tau) = \left(1 - \frac{|\tau|}{a}\right) * \sum_{n=-\infty}^{\infty} \delta(\tau - nT) \qquad 4.4.8.$$

So we see that $R_\phi(t)$ is a train of triangles of base width 2a and period T (Figure 4.4.2.). Putting 4.4.8. into 4.4.5. and observing only the first triangle we see that the Doppler signal correlation function is damped and rides on a sloping baseline (Figure 4.4.3.) This can make the deduction of the velocity somewhat difficult, especially if the pulse width is very small so the damping is large (see chapter 5).

4.5. PERIODIC SOUND FIELDS WITH SUPERIMPOSED FLOWS.

We will now discuss the case of a periodic sound field on which a steady flow is superimposed. Actually, this case does not really occur in this project but it will be discussed here for the sake of completeness. The situation corresponds to that of figure 4.1.1.(a) where the net effect of the flow is to cause a shift of the carrier frequency and the corresponding effect on the correlation function is the multiplication of equation 4.2.17. by a $\cos(\omega_0\tau)$ term where ω_0 is related to the flow velocity through equation 3.2.2. Using the approximate equation 4.2.19. we see that the correlation function is

$$R(\tau) \propto J_0(D a_n \tau) \cos(\omega_0 \tau) \qquad 4.5.1.$$

which was derived by Durrani & Greated (1977) on the assumption that the flow velocity was much greater than the oscillatory velocity. This assumption considerably simplifies the mathematics of the situation but the deduction of the acoustic velocity amplitude becomes very inaccurate because the parameters of the Bessel function (zeroes and turning points) become masked by the cosine oscillations. This is illustrated in figure 4.5.1. which shows

(a)

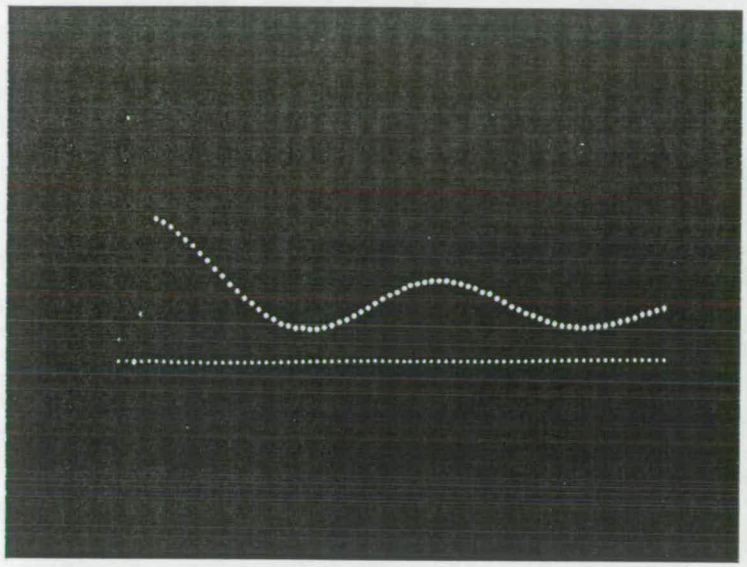

(b)

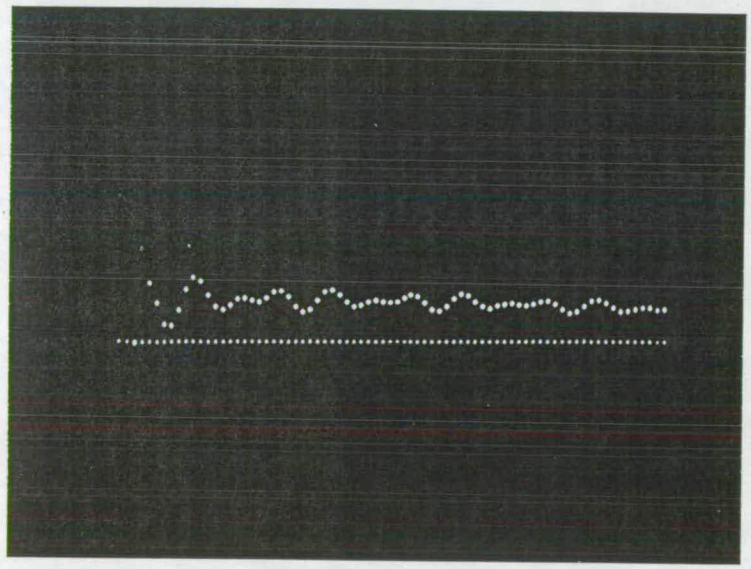

Figure 4.5.1. Effect of a steady flow (frequency shifting) on the correlation function. (a) No frequency shift. (b) Frequency shift applied.

correlation functions recorded with and without frequency shifting. (The experimental apparatus and method by which figure 4.5.1. was obtained is described in the next chapter.)

Essentially what is needed is the deconvolution of the contributions to the correlation function from the oscillatory and steady flows. This is a common type of desideratum in L.D.A. but is complicated by the truncated and statistical nature of the correlation function. Methods for this "inversion" procedure range from the simple (identification of turning points) to the highly complicated and computationally expensive (high resolution spectral estimators) [Brown & Gill 1982]. A good deal of interesting work could probably be done in this area.

Another approach is suggested by the gating technique. Since the velocity deduced from the gated correlograms represents the velocity at that particular phase position of the acoustic fluctation plus the contribution from the steady flow, then the reconstructed time history will be a sinusoid riding on a velocity pedestal. It is thus possible to deduce the velocity amplitude and mean flow from the one measurement. Unfortunately, as we shall see, the gating technique is somewhat tedious in application. We notice however that if the flow situation corresponded to that of 4.1.1.(c), then it would probably be best to use frequency shifting to move the carrier frequency well away from zero. Processing would then have to continue from 4.1.1.(a).

Finally, if there was turbulence in the acoustic field then any possibility of acoustic measurement would probably be precluded altogether if the turbulent spectral broadening became of the same order as the modulating frequency. For then the spectrum of, say, figure 4.1.1.(a) would become smeared so that the individual peaks (and hence oscillatory information) would be lost.

Chapter 5: Experiments. Measurement of Periodic and Noisy Sound Fields.

5.1. INTRODUCTION.

In this chapter the work done to verify the theory of chapter 4 will be described. The methods of acoustic calibration and the construction of the acoustic equipment will be detailed and time averaged measurements in standing and travelling wave tubes will be described both for periodic and noisy sound fields. It will be shown how the gating technique may be used to measure the phase difference between the velocity and pressure. Finally, the application of the technique to the measurement of complex acoustic impedance in an open tube will be described. This situation is well enough understood to permit theoretical calculation of the impedance but it is also realistic enough to demonstrate the use to which the technique may be put in a practical situation. Observations made in the course of these final measurements lead us to consider non-linear acoustic effects and the optical measurement of acoustic streaming. This will then be dealt with in chapter 6.

5.2. APPARATUS.

5.2.1. Acoustic Calibration - Equipment and Procedures.

Since all the L.D.A. velocity measurements to be described in this chapter will be compared against sound pressure measurements it is necessary to have an accurate and reliable procedure for calibrating the pressure microphones. In all these experiments we will be relying for our primary source of calibration on the Bruel & Kjaer (hereinafter called B & K) type 4230 sound level calibrator. This provides, for B & K half inch microphones, a sound pressure level of 94 dB (re 20μPa) to within 0.4 dB at 1000 Hz. Once a microphone has been

calibrated at this frequency its response at other frequencies can then be deduced using the data supplied by the manufacturer.

Frequently, however, we will be using the microphones with probe attachments which, due to resonance and absorption effects, greatly change the microphone response. Calibration is then achieved using another, precalibrated, microphone to sense the pressure in an acoustic coupler and the signal from this compared with the probe response. Figure 5.2.1. shows a diagram of the equipment used.

Since there are errors of about 0.1 dB in reading the scales on the measuring amplifiers we will take the total error in the pressure measurements (including the error in the type 4320 sound level calibrator) as about 0.5 dB. This value will be used throughout the present work when probe microphones are being used. An exception to this is in chapter 6 where the sound field becomes so intense that microphone distortion effects must be considered.

5.2.2. Acoustic Wave Tubes.

The acoustic fields, with which the technique was tested, were set up in either standing or travelling wave tubes. In the standing wave tube the waves emitted from one end were reflected from the other to set up (by interference) a standing wave. In the travelling wave tube the far end was terminated in such a way as to reduce this reflection to a minimum.

The standing wave tube was constructed from 2 cm i.d. glass tubing with solid rubber bungs terminating each end to provide an air column of length 46.5 cm. Acoustic excitation of the air column was provided by a probe loudspeaker inserted through one bung while pressure measurements were made with a probe microphone (1mm i.d.) inserted through the other. Location of the tube resonances was made by positioning the tip of the probe microphone at one

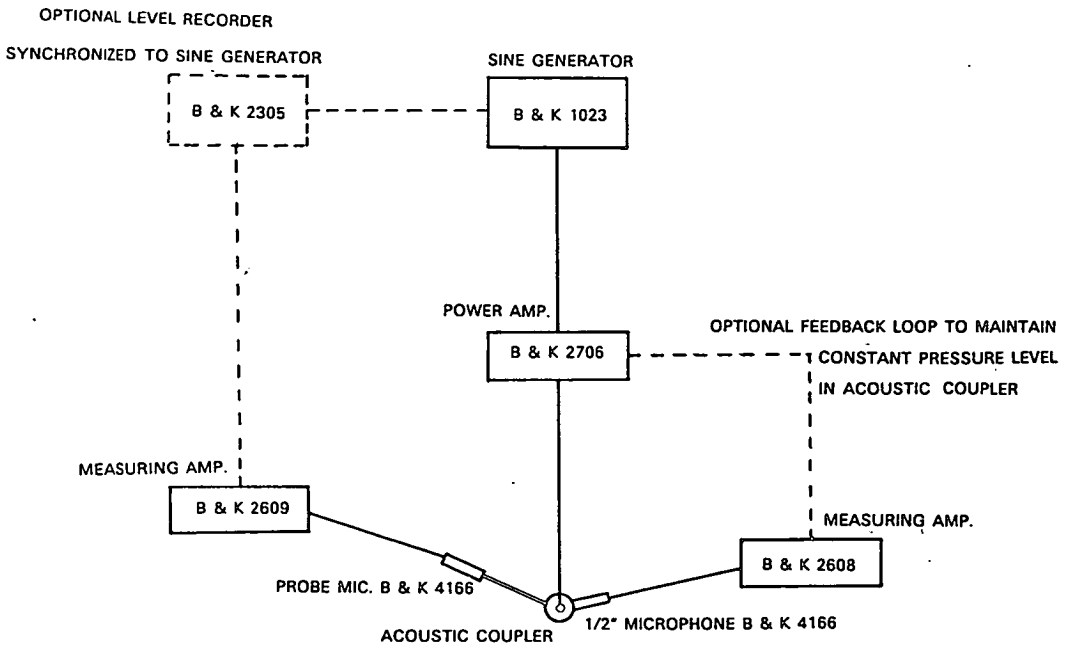

Figure 5.2.1. Apparatus for calibration of probe microphones.

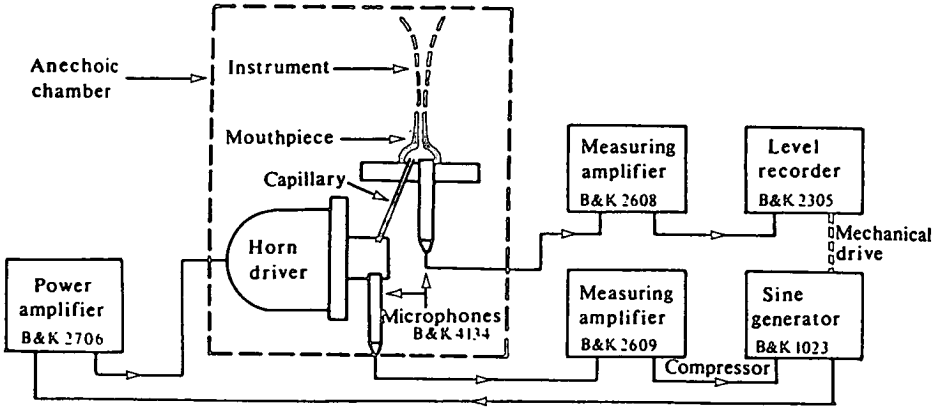

Figure 5.2.2. Apparatus used for testing the termination of the travelling wave tube (from Campbell (1987)).

closed end (a pressure antinode) and adjusting the frequency until a maximum response was seen on the measuring amplifier.

For the travelling wave tube a 1.5 metre length of 2 cm i.d. glass tubing was used with the last metre or so filled with plastic wool and foam rubber to prevent reflection of sound from the far end. Sound was introduced into the tube through a curved section of plastic tubing using a horn loudspeaker which had the horn removed. A probe microphone could be inserted through the plastic tubing to monitor the pressure. (See figure 5.2.4. which shows this tube in the working section of the L.D.A. system.)

To assess the effectiveness of the absorbing material and hence be able to adjust it for minimum reflection, the tube was examined in an anechoic chamber using the apparatus constructed by Campbell (1987) for measuring the input impedance of brass instruments (Figure 5.2.2.). This apparatus worked by supplying a constant volume velocity input through the capillary and measuring the pressure output from the system under observation. In this case, however, the musical instrument was replaced with the glass tube and interest was more focussed on reducing resonance than extracting values for impedance. The absorbing material was adjusted several times until a roughly flat response was found over quite a wide frequency range. The output from the level recorder is shown in figure 5.2.3.(a) for the final configuration of absorbing material used. For comparison the output due to a 2 m long open tube of similar diameter is shown in (b).

The effectiveness of the termination was further gauged by traversing the probe microphone some distance along the tube. Any standing waves would then manifest themselves through variation of microphone response with position. The largest ratio of sound maximum to minimum was found to be 0.8 dB (at 1260 Hz, the frequency used later). This value will be used later in

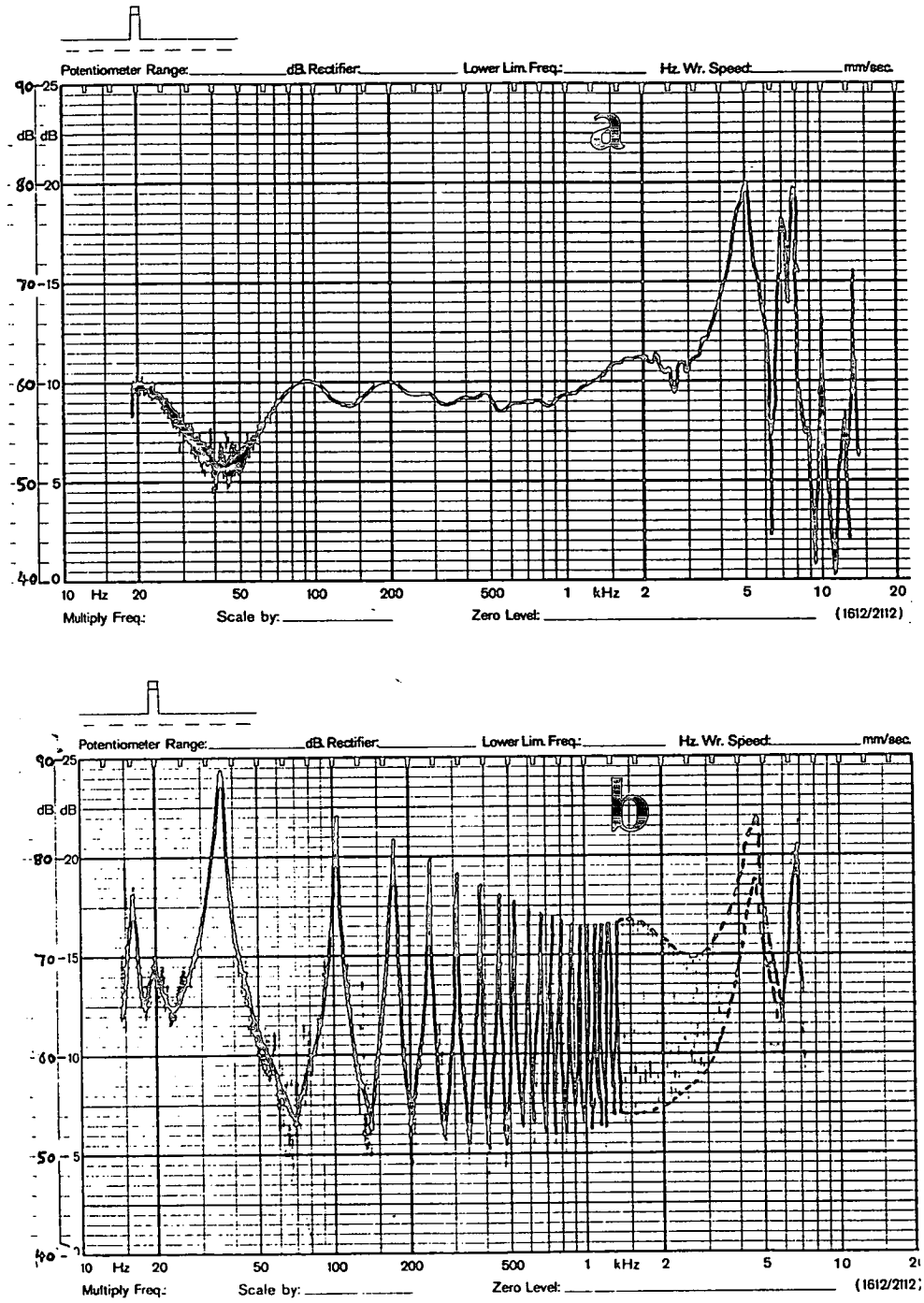

Figure 5.2.3. (a) Level recording from the travelling wave tube with the terminating material in the final configuration and (b) recording from a 2 m long open tube.

assessing the accuracy of the L.D.A. measurements.

5.2.3. Optical and Signal Processing Equipment.

A diagram of the experimental apparatus is shown in figure 5.2.4. with the travelling wave tube in the working section.

On the optics side the beam from an 8 mW He-Ne laser (λ=633nm) was split into two equal intensity, parallel beams using a beam splitter. After passing through a phase shifter (Electro Optics Developments PC 14 Light Modulator) the two beams were focussed down from a 2 cm separation using a 20 cm focal length lens. This gave a measuring volume with 35 fringes and a fringe spacing of 6.33 µm. (The number of fringes was simply found by projecting them onto a screen using a very short focal length lens and counting them.) The 20 cm focal length lens was chosen for two reasons; firstly, the fringe separation was of the order of that expected for easily generated acoustic particle displacements and secondly, the crossover point was sufficiently far from the lens to allow easy access during experimental work.

The detector was a photomultiplier with a built-in discriminator unit which produced equal sized pulses for each photon detected. Light from the observation volume was collected using a 105 mm focal length lens and was focussed through a 400 µm diameter pinhole onto the detector surface. A narrowband optical filter, just in front of the detector, only permitted the passage of red light near 633 nm - allowing measurements to be made under normal illumination conditions. The pinhole, which determines the size of the measuring volume (chapter 3), also prevented too much extraneously scattered light from entering the detector. The photomultiplier was usually angled at about 35° from the straight through position to avoid flare from the tube walls.

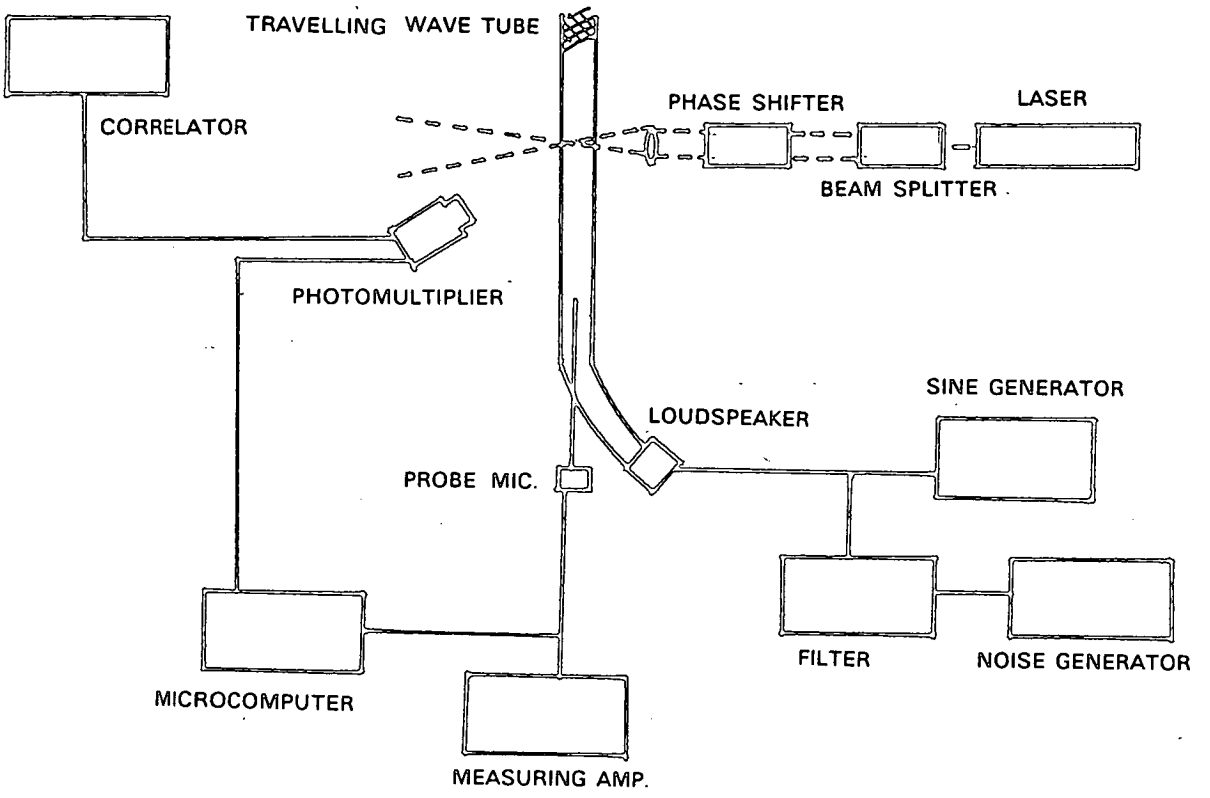

Figure 5.2.4. Laser Doppler apparatus with the travelling wave tube in the working section.

The photomultiplier signal was processed using a Malvern type K7023 digital correlator which has a minimum lag time between separate channels of 50 ns and a total of 72 channels. Measurements were made by outputting the correlation function (the correlogram) to an oscilloscope and counting the number of channels to maxima or minima. These correlograms could then be recorded, if one wished, using an oscilloscope camera.

5.2.4. The Gating Equipment.

The gating technique worked in the fashion indicated in chapter 4. The pressure signal from the probe microphone was sent to an Apple microcomputer which had been programmed to detect the positive going zero crossings of the signal and supply a pulse of preset duration and at a preset delay time from the zero crossing. The pulse length and delay time could be varied independently with the former having a minimum value of 50 μs. The pulses were then amplified and sent to the photomultiplier. Generally, during an experimental run, both the pressure signal and pulses were monitored on an oscilloscope.

As was also described in chapter 4, this gating process results in the correlation function becoming damped and riding on a sloping baseline. This can make the deduction of the velocity quite difficult, especially if the pulse width is small. The problem can be overcome (at least on this Malvern correlator) by incorporating a strobing circuit into the equipment. The intricacies of the strobing process are somewhat involved – the details can be obtained from the manufacturer – but essentially what happens is this: the Doppler signal from the photomultiplier is split into two by the strobing circuit. One part goes directly through to one input on the correlator while the other, identical, part is sampled by the gating pulses and fed to the other input. The strobe circuitry then acts on the shift registers in the correlator so that values

from the inputs are only stored when the gating pulses are high (i.e. for the duration of the pulse.) Cross correlating the two inputs then gives the autocorrelation of the gated doppler signal. No damping occurs because the correlator does not in effect see the pulses themselves.

5.3. LASER DOPPLER ACOUSTIC VELOCITY MEASUREMENT.

5.3.1. Time averaged measurement of periodic acoustic fields.

For these measurements the gating circuit, phase shifter and noise generator of figure 5.2.4. were made inactive. The standing wave tube, probe loudspeaker and probe microphone were all mounted rigidly on a piece of optical bench so that the whole assembly could easily be moved as a unit. A small quantity of tobacco smoke was introduced into the tube for seeding purposes. This rig was then put into the working section of the L.D.A. system so that the laser beams intersected on the tube axis and the air column was excited to its fourth normal mode - a frequency of 1470 Hz - using the probe loudspeaker. The laser intersection was then scanned along the tube axis by moving the tube-speaker-microphone assembly and correlograms were recorded every two centimeters. The acoustic velocity amplitude was then derived from these by counting up to the first minimum of each correlogram and applying equation 4.2.20. The pressure was also recorded at these points by traversing the probe microphone along the tube. These pressure measurements were then converted to equivalent velocity amplitudes using equation 2.2.9.. Although this equation is not directly applicable to a standing wave (chapter 2 ,section 2.2.1.) we can use it provided we remember that the velocity and pressure are 90° out of phase in this case. Figure 5.3.1. shows the correlation functions obtained for a variety of intensities - indicating how the Bessel function changes in accordance with equation 4.2.19. That a zero order Bessel function is a good approximation to the correlation function may be seen by

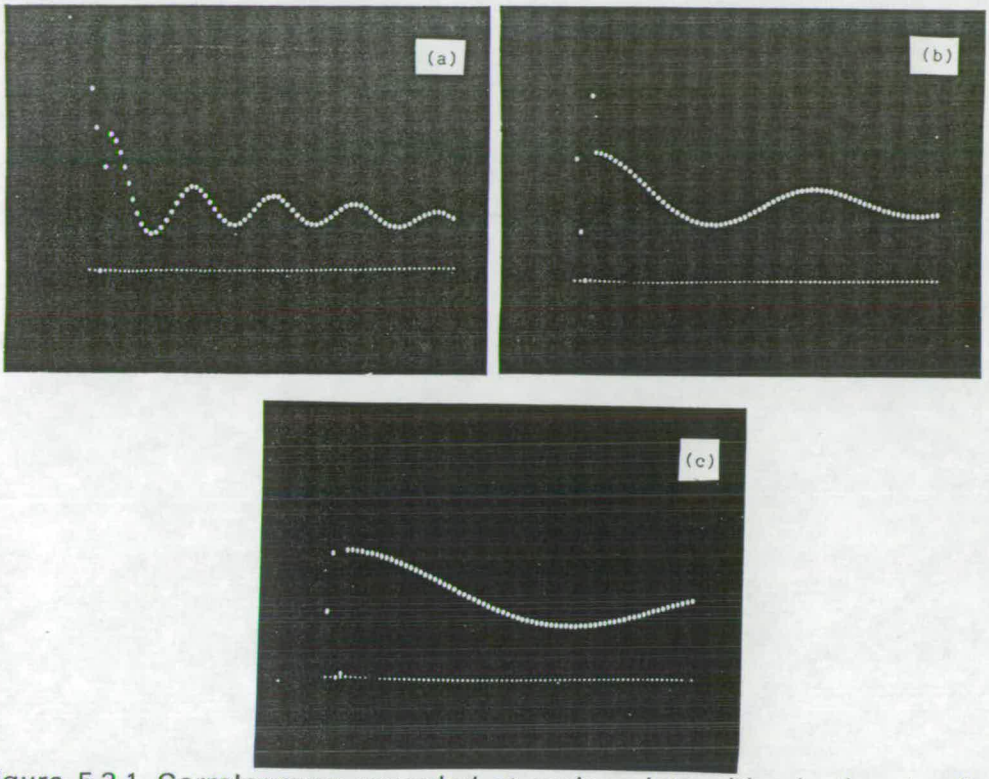

Figure 5.3.1. Correlograms recorded at various intensities in the standing wave tube. Sound frequency, 1470 Hz, sample time (time between channels on correlator) = 1.5 µs. (a) velocity amplitude = 257 mm/s, (b) velocity amplitude = 103 mm/s, (c) velocity amplitude = 8 mm/s.

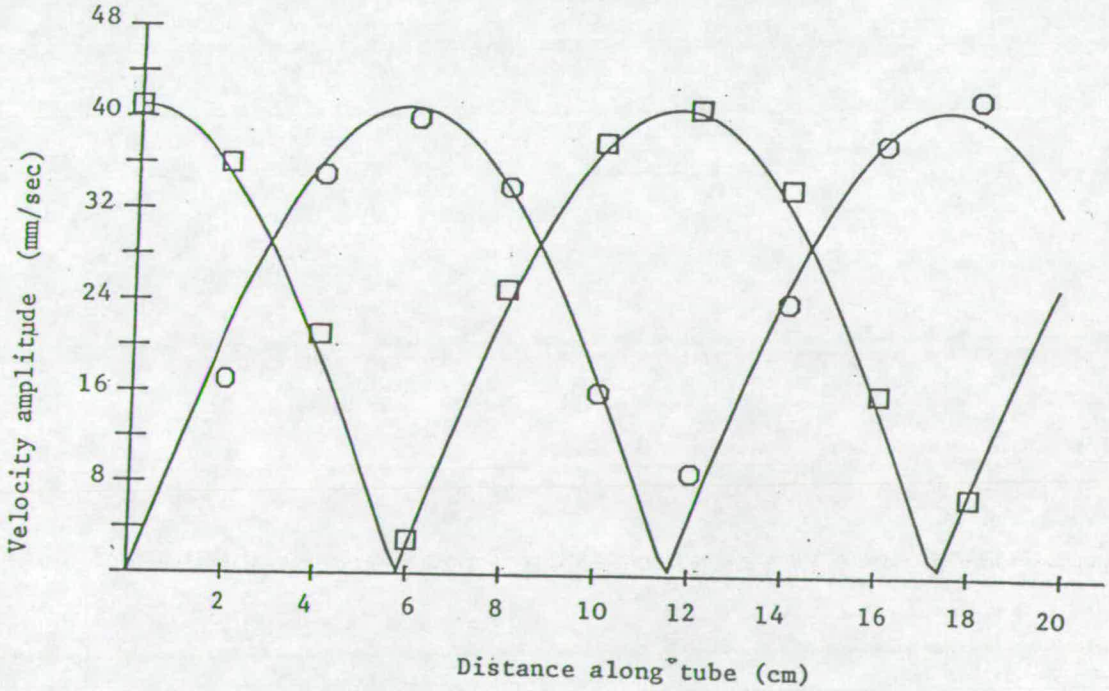

Figure 5.3.2. Pressure deduced (□) and correlogram deduced (o) velocity amplitude measurements along the standing wave tube.

calculating the velocity amplitude using the various turning points of, say, figure 5.3.1.(a) and using the tabulated values for the Bessel function. The calculations all give closely similar values.

The velocity measurements made with the L.D.A. system and those derived from the pressure measurements were then plotted as a function of distance along the tube (figure 5.3.2.). The solid lines were fitted using the velocity maximum (derived from the pressure measurement at one end of the tube) and knowing the wavelength of the sound field. Both sets of measurements show close agreement and, as would be expected for this sound field, are 90° out of phase. The accuracy to which the velocity amplitude could be deduced from the L.D.A. measurements depended on how accurately the minimum of the correlation function could be measured. Just measuring by eye it was generally possible to estimate the position of the minimum to within half a channel. This indicates an accuracy of greater than 5% for an average correlogram. Interfacing the correlator to a computer and using an interpolation and minimum-finding routine would increase this accuracy considerably. All the L.D.A. measurements however agreed with the pressure measurements to within the accuracy of the pressure microphone.

Replacing the standing wave with the travelling wave tube allowed even more direct comparison of the L.D.A. and pressure measurements since the velocity and pressure are in phase. Figure 5.3.3. shows one such correlogram obtained at a frequency of 1260 Hz. The travelling wave tube also allowed direct estimates of the dynamic range of the technique - both in terms of the intensity and frequency of the sound field.

We are now in a position to discuss the dynamic range of the technique. We will thus do this in the following section, both from a theoretical point of view and in terms of what we were able to measure. Then we will move on to the

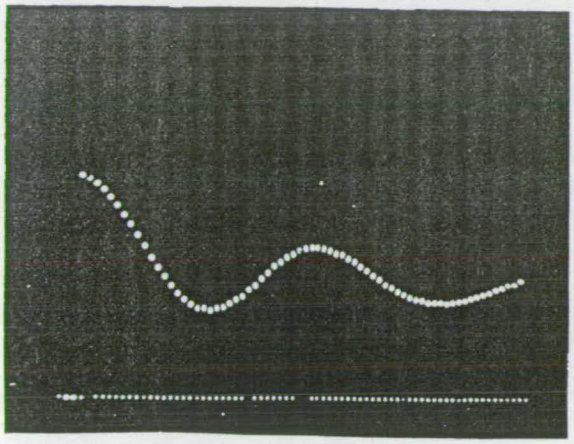

Figure 5.3.3. Correlogram recorded in the travelling wave tube at sound frequency 1260 Hz. Sample time = 3 μs. Velocity amplitude deduced from correlogram = 64.3 mm/s. Velocity amplitude deduced from microphone reading = 63.3 mm/s.

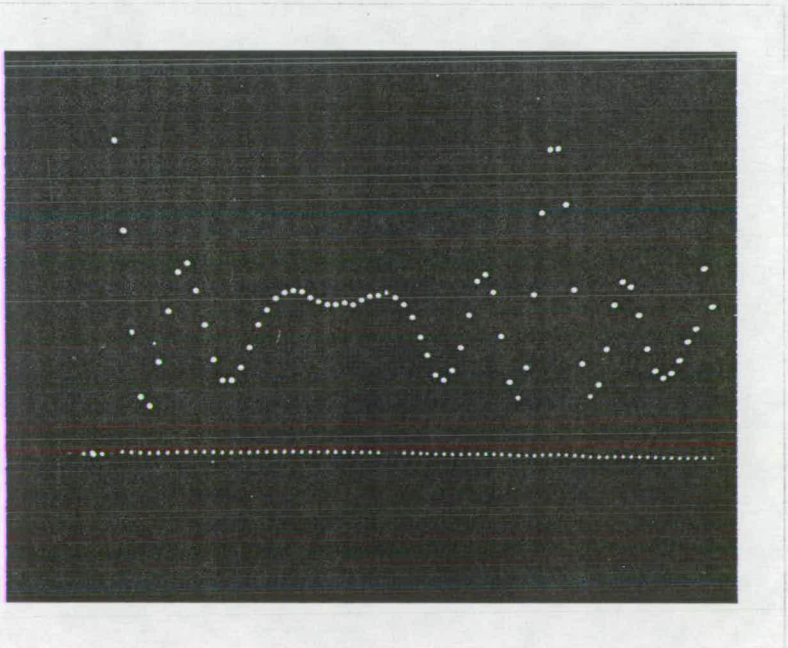

Figure 5.3.4. Effect of $\sin(\omega_m \tau/2)$ term on the correlation function (c.f. equation 4.2.9.). Sound frequency = 1260 Hz, sample time = 15 μs, sound field intensity in travelling wave tube = 118 dB.

measurement of phase and noisy sound fields.

5.3.2. Dynamic range of the technique.

As was mentioned in chapter 3, one would expect the lower intensity limit of the technique using the optical configuration described above to be about 105 dB for a 1000 Hz sound field (corresponding to a velocity amplitude of ~ 12 mm/s). In fact we found we could measure down to just over 95 dB (equivalent to ~ 5 mm/s). This perhaps reflects the motion of several particles, moving coherently, so that at any instant the fringe pattern is well sampled.

Davis & Hews-Taylor (1986) discuss the technique's dynamic range in terms of modulation indices (defined in chapter 4): for low indices very little energy is put into the sidebands of figure 4.1.1. while for high indices the energy is distributed among so many sidebands that the peaks can become masked by system noise. This argument however is, like the one in the previous paragraph, really only useful for order of magnitude estimates. For example, the level of noise in any system depends on the type of analysis system, the amount of extraneous light entering the detector, the size of the scattering particles etc.. We found, with the above optical system, that we could measure accurately up to about 130 dB. This agrees qualitatively with Davis & Hews-Taylor's work.

A more fundamental limitation on the technique at higher frequencies and lower intensities is the effect of the $\sin(\omega_m \tau/2)$ term in equation 4.2.18. For "moderate" intensities and frequencies $\sin(\omega_m \tau/2) \sim \omega_m \tau/2$. This approximation may, however, not be satisfied if ω_m becomes large or the intensity becomes low so that the lag time, τ, on the correlator must be increased to render the first minimum of the Bessel function visible. The effect of this term on the correlation function is shown in figure 5.3.4. where the

correlation function repeats for $\omega_m \tau/2 = \pi$ (remembering that $J_0(\ )$ is an even function). No information can thus be recovered (through the first minimum of the Bessel function) if the first minimum of this sinusoidal oscillation occurs before the first minimum of the Bessel function. Thus, for the velocity amplitude to be recoverable.

$$\text{LAG TIME TO MINIMUM OF BESSEL FUNCTION} \lesssim \text{LAG TIME TO MINIMUM OF SINUSOIDAL OSCILLATION}$$

$$\therefore \quad \frac{3.832}{D a_m} \lesssim \frac{\pi}{\omega_m}$$

$$\frac{a_m}{\omega_m} \gtrsim \frac{3.832}{\pi D}$$

This implies, for our 1260 Hz field, a lower velocity limit of approximately 9 mm/s - qualitatively in agreement with the experimental work.

5.3.3. Measurement of phase.

To test the gating technique the gating circuit and phase shifter of figure 5.2.4. were made active. The phase shifter, set to give a 50 kHz equivalent frequency shift, provided a 0.317 m/s velocity bias from which to determine the velocity of the acoustic fluctuation. For a 1260 Hz sound field at a velocity amplitude of 86 mm/s in the travelling wave tube, the gating pulse width was set to 100 μs and correlograms were recorded at various delay times. (A typical oscilloscope trace of the pressure signal and the pulses is shown in figure 5.3.5..) From these correlograms the velocity was deduced from the period of the correlation function. Two such correlograms are shown in figure 5.3.6. The

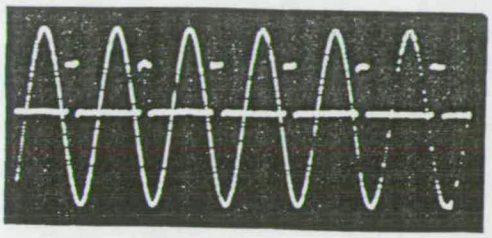

Figure 5.3.5. Pressure signal and gating pulses. Sound frequency = 1260 Hz, delay time = 400 µs, pulse width = 100 µs.

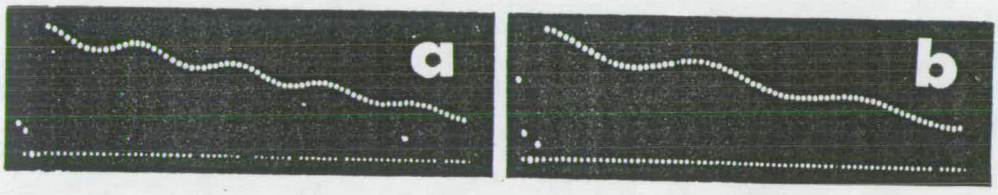

Figure 5.3.6. Gated correlograms for different delay times in the 1260 Hz cycle. Frequency shift = 50 kHz, sample time = 1 µs, pulse width = 100 µs. (a) delay = 300 µs, (b) delay = 700 µs.

damping of the correlation function is clearly visible. The velocity was then plotted as a function of delay time (figure 5.3.7.) and, as expected, shows the form of a sine curve. Unfortunately however we did not know the phase response of the probe microphone so no quantitative conclusions could be reached about the accuracy of the technique. We will however be able to do this later when complex acoustic impedance is being measured.

5.3.4. Time averaged measurement of band limited noise fields.

For these measurements the gating circuit and phase shifter were again made inactive and the travelling wave tube was used. The acoustic excitation was provided using a QuanTech type 420 noise generator with the noise filtered through a band pass filter with 24 dB/octave cutoff and centre frequency at 1260 Hz. The spectrum of the sound field is shown in figure 5.3.8.(a) with the time history in (b). Note the similarity of the latter to the diagram in figure 4.3.1. The spectrum was recorded both directly from the filter and from the probe microphone and, since these both looked identical, this was taken as indicating little or no filtering or distortion of the sound field due to the amplifier, speaker, microphone or resonance effects in the tube.

Velocity measurements were made with the L.D.A. system by estimating the standard deviation of the correlograms from the oscilloscope. This was done over a range of intensities and a typical correlogram is shown in figure 5.3.9. Comparison with pressure measurements was made by assuming that the mean pressure response of the probe microphone came at 1260 Hz and that each part of the spectrum contributed to the response on the measuring amplifier in proportion to its intensity. This was probably not too bad an assumption since the pressure response of the microphone was roughly flat in this area. A plot of velocity deduced from the pressure measurements versus those deduced from the L.D.A. system is shown in figure 5.3.10.. The straight

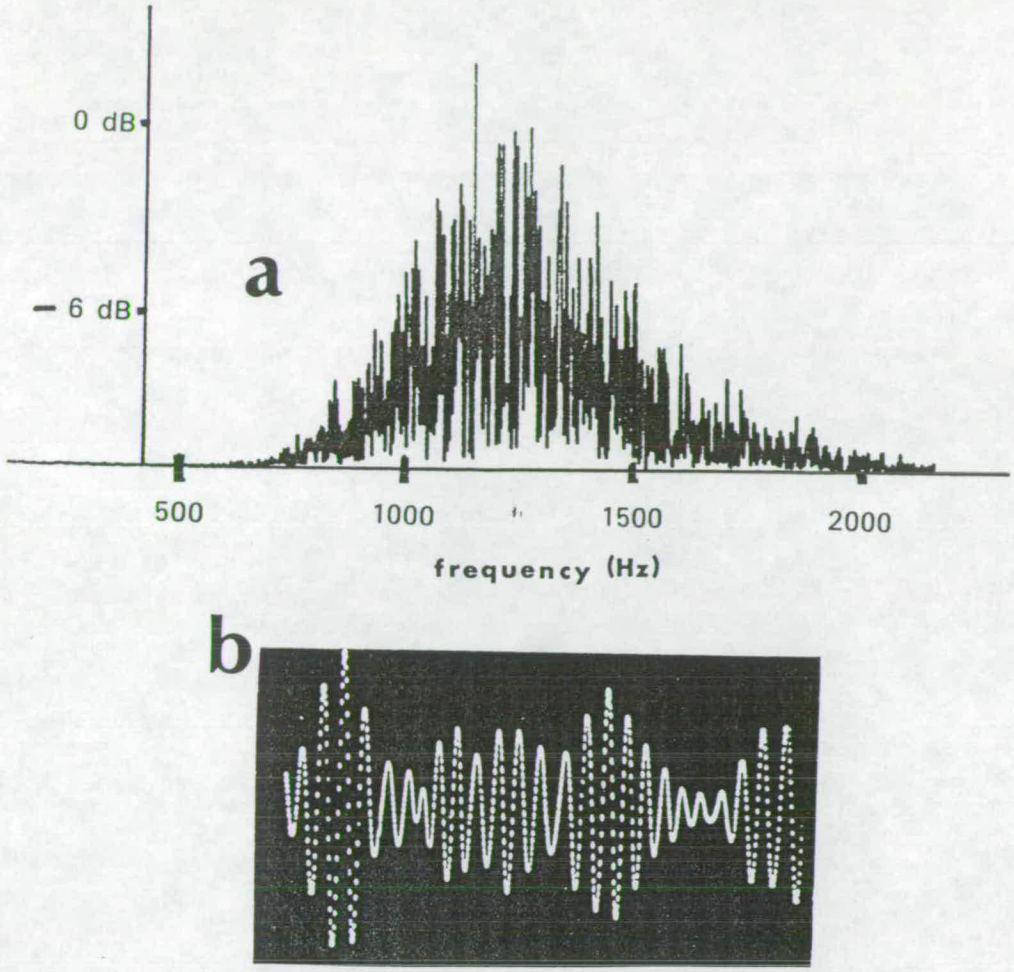

Figure 5.3.8. (a) Spectrum of noise filtered about 1260 Hz. (b) Sample of noise time history.

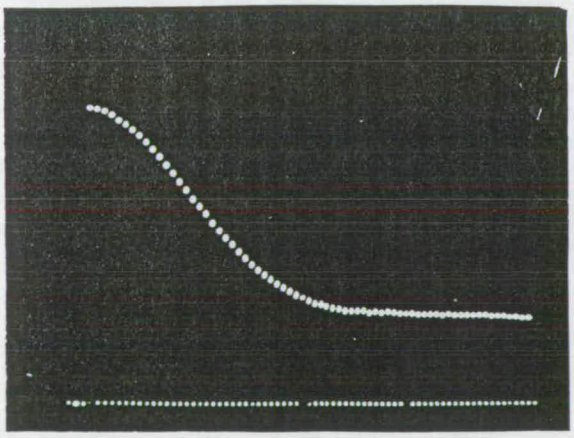

Figure 5.3.9. Typical correlogram due to band-limited noise field. Sample time = 2 μs. Mean velocity amplitude deduced from correlogram = 43.0 mm/s. Mean velocity amplitude deduced from pressure measurement = 44.8 mm/s.

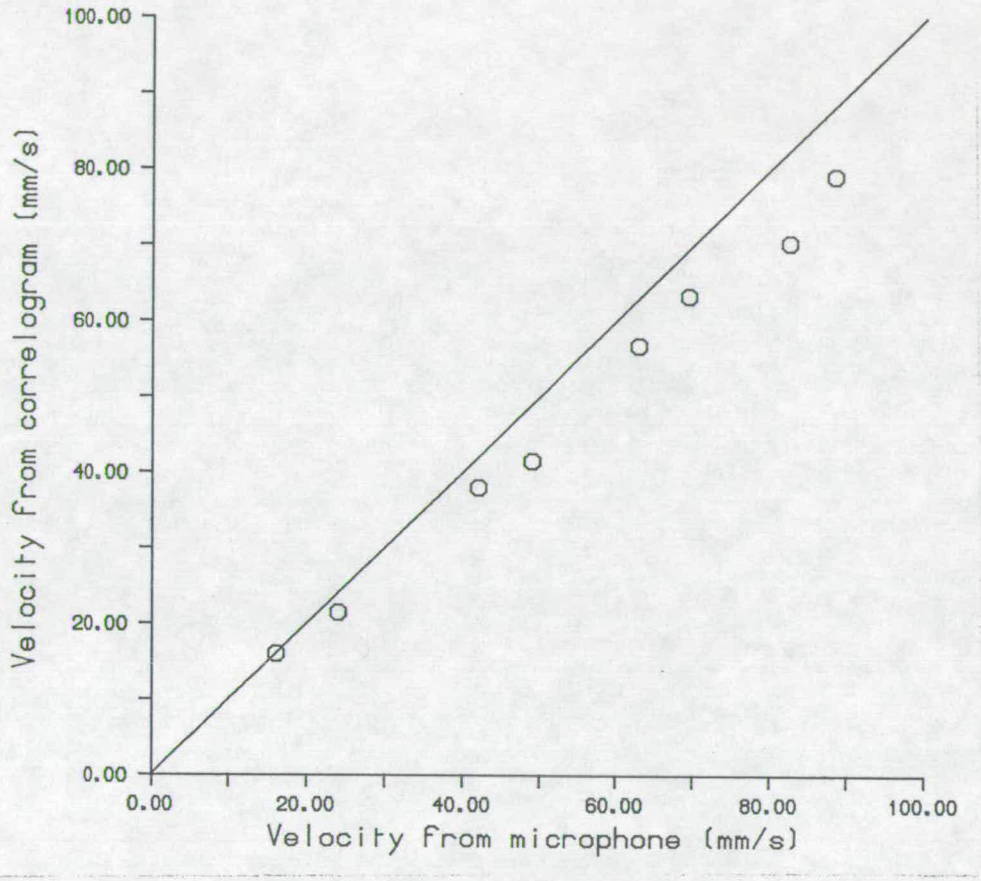

Figure 5.3.10. Mean velocity amplitudes measured by L.D.A. system versus those deduced from pressure measurements in the noise field over a range of intensities. The straight line indicates equal velocities.

line shows equal velocities. We can see that there is quite close agreement although the L.D.A. measurements seem to be lower than the others by roughly 5%. This however was considered well within the errors that could be ascribed to the assumptions and calibration errors inherent in this work e.g. the narrowband assumption, improper termination of the tube etc.

5.4. MEASUREMENT OF COMPLEX ACOUSTIC IMPEDANCE.

5.4.1. Apparatus.

A diagram of the apparatus used is shown in figure 5.4.1. with a photograph in figure 5.4.2.

A glass tube of length 1.512 metres and i.d. 2.1 cm was sealed against a brass plate which had holes bored through it to accept a capillary tube (i.d. 1 mm) and a 1/2 inch microphone (B & K type 4134). Sound was introduced into the tube through the capillary and the pressure at this (input) plane was measured using the microphone. This microphone also provided the signal for the gating pulses.

The same optical system described in the previous sections was used with the laser beams being focussed down to intersect on the tube axis at a distance of 1.5 cm from the input plane. Thus velocity measurements were not being made exactly at the end of the tube but a calculation showed (see Appendix B) that the effect of this would be to move the measured resonance frequencies up by a factor of $(1+x/L)$ where x is the distance to the input plane and L is the length of the tube. For our setup this amounted to a frequency correction of about 1% which was applied to each impedance measurement.

Further, since the L.D.A. system measures the velocity at one point (giving the acoustic particle velocity), we have to multiply this by the cross sectional area of the tube to obtain the volume velocity for calculating the acoustic

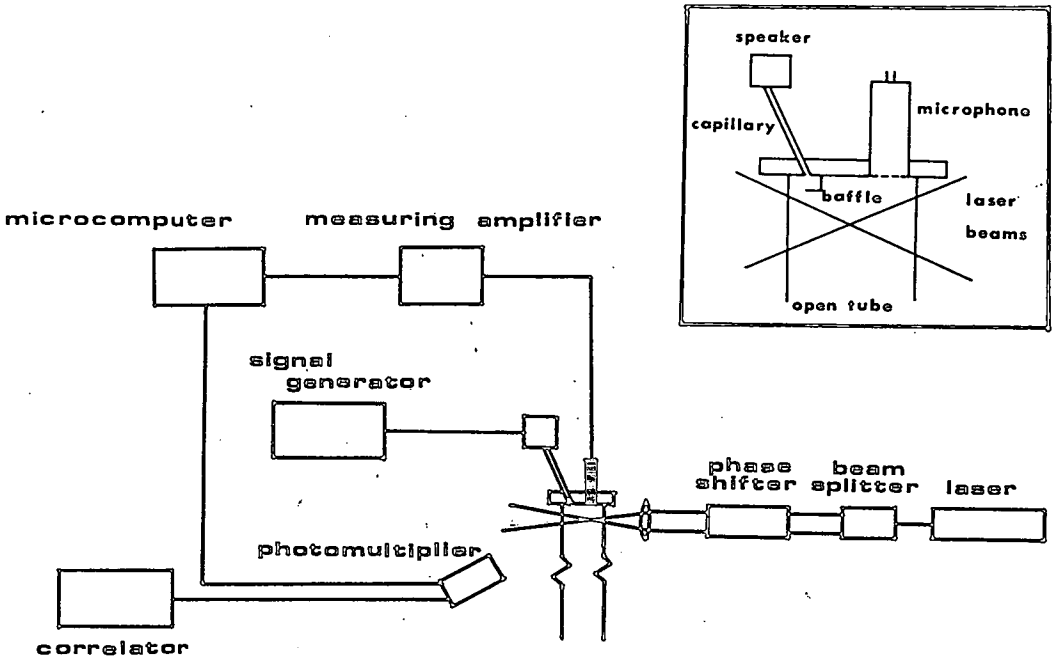

Figure 5.4.1. Impedance measurement apparatus with (inset) close-up of the closed end of the tube.

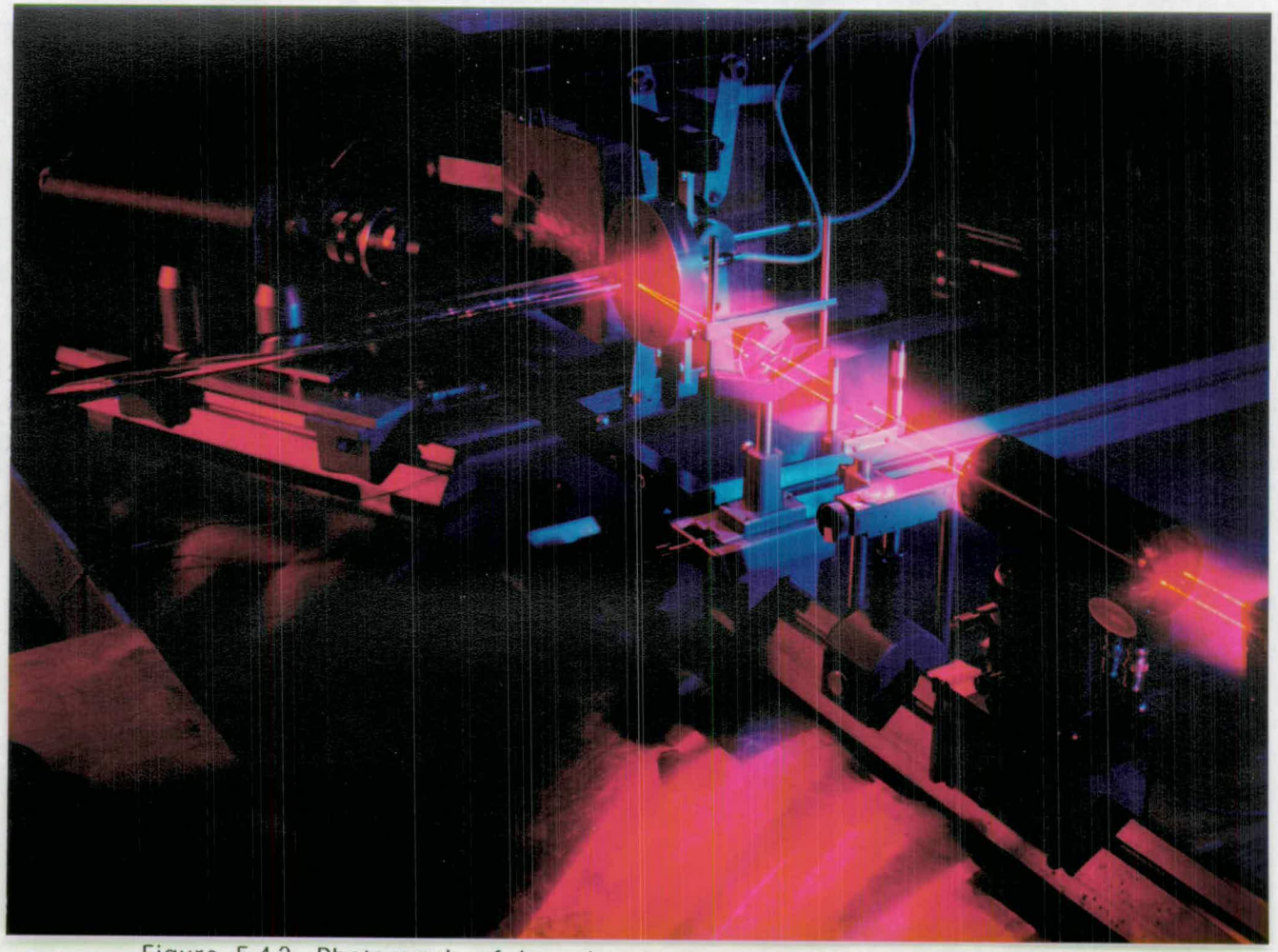

Figure 5.4.2. Photograph of impedance measurement apparatus showing the laser beams coming from the right, passing through the phase shifter, through a mask to eliminate spurious beams and then being focussed down into the glass tube. The photomultiplier can be seen on the far side of the tube, to the left.

impedance (see chapter 2). This assumes that the velocity is constant over the tube cross section but, as we saw in chapter 2, there exists viscous interaction between the flow and the tube wall which creates a boundary layer. This effectively decreases the tube's cross section. However, substituting values for the acoustic field, air viscosity etc. into equation 2.2.12. shows that even at frequencies as low as 50 Hz (the lowest frequency we used) the error incurred through neglect of the boundary layer is only of the order of 5% for our setup - and this decreases rapidly with increasing frequency. Consequently the effect was not considered any further.

When the laser beams were on and a sound field was being introduced into the tube it was noticed that turbulent motions of the air of the order of centimetres per second were being produced near the capillary exit at certain frequencies. Since these motions could have upset the measurements, a small baffle of thin plastic was constructed round the capillary exit. This reduced the motion near the laser beam intersection and measurements could then be made with some confidence. Further investigation seemed to indicate that the motions were due to non-linear interaction between the sound field and the region round the capillary tip. A discussion and qualitative explanation of the effect is given in Appendix A.

5.4.2. Measurement of impedance amplitude ($|Z|$).

Measurement of the impedance amplitude was carried out over a range of frequencies from about 50 Hz to 700 Hz by making separate measurements of the pressure and velocity. The recorded sound pressure levels were converted to pascals (equation 2.2.8.) and the velocities deduced from the correlograms using equation 4.2.19. Each particle velocity amplitude was then converted to r.m.s. volume velocity and combined with the pressure measurement at that frequency to yield $|Z|$ which is expressed in acoustic ohms.

A theoretical impedance curve was calculated using the method outlined in section 2.2.2. with values for constants such as the viscosity, speed of sound in air etc. at various temperatures taken from Benade's (1968) paper. The theoretical curve and experimental points are shown in figure 5.4.3. where the experimental points have been moved down in frequency by 1% due to the different planes of velocity and pressure measurement. As can be seen, the agreement is very good. The error bars were calculated assuming a 0.5 dB error in the pressure measurements and that the velocity could be measured to about 2% accuracy from the correlograms.

5.4.3. Measurement of phase (ϕ).

In order to demonstrate the measurement of phase, recordings were taken at 155, 165, 170, 175 and 180 Hz; a range which we knew to straddle a resonance peak and hence to have a large phase change. The pulse width in this case was 500 µs with the delay being incremented in units of 500 µs. A phase shift of 20 kHz was used providing a bias velocity of 0.1266 m/s. At each delay setting a velocity measurement was taken and the process repeated until at least one whole pressure (and hence velocity) fluctuation had been covered. Figure 5.4.4. shows two velocity versus delay time curves recorded at different frequencies and clearly shows a phase change.

Since, in this experiment, we were using a microphone without a probe attachment, it was possible to estimate the microphone phase response using the data supplied by the manufacturer [Bruel & Kjaer 1982]. Knowing this we were then able to deduce the phase difference between the acoustic velocity and pressure. Figure 5.4.5. shows the measured points and the theoretically deduced phase curve. The error bars were calculated by estimating how accurately the phases of the velocity versus delay curves could be deduced.

As may be suspected this method of measuring phase is very tedious when

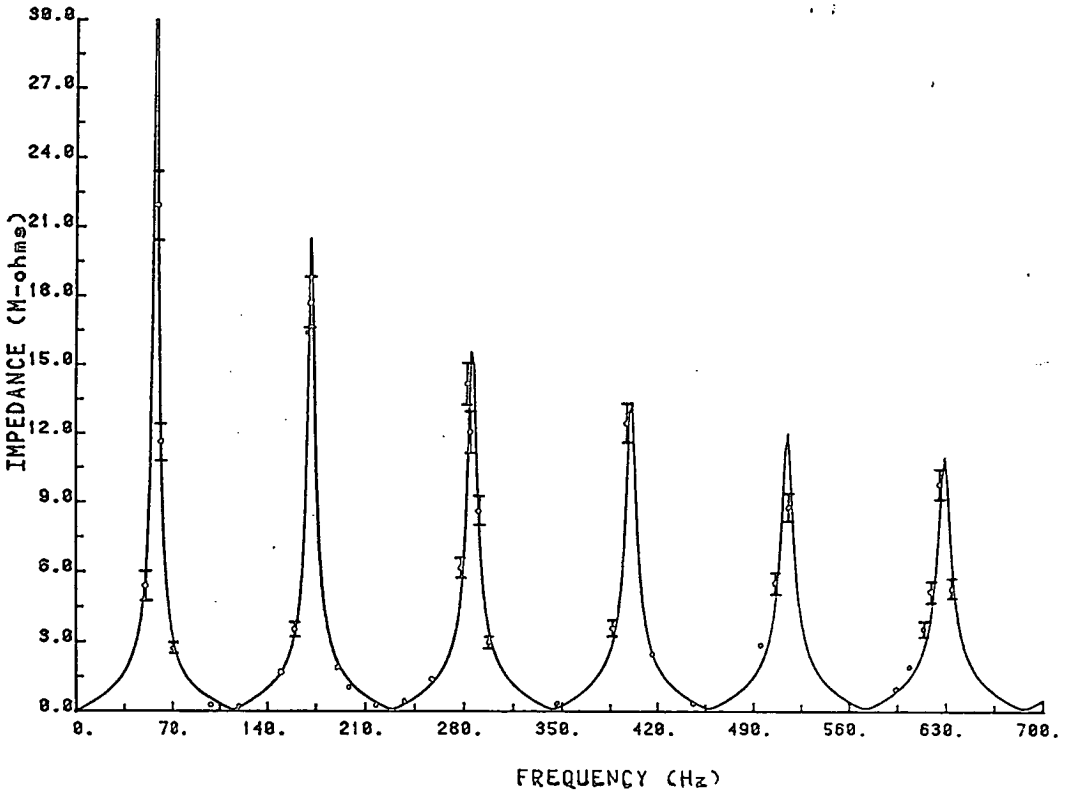

Figure 5.4.3. Theoretical impedance magnitude (solid curve) and experimental points.

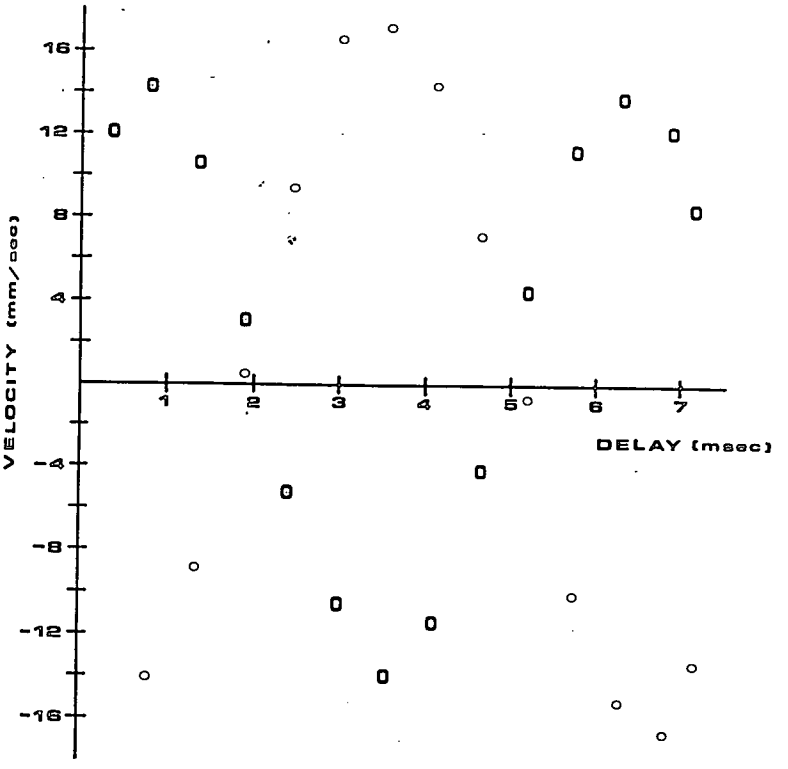

Figure 5.4.4. Two velocity versus delay time curves. Frequencies = 155 Hz (o) and 175 Hz (o).

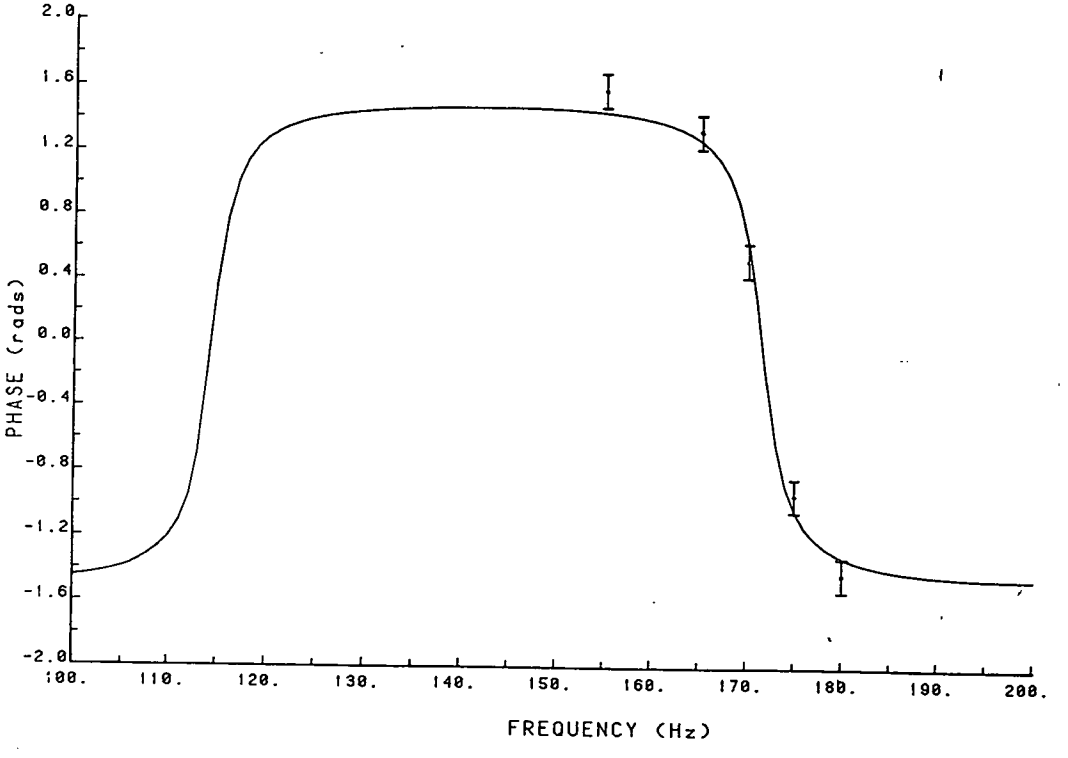

Figure 5.4.5. Theoretical phase (solid curve) and experimental points.

done manually. Discussion of how the procedure may be speeded up will be deferred to the conclusions and discussion of chapter 7.

Chapter 6: Acoustic Streaming and Particle Image Velocimetry.

6.1. INTRODUCTION.

It was seen in the last chapter how acoustic streaming effects arose in connection with the measurement of complex acoustic impedance. During the course of finding out more about this streaming it was realised that the photographic technique of Particle Image Velocimetry (P.I.V.) could be applied to the measurement of this effect. This would be interesting primarily because it is difficult to use material probes to measure streaming and also because P.I.V. ties in well with the more common flow visualisation method of comparing streaming observations with theory.

In fact, P.I.V. had been considered earlier in this project for the measurement of acoustic particle velocities but had been left aside after a few preliminary experiments had indicated that any measurements would have low resolution and have required very large laser powers. Work on acoustic streaming would therefore also allow a more complete assessment of this early work

Although L.D.A. could perhaps also be applied to acoustic streaming measurement we notice that, for slow flows, the correlation function can take a very complex form and for faster flows there is still the problem of sorting out the contributions due to the oscillatory and flow motions. (c.f. Chapter 4.)

6.2. ACOUSTIC STREAMING.

Acoustic streaming is the generation of non-zero mean flows by a sound field. The phenomenon typically (though not exclusively [Andrews & McIntyre 1978]) arises due to attenuation or dissipation of the sound field in the propagating

medium or, when a solid wall is present, in the boundary layer [Lighthill 1978a]. It is this attenuation that provides the mechanism for transferring momentum into the body of the fluid. There are several articles dealing with acoustic streaming (e.g. [Lighthill 1978a,b , Beyer 1974]) but the topic as a whole has perhaps been rather neglected. This is probably because streaming effects only arise when the acoustic field is very intense and such regimes occur only infrequently at normal audio frequencies (<20kHz). Exceptions arise when the field is very curved (as discussed in appendix A) or, occasionally, in musical instruments. For example, the intensity can be as great as 160 dB in the mouthpiece of a clarinet [Keefe 1983] and, although streaming does seem to have some effect on the performance of the instrument, this has not yet been rigorously quantified.

The topic has perhaps also been somewhat neglected because of the difficulty of accurately measuring streaming due to the measuring probe (e.g. hot wire anemometer) creating its own boundary layer and upsetting the flow under investigation. (This could be a possible explanation for the low Reynolds numbers found by Merkli & Thomann (1975) for the transition to turbulence in oscillatory pipe flow.) Consequently, one sees in the literature qualitative statements about "strong" or "weak" streaming [Keefe 1983] and measurements made on the basis of flow visualisation [Beyer 1974].

Another region where streaming occurs is at ultrasonic frequencies (>20 kHz) and indeed the availability of reliable ultrasonic transducers in the 1940s seems to have provided an impetus for the study of streaming effects around that time [Westervelt 1953 , Nyborg 1953]. Here streaming can be much more vigorous with jet velocities of the order of meters per second being readily obtainable [Lighthill 1978a]. We will not be dealing with ultrasound in this work though it should perhaps be noted that with the advent of a new generation of ultrasonic sources and research being carried out now on using ultrasound for

mixing and inducing chemical reactions much more careful research on streaming will perhaps be required.

For the purpose of this work we will confine ourselves to the type of streaming known as Rayleigh streaming since it is well understood, can be easily generated and the streaming velocities can be independently estimated by measuring the pressure of the sound field causing it.

6.3. RAYLEIGH STREAMING.

This form of streaming was first explained by Rayleigh himself in his Theory of Sound (1896) and occurs due to the viscous attenuation of the sound field in the boundary layer when a solid wall is present. The most common configuration in which to observe this effect occurs when a standing wave is set up in a circular tube. The form the streaming takes is illustrated in figure 6.3.1. with the direct current (along the walls) always pointing towards the velocity nodes and the return current (along the tube centre) going towards the antinodes.

For a standing wave of the form

$$u(x,t) = u(x) \sin \omega t \qquad 6.3.1.$$

Rayleigh's Law gives the velocity at the wall as

$$u_w(x) = -\frac{3}{4} \omega^{-1} u(x) \frac{du(x)}{dx} \qquad 6.3.2.$$

It is interesting to note that the streaming velocity is independent of the fluid viscosity for, although the viscosity drives the streaming, the resistance to the flow also depends on the viscosity and consequently explicit dependence on it drops out of equation 6.3.2.

It is possible then to calculate the streaming velocity at any point in the tube

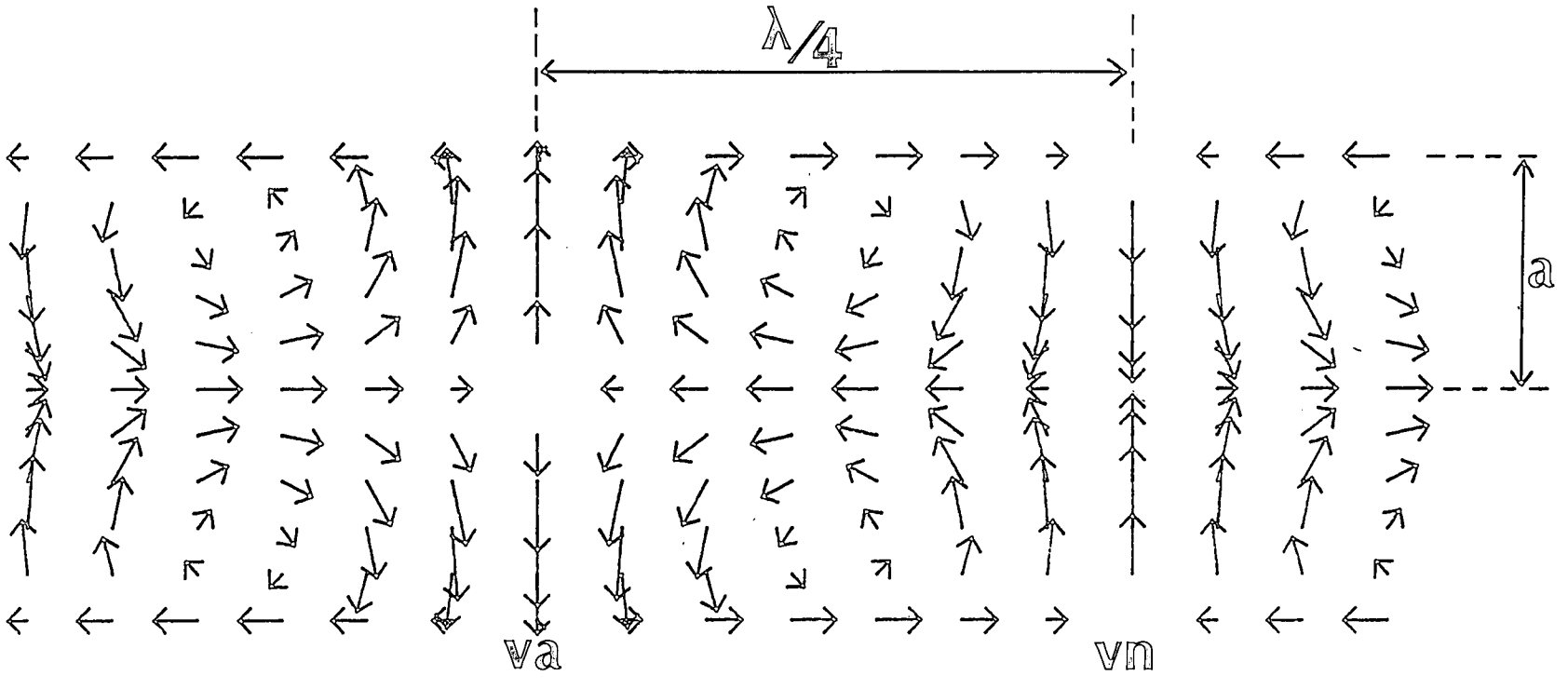

Figure 6.3.1. Form of Rayleigh streaming in a circular tube of radius a. The length of each arrow is proportional to the velocity at that point. va = velocity antinode, vn = velocity node. (The boundary layer at the tube edge is neglected).

and to deduce that the velocity across the tube, perpendicular to the axis, takes the form (neglecting the boundary layer)

$$u_s = u_w(x)\left(1 - \frac{2s^2}{a^2}\right) \qquad 6.3.3.$$

where a is the tube radius and s the distance from the tube centre.

Strictly speaking this result only holds for very low Reynolds numbers ($R_e < 1$) where one can neglect inertial terms in the Navier - Stokes equation [Lighthill 1978a]. However, Keefe (1983) has shown that this is not a precisely rigorous requirement provided the streamtubes of the flow are not too curved.

Note also that, using the well known equations relating acoustic pressure and velocity (Chapter 2.), it is possible through equations 6.3.2 and 6.3.3 to deduce the streaming velocity at any point in the tube by measuring the pressure.

6.4. PARTICLE IMAGE VELOCIMETRY. (P.I.V.)

P.I.V. is a relatively recent photographic method for measuring fluid velocity [Dudderar & Simpkins 1978] and relies on photographing, under intermittent illumination, small particles contained in and faithfully following the flow under investigation. The technique arose from speckle photography, the well known solid body deformation measurement technique [Dainty 1975] and P.I.V. is still occasionally called speckle velocimetry. This is however rather a misleading term because the generation of true speckle relies on the coherent illumination of a microscopically rough body to produce a complex interference pattern in the space around the body. P.I.V. relies purely on photographing particle images and does not in fact require the illuminating light to be coherent [Bernabeau et. al. 1982] though lasers are generally used because they provide high light density in an easily controlled form. A schematic diagram of a P.I.V. system is shown in figure 6.4.1. Light from a laser is expanded into a sheet and projected into the flow. The laser is then pulsed (either by Q-switching or chopping the beam) so that successive

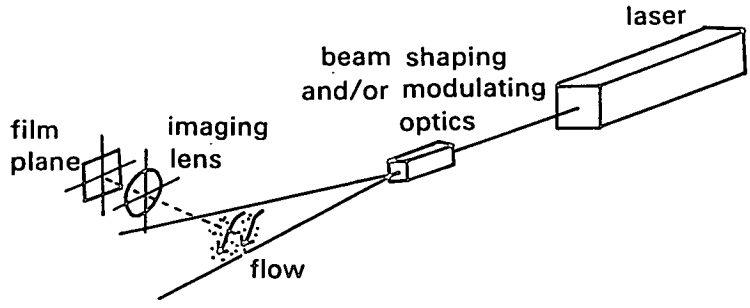

Figure 6.4.1. Schematic diagram of P.I.V. system.

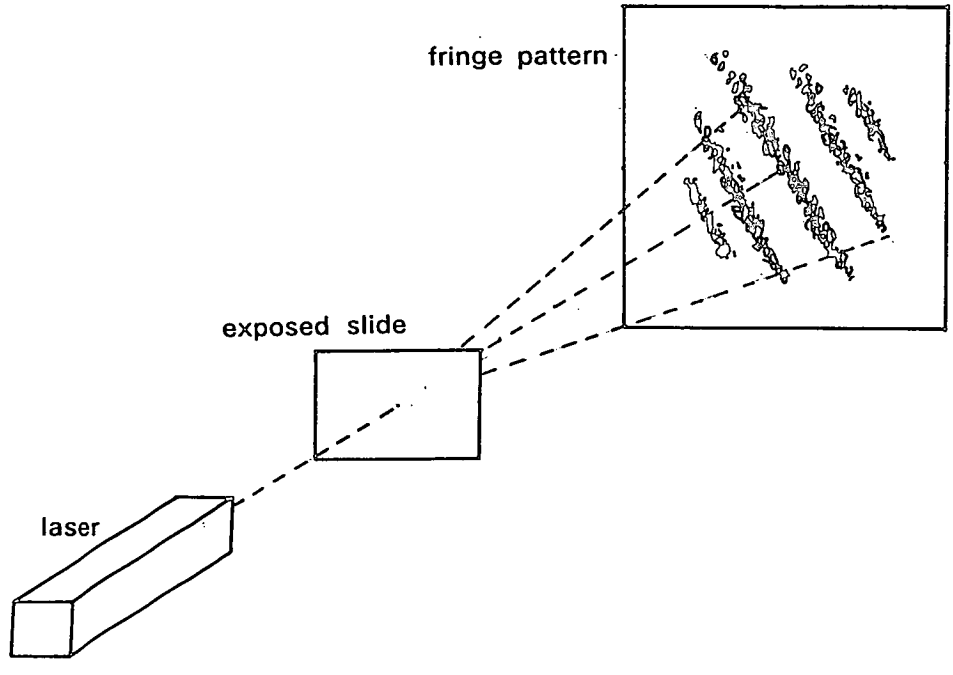

Figure 6.4.2. Production of P.I.V. fringes.

particle images are recorded on the film plane of a camera placed at right angles to the expanded sheet of laser light.

The velocity information is then recovered by ascertaining the separation of the particle images on the film plane. This can be done by either observing the film directly using a microscope or, more commonly, by interrogating each point on the film using a low power laser beam to produce, in the far field diffration zone, a series of fringes analagous to those produced in the Youngs double slit experiment (figure 6.4.2.). The distance between the fringes is inversely proportional to the particle image separation at that point on the film and their orientation is perpendicular to the flow direction (to within a 180° ambiguity). Knowing the magnification of the camera and the time between the light pulses it is then an easy matter to deduce the local flow velocity.

As may be appreciated, if the particle images are too close then the fringes will be so far apart so that perhaps only one will be visible or, if the images are too far apart, then the fringes will be too close to be resolvable. Such limitations on the dynamic range of the technique have been discussed previously [Meynert & Lourenco 1984] though a convenient rule of thumb is that, on the film plane, the particle images should be separated by approximately 0.1 mm. It is necessary therefore (if one wants to avoid much tedious work) to be able to estimate roughly the range of velocities in the flow under investigation.

Since a typical region needing analysis can contain from say fifty to several hundred points it is necessary in practice to analyse the fringes automatically. This is most commonly done by capturing the fringe pattern using a video camera and frame grabber and using a computer to extract the velocity information. Such a system has been developed at our institution [Gray & Greated 1988a] and there are many publications describing the speed etc. of

various implementations of the technique e.g. [Robinson 1983, Erbeck 1985, Huntley 1986]. In our implementation the slide is automatically scanned using a computer controlled micropositioner, the fringes at each point captured using a video camera and the velocity information extracted using a two-dimensional Fast Fourier Transform.

6.5. P.I.V. THEORY.

In this section we introduce briefly the theoretical background to P.I.V. This will aid us later when discussing the limitations of the technique and will also allow us to highlight the analogies that can be drawn between L.D.A. and P.I.V.

First imagine a small area of the flow over which the velocity is constant and which is photographed to produce on the developed film images of the particles in the flow. Under a single exposure (one pulse from the laser) there will be a random distribution of particles. Under a double exposure this random pattern is displaced by an amount proportional to the velocity of the flow. Our task is to deduce the separation of the particles.

As said above, this can either be done directly by observing the slide and calculating the separations (most conveniently done by calculating the image intensity autocorrelation function) or indirectly by illuminating the area with coherent light to produce (by the Wiener - Khinchine Theorem) the Fourier transform of the image intensity autocorrelation function (the fringe pattern). This can then be re-transformed to get back to the autocorrelation function. The indirect approach is of course faster due to the speed of the Fast Fourier Transform algorithm.

To put all this on a more mathematical footing we note first that, under a single exposure, the size of the particle images is measured by the image intensity autocorrelation function.

$$R_p(x) = \langle I(r_i)\, I(r_i + x) \rangle \qquad 6.5.1.$$

where r_i is the position of the ith particle. The <> brackets indicate ensemble averaging and will be used to distinguish this two-dimensional case from the one-dimensional case of chapter 4 where the expectation operator E[] was used.

If two exposures are made, between which the particles move a distance ξ then the total irradiance falling on the film and hence the image intensity is given by

$$I(r_i - \xi/2) + I(r_i + \xi/2) = I(r_i) * \amalg(\xi) \qquad 6.5.2.$$

where * denotes convolution and $\amalg(\xi)$ is the symbol introduced by Bracewell (1986) to denote two delta functions separated by ξ

$$\amalg(\xi) = \frac{1}{2}\left(\delta(x - \xi/2) + \delta(x + \xi/2)\right) \qquad 6.5.3.$$

Note that in 6.5.2. we are neglecting constant factors such as the exposure time and scattering efficiency of the seeding particles. The autocorrelation function of the transparency then becomes

$$R_T(x) = \langle I(r_i) * \amalg(\xi) \times I(r_i + x) * \amalg(\xi) \rangle \qquad 6.5.4.$$

which on expansion and simplification becomes

$$R_T(x) = 2\left\{ R_p(x) + R_p(x) * \amalg(2\xi) \right\} \qquad 6.5.5.$$

Then, taking the Fourier transform of both sides and using the convolution theorem we get

$$\mathcal{F}(R_T(x)) = 2\mathcal{F}(R_p(x)) + 2\mathcal{F}(R_p(x)) \times \mathcal{F}(\amalg(2\xi)) \qquad 6.5.6.$$

$$= 2\mathcal{F}(R_p(x))[1 + \cos 2\pi\alpha] \qquad 6.5.7.$$

where α is a measure of the spatial frequency. We see immediately that equation 6.5.7. has a form identical to that for the laser Doppler fringe intensity (equation 4.2.1.). The cosine term represents the particle spacing information in which we are interested while the multiplying term represents the statistics of the particle size distribution. For example, if the particles all gave identical circular images then the $\mathcal{F}(R_p(x))$ term modulating the fringes would be an Airy disc. Or, if the particles had a random distribution in size then the envelope would be (by the central limit theorem) a Gaussian. Removal of this low frequency term (which can sometimes swamp the fringe frequency when there is a low fringe density [Pickering & Halliwell 1984]) is a recurrent problem in P.I.V. and is compounded by the noisiness of the fringe images due to the use of coherent light (true speckle!). In our fringe analysis system [Gray & Greated 1988a] following Huntly (1986) an average halo is collected from all points of the P.I.V. slide and is subtracted from each fringe pattern. Processing then proceeds by two-dimensional FFT. We note that in practise more than two exposures may be used so that multiple images are obtained on the film plane. This has the effect of sharpening the fringe pattern and increasing the fringe visibility (c.f. using multiple slits or a diffraction grating as opposed to just two slits in Young's experiment).

6.6. P.I.V. EXPERIMENTAL APPARATUS.

A diagram of the experimental setup for recording the P.I.V. images is shown in figure 6.6.1. Light from a 32 mW He-Ne laser (λ=633nm) was expanded

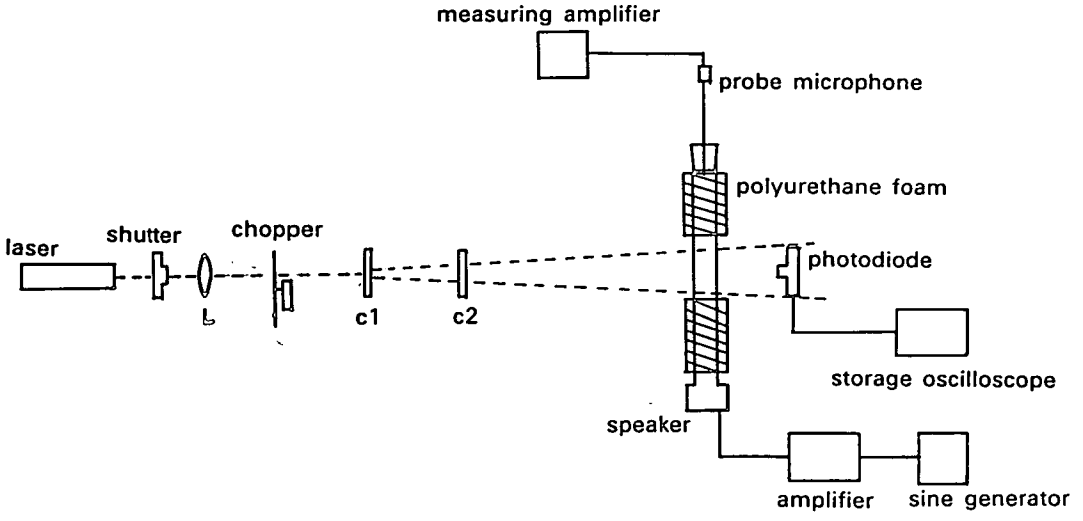

Figure 6.6.1. Apparatus used to acquire P.I.V. photographs (see text).

using a circular lens, L, and the two cylindrical lenses C1 and C2 to produce a thin sheet of light which, when it entered the tube through the axis, was approximately two centimeters high and 1/2 mm thick. A chopper, which was a rotating disc with a slot cut in it, was placed at the focus of L and produced the pulses of light while a shutter placed just before L dictated the number of pulses that got through. This use of an external shutter, rather than the shutter on the camera, was employed to reduce vibration in the film plane to a minimum. Although the chopper (Scitec Model 300 CD) came complete with an electronic readout to indicate the frequency of rotation of the disc, it was found that at the low speeds required for this experiment the readout was unreliable and so an external photodiode was connected to a storage oscilloscope to give an accurate measure of the pulse separation and duration.

The camera, a 35mm Nikon with a 50mm flat focus lens at a magnification of 0.773, placed at right angles to the sheet of light, recorded the P.I.V. photographs. It was found necessary to use a flat focus lens if one wanted to avoid distortion in the off-axis region. The film used was Kodak T-Max 400 which provided good sensitivity (400 ASA) with adequate resolution (~100 lines/mm, depending on contrast). The picture was always taken against a black background to increase contrast and during experimental runs the laboratory was only illuminated with extremely subdued light.

The amount of distortion in the image plane due to the curvature of the glass tube was estimated by putting a piece of graph paper in the tube, photographing it, and examining the developed film with a travelling microscope. A negligible amount of distortion was found except at approximately 1 mm or so from the tube wall. Since, as it turned out, the amount of flare from the wall of the tube tended to make any measurements in this region impossible anyway it was not necessary to calculate correction factors for this effect.

using a circular lens, L, and the two cylindrical lenses C1 and C2 to produce a thin sheet of light which, when it entered the tube through the axis, was approximately two centimeters high and 1/2 mm thick. A chopper, which was a rotating disc with a slot cut in it, was placed at the focus of L and produced the pulses of light while a shutter placed just before L dictated the number of pulses that got through. This use of an external shutter, rather than the shutter on the camera, was employed to reduce vibration in the film plane to a minimum. Although the chopper (Scitec Model 300 CD) came complete with an electronic readout to indicate the frequency of rotation of the disc, it was found that at the low speeds required for this experiment the readout was unreliable and so an external photodiode was connected to a storage oscilloscope to give an accurate measure of the pulse separation and duration.

The camera, a 35mm Nikon with a 50mm flat focus lens at a magnification of 0.773, placed at right angles to the sheet of light, recorded the P.I.V. photographs. It was found necessary to use a flat focus lens if one wanted to avoid distortion in the off-axis region. The film used was Kodak T-Max 400 which provided good sensitivity (400 ASA) with adequate resolution (~100 lines/mm, depending on contrast). The picture was always taken against a black background to increase contrast and during experimental runs the laboratory was only illuminated with extremely subdued light.

The amount of distortion in the image plane due to the curvature of the glass tube was estimated by putting a piece of graph paper in the tube, photographing it, and examining the developed film with a travelling microscope. A negligible amount of distortion was found except at approximately 1 mm or so from the tube wall. Since, as it turned out, the amount of flare from the wall of the tube tended to make any measurements in this region impossible anyway it was not necessary to calculate correction factors for this effect.

6.7. MEASUREMENTS AND RESULTS.

The apparatus was set up as indicated in figure 6.6.1. Sound of frequency 2460 Hz was introduced into the tube (length 450 mm, internal diameter 23.3 mm) using a horn loudspeaker with the horn removed. The tube was sealed at the other end with a rubber bung which had a tightly fitting metal plate attached to its inside face to ensure a rigid termination. The sound field thus corresponded to the 7th normal mode of the air column. A probe microphone, (Bruel & Kjaer type 4166 with 2 mm i.d. probe attachment) inserted through the rigid end monitored the pressure. The probe microphone had previously been calibrated to within 0.5 dB using an acoustic coupler. Although the intensities required to produce streaming were near the limits of the microphone's range [Bruel & Kjaer Data Handbook 1982.] they were still within the 10% distortion limit - leading to a possible error of around 1 dB. So, although the pressure measurements were not highly accurate they did provide a useful independent check on the streaming velocities.

Tobacco smoke was introduced into the tube to provide the seeding particles and streaming was set up, the field having a pressure of 151 dB (re 20 μPa) at the rigid end. Because of the limited dynamic range of the P.I.V. technique (see section 6.4.) the streaming velocity was first estimated by eye and the chopper then set to provide pulses with a separation of 0.114 seconds and duration 0.0057 seconds. It is necessary to have the ratio of pulse separation to duration so large because if the particle displacements and separations are of a similar order, they will give rise to similarly sized contributions in the spatial frequency domain which will lead to a loss of velocity information. Also, since the time between pulses is much shorter than any relevant time scale for the flow, the velocity measurement is essentially instantaneous. Such details of the technique are well discussed in Meynert & Lourenco (1984). The shutter, set to 0.5 second, allowed 4 pulses through.

Photographs were taken near a velocity node and a print of the film used to provide the measurements quoted here is shown in figure 6.7.1. The individual particle images can be clearly seen. In fact, measurements could not be made far from the velocity nodes because, at the frequencies and intensities used here, the vibrational displacement amplitudes became of the same order as the particle displacements required to give fringes. This is quite an important point and will be returned to and discussed at some length in section 6.7.

The film was analysed in the fashion indicated in section 6.4. It is clear from figure 6.7.1. that not all areas of film yielded a velocity measurement, due either to flare from the tube walls or uneven seeding. The latter is a problem in all P.I.V. measurements and seems to be more difficult to overcome in air than in water. Perhaps this is due to the larger convective currents found in air, coupled with its lower viscosity.

The measurements were transferred to a computer which, after interpolating missing points and smoothing the velocities using a third order Chebyshev interpolation routine, drew a velocity map (see figure 6.7.2.). As can be seen, the measurements look slightly asymmetric with the velocities in the upper left vortex seeming to sweep over too much to the right. This was probably due to outside air currents. As a check on the accuracy of the measurements it is noticed from equation 6.3.3. that the axial velocity should be parabolic across any section of the tube with maximum velocity given by equation 6.3.2. and zeroes at distances r=0.707a from the axis of the tube. Axial velocities were therefore computed from the original unsmoothed data for three separate lines across the tube a few millimeters from the velocity node (figure 6.7.3.). The solid parabolae were fitted using the measured velocity maxima and the theoretical zero points. The fits are quite good though the velocities do show some deviation near the left crossover point, reflecting the assymmetry mentioned earlier. A calculation using equation 6.3.2. and a value

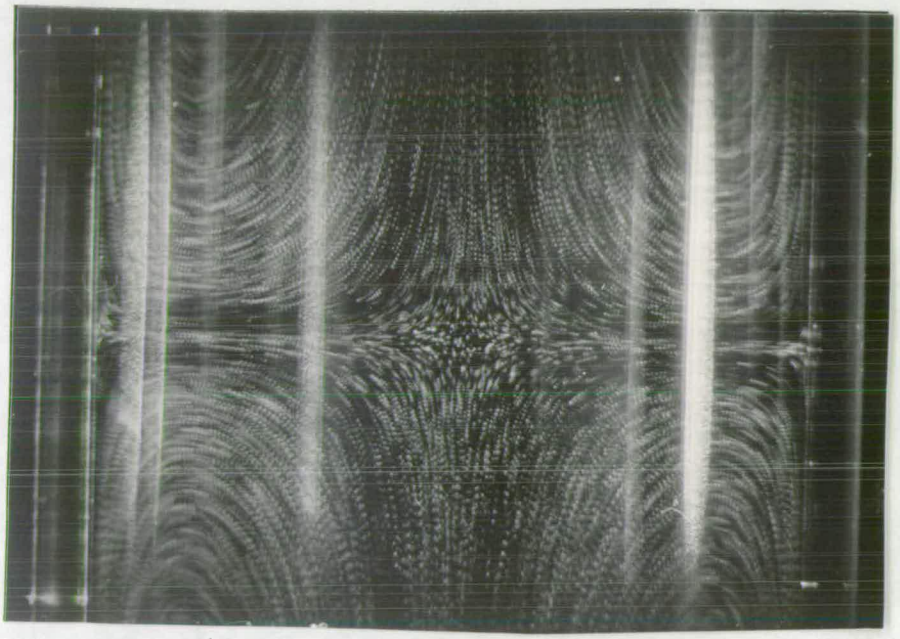

Figure 6.7.1. Print of P.I.V. transparency used to provide measurements. The individual particle images can be clearly seen.

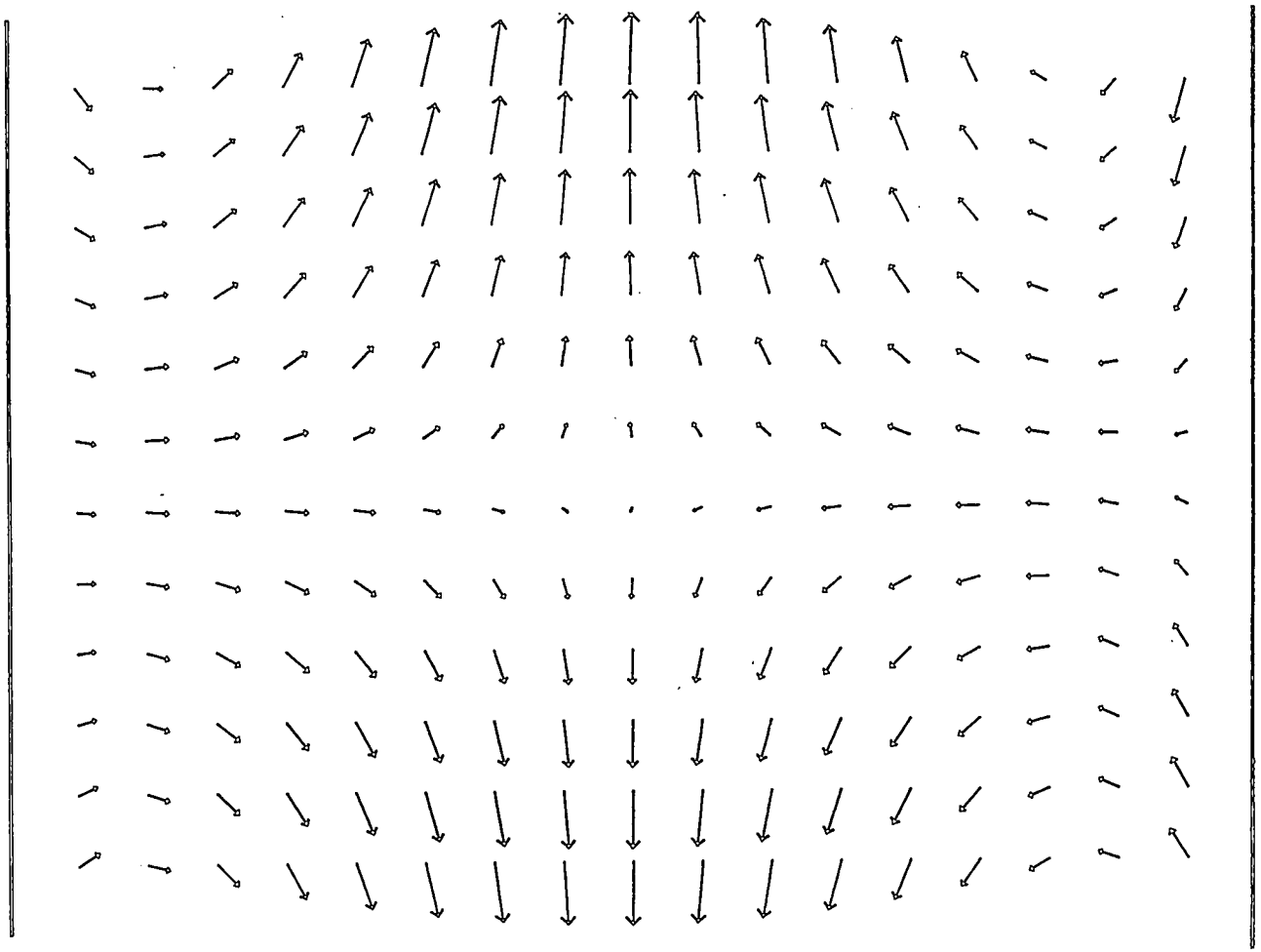

Figure 6.7.2. Velocity map. (1 cm = 4.37 mm/s).

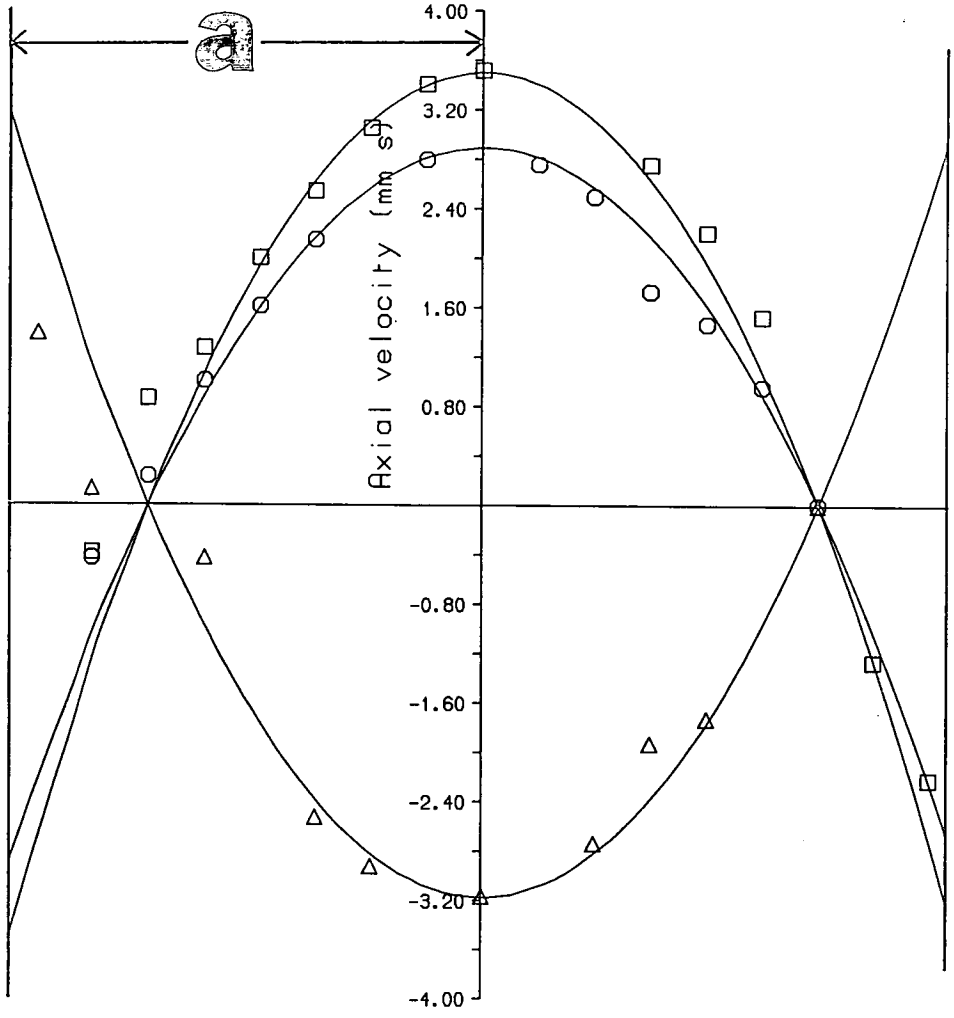

Figure 6.7.3. Experimentally deduced axial velocities in the tube (symbols) and theoretical curves.

of 151 dB for the maximum pressure indicates a maximum slip velocity of ~6.5 mm/s, giving the corresponding maximum axial velocity a few millimeters from the velocity node to be of the order of 3-4 mm/s - in agreement with figure 6.7.3. The cross sectional velocity measurements agree with the theoretical curves to within about 10% in the region of the central return velocity but deteriorate in the outer regions. This is due not only to extraneous air currents but to the fact that small positional errors in the interrogating laser beam lead to large velocity errors because of the large velocity gradient in these regions. Inaccuracies also occur due to the finite area of the interrogating laser beam. That is, in regions where the seeding is quite sparse the particle images which produce the fringe pattern may not lie, on average, at the centre of the laser beam which is where the velocity is taken to be measured. The measured velocities in figure 6.7.3. also show significant scatter about the theoretical lines and this reflects a basic problem in P.I.V.: because the measurement is taken effectively instantaneously effects such as particle diffusion and random particle distributions which can upset an individual velocity measurement are not averaged out. It is impossible thus to assign a statistical measure (in terms of these effects) to each separate velocity. It is however possible to assign a measure in terms of the point's nearest neighbours because we know that in this case the flow is continuous. This is the justification for using the velocity smoothing routine mentioned earlier.

6.8. DISCUSSION AND CONCLUSIONS.

It has been demonstrated that P.I.V. can accurately measure acoustic streaming effects; an area that cannot be tackled using conventional probe devices. Also, in contrast to the more common optical technique of Laser Doppler Anemometry (L.D.A.), it can measure "instantaneously" over a whole field. To make the type of measurements described here using L.D.A. would require a

two component L.D.A. system, a carefully controlled environment to prevent changing ambient conditions from upsetting the streaming over the time (many hours) that would be required to make the measurements and some method of traversing the L.D.A. measuring volume accurately to each point in the flow.

There are however several limitations to the P.I.V. technique. Firstly, any flows measured must be essentially two-dimensional: if there is too much out of plane motion then the particle images will become decorrelated and no velocity information can be extracted. Secondly, and just as importantly for acoustic streaming, if the vibrational displacement of the sound field becomes too large then it can effectively swamp the velocity displacement images (the particle images become streaked and overlap). Such an effect was noticed in this work (section 6.7.) Furthermore, in regions not too far from the velocity node the streaking of the particles causes the circular halo in which the fringes are confined to become elongated and outer lobes to become visible, an effect of the $\tilde{\mathfrak{I}}(R_p(x))$ term in equation 6.5.7. (see figure 6.8.1.). This can have serious implications for the fringe analysis system since, in our implementation, an average circular halo is subtracted from each fringe pattern in order to remove low frequencies which could otherwise swamp the fringe frequency [Gray & Greated 1988a]. Clearly it is impossible to define such a halo if it changes for different portions of the film. We get round this problem by instructing the computer to make measurements on successive lines perpendicular to the tube axis across which the vibrational amplitudes are constant. The computer can then gather an average halo from each of these lines and use it to remove the low frequencies for that line.

In fact, because the particles move more slowly at the extremities of their displacements and hence scatter off more light from these positions, the particle images are not just streaked but are somewhat dumbell shaped (this is

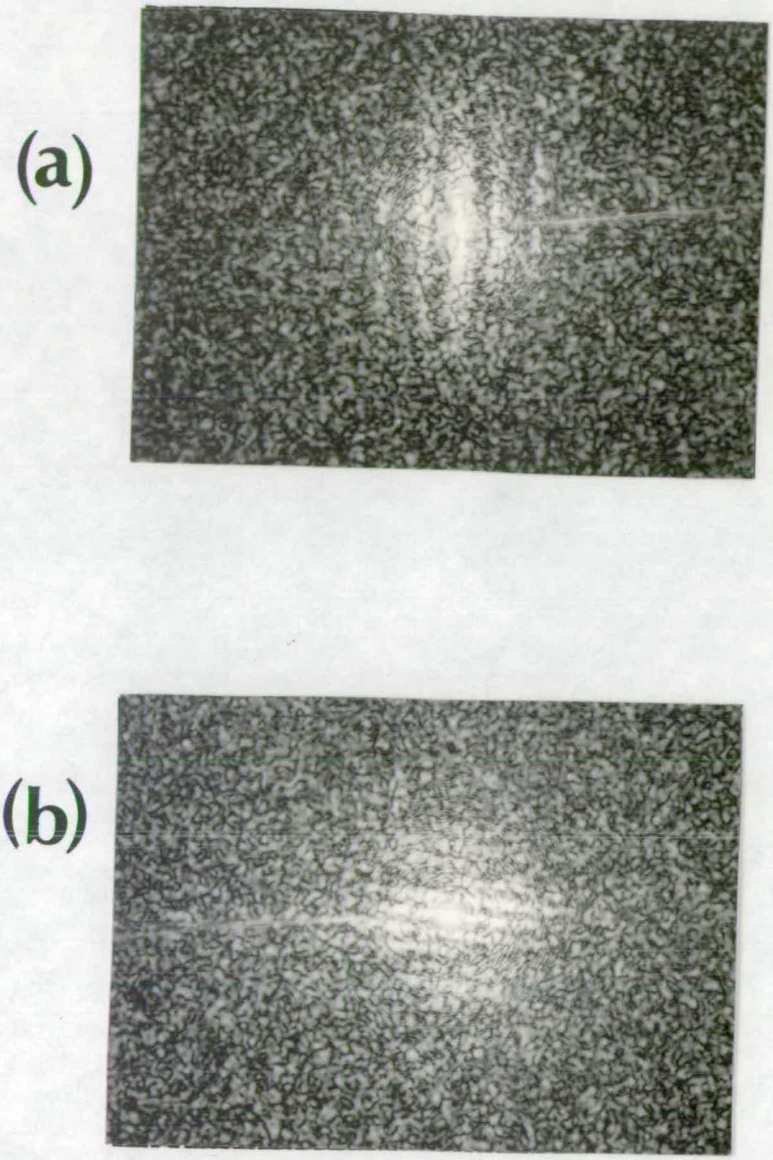

Figure 6.8.1. P.I.V. fringe patterns. (a) acquired near velocity node and (b) acquired away from node, showing the appearance of lobes due to streaking of the particle images.

nicely shown in Brandt *et. al.* (1937)). The halo, in the direction parallel to the particle oscillations, then takes the form of a squared zero order Bessel function from which it would be possible to estimate the magnitude of the particle displacements [Tiziani 1971]. Such estimates would however probably be of quite low accuracy and such measurements would perhaps be of little practical use anyway. It may however be of interest to note that, knowing the sound field and the particle's density, it would be possible in principle to deduce the particle sizes from their displacement amplitudes.

We see therefore that we are faced with a similar problem as in L.D.A. In that case (c.f. Chapter 4.) the zero order Bessel function in the temporal autocorrelation function due to the oscillatory motion was multiplied by a cosine term when a flow was present. Now, in P.I.V., when we wish to measure the flow, we find a (squared) zero order Bessel function modulating the fringe pattern in the Fourier Transform of the spatial autocorrelation function.

A way round the above problem would be to pulse the laser fast enough to "freeze" the particle images, the pulse former being triggered from the sound field to capture the images at the same phase positions. To illuminate the particle for say 1/10 of its period would require, for frequencies of the order we have here, laser pulses lasting only small fractions of a millisecond. This would then require (if we scale up the intensities used here) laser powers of the order of several watts. Such lasers are not uncommon though their use does entail certain difficulties and hazards. It may be noted however that more effective use can be made of available laser light by employing scanning beam technology [Gray & Greated 1988] or by using more sensitive films and sacrificing resolution.

However, despite these limitations the technique should be of considerable interest both to acousticians and fluid dynamicists. It may also be noted that

in other areas the technique would perhaps not suffer from the aforementioned difficulties. For example, in the regions of much higher frequencies, say 20 kHz upwards, the vibrational amplitudes can become quite small though the streaming effects are very large [Lighthill 1978a , Bergmann 1938].

Chapter 7: Discussion and Conclusions.

7.1. RESUMÉ OF WORK DONE.

The main achievements of this project may be summarised as follows:

1. After a brief introduction to acoustics and laser Doppler anemometry a critical examination is made of the factors affecting the laser Doppler measurement of acoustic velocity fluctuations.

2. A rigorous derivation of the photon correlation function is presented for the case of periodic and noisy sound fields. It is shown how the parameters of the acoustic velocity field may be extracted from the observed correlation function. A gating technique, which may be used to measure the phase difference between the acoustic velocity and pressure, is described and the effect this gating can have on the correlation function is detailed.

3. Experiments are described which verify the above theory and the limits of the technique are assessed. Measurements of the complex impedance of an open tube are shown to give good agreement with theory.

4. Observations made in connection with the measurement of complex impedance lead to consideration of acoustic streaming and the realization that particle image velocimetry could be applied to the measurement of this phenomenon. The technique is applied to the case of Rayleigh streaming and the measured velocities are shown to give good agreement with theory.

Laser Doppler anemometry and particle image velocimetry have thus been proved capable of performing accurate measurement on a useful and interesting range of acoustic phenomena.

7.2. LIMITATIONS OF THE TECHNIQUES.

The L.D.A. technique is somewhat limited in several respects. Firstly, there is the restricted dynamic range. With the apparatus described in chapter 5 one can measure from roughly 95 to 130 db in a 1000 Hz sound field. The lower limit can be decreased however by decreasing the fringe spacing (recall the

argument in chapter 3 relating fringe spacing and displacement of the scattering particles). This can be achieved both by increasing the intersection angle of the beams and using light of shorter wavelength. For example, using say a wavelength of ~ 0.45 μm and an intersection angle of 60° gives a fringe spacing of ~ 0.45 μm and the lower limit of measurement as ~ 86 db for a 1 kHz field. This is perhaps a practical lower limit of measurement since it is difficult to obtain laser light of shorter wavelength and also, obtaining such a large intersection angle produces its own problems such as non-paraxiality of lens systems and difficulties of conveniently introducing the measuring volume to the area of interest.

The problem of raising the limit of the technique is not quite so fundamental since one can reasonably easily make the structure of the light pattern through which the scattering particles pass as large as required.

Then there are the complications due to any superimposed flows in the sound field. This was discussed in chapter 4 but no work was done to see how acoustic parameters could be extracted from the correlation function. This would probably be quite an interesting area of study and will certainly have to be tackled if the L.D.A. system is to find widespread use in acoustic measurement.

Also, in the system we have used in this project, velocities were only measured in one dimension. This was not a limitation for the essentially planar sound fields studied here but for a totally unknown sound field several measurements would have to be taken at each point. Alternatively, a two or three component L.D.A. system could be used though this dramatically increases the complexity (and price) of the apparatus.

Another point, not explicitly mentioned so far, is that an optical path must be provided to the area where acoustic measurement is to be made. If one

wanted to make measurements in musical instruments, say, then special transparent sections would have to be constructed.

A limitation which was not fully investigated in this project was the gating technique. It was mentioned in chapter 5 that it can be difficult to deduce the flow velocity when the duration of the gating pulse is small - this being due to the damping effect of the gating process. It was also mentioned how the problem could be got round by using extra electronic circuitry. However, when the gating pulse is very small, very little light gets through to the photodetector and it can take a prohibitively long time to build up a correlation function (over a minute as opposed to a few seconds without gating). This further slows down the already rather tedious gating procedure because, to make the measurements described in section 5.4.3. at least five or six correlograms must be recorded in order to accurately reconstruct the time history at *each* phase point. The process could be speeded up by using an on-line computer to the correlator. This facility was not however available during the present work.

For the reasons given above the author sees the technique, in its present form, more as a research tool than as a tool for routine "industrial" measurement in the manner of conventional fluid velocity measuring laser Doppler systems. Applications could include laboratory measurement of specific sound fields of special interest or the technique could be used as a calibration standard in national standards laboratories. Also, because the technique is more suited to sound in the higher intensity range, applications would probably be more easily found in these regimes. This could include, for example, measuring the sound field near a jet engine for diagnostic or environmental purposes.

The limitations of the P.I.V. technique were largely noted and discussed in

chapter 6 but we can briefly recap here by noting the need for a certain amount of *a priori* information about the flow under investigation. This is because of the limited dynamic range and two dimensionality of the technique. For measurement of large flow fields large lasers are also needed - increasing the cost and hazardousness of the system.

7.3. PROPOSED FURTHER WORK

There are several directions in which the work undertaken in this project could be extended. On the L.D.A. side the technique could be refined by interfacing the correlator to a computer and investigating the best way to extract information from the correlation function. This could include the use of curve fitting or high resolution spectral estimators and investigation of the technique when steady flows are present. It would be very interesting to apply the technique to some practical measurements, for example, measurement of the input impedance of brass musical instruments or the sound field near loud industrial machinery. This latter sound field would perhaps be of some interest in connection with the measurement of band limited noise since the noise from say a jet engine could be thought of as a dominant tone with a certain amount of noise pollution round it. Another interesting area of study would be an investigation of the boundary layer when acoustic fields are adjacent to walls. This is a phenomenon which can really only be investigated using optical probes since material probes would probably upset the flow too much.

The P.I.V. technique perhaps offers even more scope for further work. Firstly, no complete statistical analysis has yet been offered relating the output from the P.I.V. system (the fringe pattern) to the parameters of the flow (density of seeding particles, presence of velocity gradients, turbulent flows etc.). There could also be a lot more work done on the image analysis side of the technique. We saw in chapter 6 how the Fourier transform based image

analysis algorithm failed when the particle images became streaked due to the amplitude of the acoustic particle displacements. We got round the problem in a rather *ad hoc* way but it should be possible to devise more robust algorithms – perhaps based on pattern recognition principles. Further work could also include extending the technique to three dimensional flows. Some work has already been done in this area using holographic and stereoscopic methods [Royer 1988, Gauthier & Riethmuller 1988] but these techniques still suffer from considerable drawbacks.

It would be interesting to use P.I.V. to look into acoustic streaming in more detail – as mentioned before little quantitative experimental work has been done in this area. At present there is also a growing interest in the application of ultrasonic techniques for industrial machining, mixing etc. Since ultrasonic fields can induce powerful streaming effects without large particle displacements, P.I.V. should be ideally suited to making measurements in these velocity fields. The author feels that this could be an area of considerable academic and commercial interest.

Appendix A: Streaming from an acoustically excited capillary tube.

It was seen in chapter 5 that some form of jet or streaming motion seemed to be produced from the tip of the capillary tube used to provide the acoustic excitation in the impedance measurements. This was thought worthy of further investigation and, in fact, led on to the work of chapter 6. Here we will discuss how the effect came to be recognised as a phenomenon of non-linear acoustics and a qualitative explanation will be offered for it.

In order to study the phenomenon more closely a capillary tube (i.d. 1mm) was attached through a rubber bung to a horn loudspeaker which had the horn removed (Figure A1). With the sound intensity turned up a stream of air could easily be felt coming from the tip of the capillary. This jet, which was strong enough to blow out a candle, varied in strength not only with the sound intensity but also with frequency with the frequencies of maximum jet strength appearing to coincide roughly with the expected resonance frequencies of the tube. Visualising the flow using tobacco smoke and a sheet of laser light revealed that it took the form illustrated in figure A1. That is, the flow took the form of a central jet with recirculating vortices.

In order to study this more closely a similar capillary was attached to an air pump and the air flow adjusted until it felt roughly the same as that from the sound induced flow. When the jet due to the pumped air was visualised no vortices were observed, except those set up occasionally by entrainment of adjacent fluid. Also the smoke became diluted or dissipated vey quickly unlike in the acoustic case where the jet and vortices remained visible for several

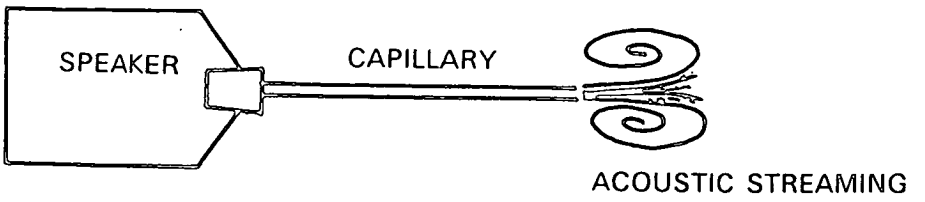

Figure A.1. Production of acoustic streaming due to sound emitted from the tip of a capillary tube.

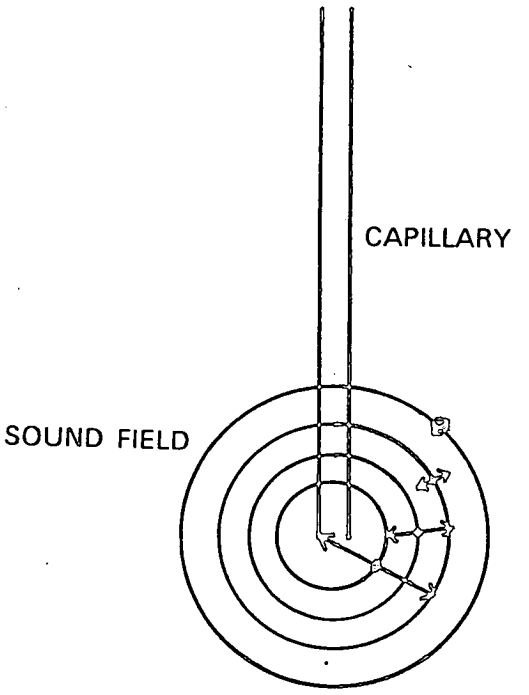

Figure A.2. Spherical sound field round the capillary tip. The double headed arrows represent the magnitude of the acoustic velocity.

minutes. This all implied that a more complex dynamical situation than just some pumping mechanism was at work. The tips of both capillaries were then placed underwater. That attached to the air pump immediately began to vigorously blow bubbles but the other did not. In fact, the small plug of water drawn up into the acoustic capillary was sufficient to stop the streaming while shaking it out restored the jet. This implied that the streaming was due to the sound field interacting with the outside medium or the capillary boundary layer and led us to consider the radiation pattern of the emitted sound field.

If the air column in the capillary is oscillating so that the at the capillary exit the air can be thought of as a small oscillating piston, then the radiation pattern in such a situation is governed by the parameter ka where k ($=2\pi/\lambda$) is the wavenumber and a the capillary radius. For the typical frequencies used here ($\sim$1kHz) and a=0.5mm, $ka << 1$ which implies [Kinsler *et. al.* 1982] that an almost perfect spherical wave is being emitted i.e. the capillary tip was behaving as a point source. This was further tested in the anechoic chamber where it was found that the field intensity decreased with inverse distance squared i.e. in a manner consistent with the spherical wave assumption.

If we now consider how pressure and velocity are related in a spherical wave we see that, for distances close to the source, the acoustic velocity is given by [Kinsler *et. al.* 1982]

$$u \simeq \frac{P}{\rho_0 c k r}$$

where P is the pressure and r the distance to the source (c.f. eqn. 2.2.5.). Thus moderate acoustic intensities can generate large velocities close to the source. The acoustic field then takes the form illustrated in figure A2 where the arrows indicate the magnitude of the velocity.

Recalling the discussion of Rayleigh Streaming in chapter 6 we see that the velocity field could perhaps be generating the streaming through interaction with the capillary boundary layer. This was qualitatively tested by inserting the capillary tube into the standing wave tube used in chapter 6 so that its tip was near a velocity antinode. The streaming observed is shown in figure A3 (c.f. figure A2). Inserting a thin metal bar in place of the capillary caused identical streaming to be generated. Moving the tip of the bar to a velocity node caused the streaming to stop. Our supposition that the capillary streaming is a boundary layer phenomenon forced by the large acoustic velocities near the source of spherical waves thus seems to be correct.

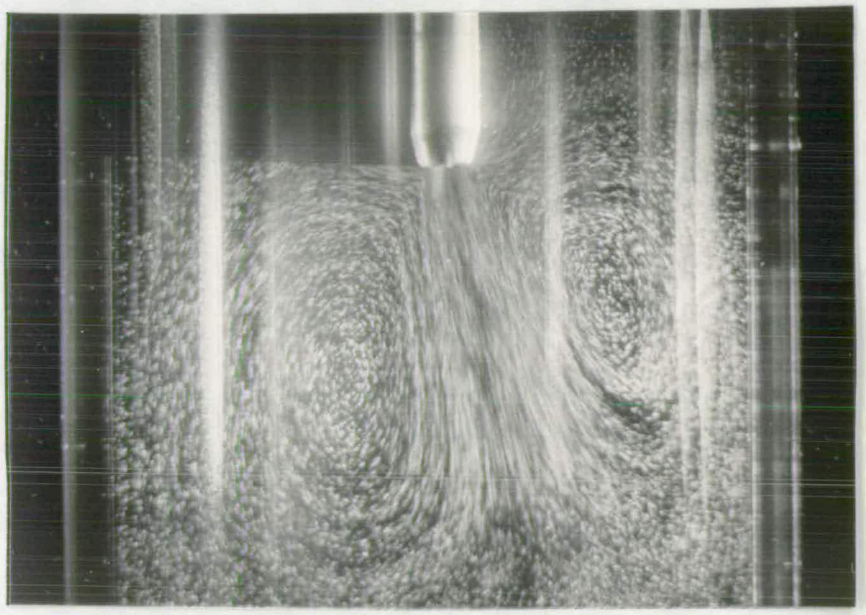

Figure A.3. Acoustic streaming due to a small tube being placed near a velocity antinode in a standing wave tube. Note that the streaming takes the form illustrated in figure A.1.

Appendix B: Input impedance of an open tube.

In chapter 5 use was made of a theoretical expression for the input impedance of an open tube. How this expression was derived was explained in chapter 2. Here we will derive the input impedance expression in another way and will go on to show how a frequency correction factor may be applied to measured impedance values when the pressure and velocity are measured in different planes.

Consider a circular tube of length L and radius a where L is much greater than the wavelength of any sound field we will examine and a is much smaller. Sound waves will therefore only propagate along the axis of the tube. A sound field is driven into one end through a capillary tube with the other end open. The impedance of the driven end is then large enough to justify the assumption that the driven end is closed. Then, neglecting radiation from the open end and assuming a pressure node at that end we can write the pressure at any point in the tube as

$$p(x,t) = A\left\{\exp i\left[\omega t + \underline{k}(L-x)\right] - \exp\left[\omega t - \underline{k}(L-x)\right]\right\}$$

$$= \frac{A}{2i}\,\sin\left[\underline{k}(L-x)\right]e^{i\omega t} \qquad B1$$

where A is the amplitude and ω the frequency of the sound field. $\underline{k}$ is the complex propagation constant, $\underline{k} = k + i\alpha$ where k is the wavenumber and α the attenuation coefficient. In equation B1 we have assumed that the load impedance is zero. This is not quite true for there is always a small radiation impedance. We can however take this into consideration by redefining the tube length to be $L' = L + 0.61a$, the well known end correction for an open tube [Kinsler *et. al.* 1982].

The velocity can then be written, using the so called linear inviscid force equation, as

$$u(x,t) = -\frac{1}{\rho_0}\int\left(\frac{\partial p(x,t)}{\partial x}\right)dt$$

$$= \frac{-\underline{k}A}{2\rho_0\omega}\cos\left[\underline{k}(L'-x)\right]e^{i\omega t} \qquad B2$$

where ρ_0 is the density of the air.

This gives for the input impedance, Z_i

$$Z_i = \frac{p(0,t)}{u(0,t)} = \frac{-\rho_0\omega}{i\underline{k}}\tan\left(\underline{k}L'\right) \qquad B3$$

Writing $\underline{k}$ in full and expanding the tangent gives

$$Z_i = \frac{\rho_0 c}{1-\frac{i\alpha}{k}}\left(\frac{\tanh\alpha L' + i\tan\alpha L'}{1 + i\tan kL'\tanh\alpha L'}\right)$$

$$\simeq \rho_0 c\left(\frac{\alpha L + i\tan kL'}{1 + i\alpha L\tan kL'}\right) \qquad B4$$

for $\alpha L << 1$. This is the same as equation 2.2.11. Examination of equation B4 shows that impedance maxima (resonances) occur for values of the wavenumber that satisfy

$$k = \frac{\pi}{L'}\left(n + 1/2\right) \qquad n = 1, 2, 3, \ldots$$

When, however, the pressure is measured at the input plane and the velocity is measured at a distance x along the tube, the impedance Z_{ix} is given by

$$Z_{in} = \frac{p(0,t)}{u(x,t)} = \frac{-\rho_0 \omega}{i\underline{k}} \left(\frac{\sin \underline{k} L'}{\cos [\underline{k}(L'-x)]} \right) \qquad B5$$

so that, in the absence of damping ($\alpha = 0$) resonances occur for values of the wavenumber, k', such that

$$k' = \frac{\pi}{L'-x} (n + 1/2) \qquad n = 1, 2, 3, \ldots .$$

So that

$$\frac{k'}{k} = \frac{L'}{L'-x}$$

$$\simeq (1 + x/L') \qquad \text{for } x \ll L \qquad B6$$

For the experimental situation described in chapter 5 this amounts to a correction of ~1% being applied to the frequencies at which the impedances were measured.

Neglecting the end correction for an open tube would have caused the calculated resonances to move by a smaller amount, ~0.4%, an amount that would have become more noticeable if measurements had been carried out at higher frequencies.

Appendix C: Publications.

The work undertaken in this project generated several reports and publications: the following is a list of articles which have either been published or accepted for publication.

- Easson, W. J., Griffiths, M., Sharpe, J. P. and Greated, C. A. (1986) "Measurement of fluid velocity and acceleration using pulsed correlation techniques." Proceedings of Electro-Optics and Laser U. K. 1986.

- Sharpe, J. P. & Greated, C. A. (1987) "The measurement of periodic acoustic fields using photon correlation spectroscopy." Journal of Physics D (Applied Physics.) 20 418-423

- Sharpe, J. P. & Greated, C. A. (1987) "Acoustic measurement using photon correlation spectroscopy." S.P.I.E. Vol. 808. (Inverse Problems in Optics.)

- Sharpe, J. P. & Greated, C. A. (1987) "Laser measurement of random and periodic sound fields." Proc. Inst. Acoust. 9(3) 183-191.

- Sharpe, J. P., Greated, C. A. & Campbell, D. M. (1989) "The measurement of complex acoustic impedance using photon correlation spectroscopy." To appear in Acustica 67(4).

- Sharpe, J. P., Greated, C. A., Gray, C. A. & Campbell, D. M. (1989) "The measurement of acoustic streaming using particle image velocimetry." To appear in Acustica 68(3).

The work described in the above papers has also been the subject of a cover story in the December 1987 issue of the technical magazine "Laser Focus."

DBI P2 HIRZEL 3 ACUSTICA SPALTEN ACU WK-4068-1
16.06.88 10:04:52

PROOF COPY.

The Measurement of Complex Acoustic Impedance using Photon Correlation Spectroscopy

by J. P. Sharpe, C. A. Greated, and D. M. Campbell
Fluid Dynamics Unit, Physics Department, Edinburgh University, Edinburgh, U.K.

□□□

1. Introduction

In acoustics one of the most important quantities that can be measured is the specific acoustic impedance, z, defined as the ratio of pressure to acoustic particle velocity,

$$z = \frac{P}{V}. \tag{1}$$

In dealing with the transmission of acoustic radiation in pipes or horns it is more convenient to use the acoustic impedance, Z, which is defined, for a fluid acting on a surface of area S, as the complex quotient of the pressure at the surface divided by the volume velocity at the surface [1].

$$Z = \frac{P}{U} \tag{2}$$

or

$$Z = |Z| e^{j\phi}, \tag{3}$$

where $|Z|$ is the impedance amplitude and ϕ the phase difference between the velocity and pressure. The specific acoustic impedance and impedance are thus related by,

$$Z = \frac{z}{S}. \tag{4}$$

The measurement of the acoustic pressure is easily accomplished using microphones but the measurement of velocity is much more difficult. A method which has been developed in recent years is the pressure gradient microphone [2, 3] which uses two closely spaced pressure microphones and transforms the pressure gradient between them into velocity using the equations of motion for the acoustic field. Such a device however requires calibration in frequency, assumptions to be made about the field under investigation, and the application of empirical correction factors depending on source proximity and directivity [4, 5]. Other methods such as hot wire anemometers [6] are difficult to calibrate and, like pressure microphones, can distort the field under investigation. Indirect methods of assessing acoustic impedance have also been devised, especially in the measurement of the input impedance of brass musical instruments where a constant volume velocity input is applied via a high impedance series resistance to the instrument mouthpiece. This makes it only necessary to measure the pressure at the input plane to deduce the impedance [7].

More recently the technique of Laser Doppler Anemometry (L.D.A.) has been applied to the measurement of acoustic velocities [8, 9, 10, 11]. The technique, which is both absolute and non-intrusive, has been shown to work well in the range of (plane wave) intensities of roughly 90 dB to 120 dB (re $10^{-12}\,\mathrm{Wm}^{-2}$) and up to frequencies of approximately 3 kHz [12].

In this paper the measurement of the input impedance for an open tube utilizing direct L.D.A. velocity measurement will be described. The theoretical impedance for this situation can easily be calculated and hence comparisons with the measured values made. Measurements are also made of the relative phase difference between the velocity and pressure, the aim being to demonstrate the applicability of L.D.A. to direct measurement of complex acoustic impedance.

2. Description of the L.D.A. technique

The L.D.A. technique relies on the scattering of light from small particles contained in, and faithfully following, the flow under investigation. This light is then collected and analysed to reveal the parameters of the flow. It has been shown [8, 13] that, for the case of tabacco smoke particles in air, the particles will faithfully follow the flow up to frequencies of the order of 10 kHz. The frequencies under investigation in this paper are well within this regime.

In the most common L.D.A. setup (which is used here) a laser beam is split into two beams which are focussed down to intersect in the flow. At the point of intersection a fringe pattern is set up which the particles in the flow pass through. Light scattered from this region is then collected and the resulting signal analysed in either the time or frequency domains, the various techniques being well documented in the literature, e.g. [14].

In our experiments we use the photon counting correlation technique which operates in the time domain. This employs a photomultiplier to collect the light and send the digital signals to a correlator which counts the number of photons arriving in small time intervals and calculates the autocorrelation function of the signal.

For the case of sinusoidal oscillations the form of the autocorrelation function has been deduced by us [11] and takes, to a good approximation, the form of a zero order Bessel function. The velocity amplitude of the fluctuation can be calculated by counting the number jof points on the correlogram up to the first minimum of this Bessel function and applying the formula

$$a_m = \frac{3.832}{D s \tau}. \tag{5}$$

where a_m is the velocity amplitude, τ is the sample time (the time between points on the correlogram), s is the number of points up to the first minimum of the Bessel function, and D is the frequency to velocity conversion factor which depends only on the wavelength of the laser light and the intersection angle of the beams. The method is fully described in [11] and a typical correlogram is shown in Fig. 1.

In order to determine the phase of the velocity with respect to the pressure we have also developed a gating technique [11, 15] which works as follows: The signal from a microphone in the sound field is sent to a microcomputer which detects the positive-going zero-crossings of the pressure signal. The computer then sends a pulse of predetermined width and at a predetermined delay time from the positive-going zero-crossings to the photomultiplier. Only for the duration of this pulse is the Doppler signal analysed so the photomultiplier only "sees" a small portion of the fluctuation at a specific time delay where the velocity is approximtely constant. A phase shifting device incorporated into the optics of the setup allows the direction of the velocity to be determined. Thus by varying the delay time, it is possible to reconstruct the velocity curve and hence its phase with respect to the pressure signal.

It should be noted of course that to implement the L.D.A. technique an optical path must be provided into the sound field to allow access for the laser beams and for collection of the scattered light. Thus, if one wanted to make measurements in say the throat of a trumpet, a specially made transparent section would be required.

Other workers [8–10] have used a frequency domain method for analysing the Doppler signal. We consider, however, that the photon correlation technique is faster and more robust and it is capable of dealing with the low level of scattered light generally found in air flows.

3. Experimental apparatus

A diagram of the apparatus used for the acoustic impedance studies is shown in Fig. 2 with a closeup of the measuring area in Fig. 3.

Light from a 32 mW He-Ne laser ($\lambda = 633$ nm) is split into two beams which, after passing through the phase shifter, are focussed down to a point on the axis of the tube using a 20 cm focal length lens. A small quantity of tobacco smoke was generally introduced into the tube for seeding purposes.

Sound from a speaker is fed through a capillary into a glass tube of length 1.512 m and internal radius 1.05 cm. A small baffle was constructed round the exit of the capillary to reduce the streaming which was observed to occur, especially at higher intensities. A Bruel & Kjaer $\frac{1}{2}$ inch microphone (type 4134), mounted in the input plane, measured the pressure and could also provide the signal for the gating pulses. The laser beam intersection was placed about 1.5 cm in front of the input plane. The velocity measurement point was not therefore exactly at the end of the tube but a calculation showed that the effect of this would be to cause the measured resonance frequencies to move up by a factor of $1 + x/L$, where x is the distance from the input plane to the velocity measurement point and L is the length of the tube. For our experimental setup this amounted to a correction of about 1% which was applied to the measured frequencies. Also, since the L.D.A. system effectively measures the acoustic particle velocity at the point of intersection, the velocities were converted to volume velocities by dividing by the cross-sectional area of the tube. No correction was made for the effect of the boundary layer when calculating the volume velocity since even at the lowest frequency used (50 Hz) this only amounted to a correction of some 5% to the velocity [7] which decreased rapidly as the frequency increased. In a more elaborate experimental setup (see section 6) this correction factor would be automatically computed at each frequency where measurements were taken. The temperature in the laboratory was maintained at $26\ ^{\circ}C \pm 1\ ^{\circ}C$.

4. Measurement of impedance amplitude ($|Z|$)

Measurements of $|Z|$ were carried out at varius frequencies in the range of about 50 Hz to 700 Hz by making separate measurements of the pressure and velocity. Pressure measurements were made in the input plane with the microphone which had been calibrated to within 0.5 dB. The recorded sound pressure level (SPL) was then converted to pascals using the formula [16]

$$\text{PRESSURE (Pa)} = 10^{\left[\frac{\text{SPL}-94}{20}\right]}. \tag{6}$$

For the velocity amplitude measurements the gating circuit and phase shifter were made inactive and the amplitudes deduced using eq. (5). Each particle velocity amplitude measurement was then converted to r.m.s. volume velocity and combined with the pressure measurements at that frequency to yield $|Z|$ which is expressed in acoustic ohms.

A theoretical impedance curve for the tube was calculated using the method of [6]. This considers the tube in analogy with a terminated transmission line of length l with distributed loss so that the input impedance can be written as [17]

$$Z_i = Z_0 \left| \frac{Z_L \operatorname{Cosh} \Gamma l + Z_0 \operatorname{Sinh} \Gamma l}{Z_0 \operatorname{Cosh} \Gamma l + Z_L \operatorname{Sinh} \Gamma l} \right|, \tag{7}$$

where Z_0 is the characteristic impedance and Z_L the terminating (load) impedance. Γ is the propagation constant which is generally complex and equal to $\alpha + \mathrm{i}\beta$, where α is the attenuation coefficient and β the wavenumber. It is then possible, knowing the form of the load impedance and by making the "large" tube approximation, to deduce the following simplified form for the input impedance,

$$Z_i = Z_0 \frac{\alpha l + \mathrm{j} \tan \beta l'}{1 + \mathrm{j}\, \alpha l \tan \beta l'}, \tag{8}$$

where $l' = l + 0.61\, a$. a being the internal radius for the tube.

This expression was used to compute values for the impedance amplitude and phase. Values for constants such as the viscosity and speed of sound in air at various temperatures are to be found in [18]. The theoretical curve and experimental points for the impedance are shown in Fig. 4.

The error bars were computed assuming a 0.5 dB error in the microphone measurements and that the velocity could be measured to about 2%. A fuller discussion of errors will be deferred to section 6.

5. Measurement of phase (ϕ)

In order to demonstrate the measurement of phase, a region of frequency about 170 Hz was chosen, this corresponding to the region of an impedance peak. Measurements were taken at 155, 165, 170, 175 and 180 Hz using the following procedure:

At the frequency selected the pressure signal was sent to the microcomputer which detected the positive-going zero-crossings of the pressure signal and generated a pulse of width 500 μs. The delay time was incremented in units of 500 μs and at each point a measurement taken of the velocity. This process was repeated until at least one whole cycle of the pressure (and hence velocity) fluctuation had been covered. It was thus possible to reconstruct the velocity curve with respect to the delay time and hence deduce its phase relative to the pressure signal. An example of pressure signal and pulses is shown in fig. 5, while Fig. 6 shows typical velocity versus delay time points.

Although we did not have the facilities for calibrating the microphone for phase, it was possible to estimate the phase response using the literature supplied by Bruel and Kjaer [19]. Applying this to the velocity versus delay time curves allows the phase difference between the pressure and velocity to be deduced. The experimental points and theoretical phase curve (computed using equation 8) are shown in Fig. 7.

The error bars were obtained by estimating the accuracy with which the phase difference between separate velocity versus time delay curves could be deduced. In the present paper estimation of the phase difference was done by simply sketching the curves on graph paper, though it should not be difficult to implement a computer curve fitting routine in order to improve the accuracy. This will be discussed more fully in section 6.

6. Conclusions

As can be seen from Fig. 4 the theoretical and measured impedances agree very well, the main source of error coming from the pressure measurements. The velocity accuracy could be improved if an on-line computer link to the correlator was available to interpolate between points on the correlation function. The effect of turbulence and non-zero mean motions on the correlation function have not been mentioned since they are small and would only contribute a damping to the correlograms which does not affect the position of the minimum of the Bessel function to any great extent.

The phase measurements are subject to the dual inaccuracy of fitting a curve to the velocity versus delay time points and then estimating the phase of this curve. As mentioned before this process was done by hand though it could easily be adapted to run on a computer. Furthermore, the actual gating process used causes unwanted side effects on the correlation function [15] i.e., the correlogram is damped and rides on a sloping baseline. This is due to the fact that the input signal is gated and it makes the deduction of the velocity somewhat difficult. It is however possible, using a more sophisticated correlator (we use the basic Malvern K7023), to gate the signal internally and eliminate this problem. Again, an on-line computer link would speed up the process.

It may be mentioned here that, as yet, no complete stochastic model has been offered to quantify rigorously the limits of applicability of the technique. In our earlier work [11, 20] we used an extension of existing L.D.A. theory which seems to apply, while other researchers [7] have simply applied the well known equations of frequency modulation. The latter approach does not take into account the statistical nature of the scattering process. The problem is by no means trivial and is one on which the authors are at present engaged.

However, we have demonstrated that it is possible to measure complex acoustic impedances in a practical situation using direct measurement of velocity from a laser Doppler anemometer. Although the procedure described is somewaht tedious in application (especially the phase measurements), it can be automated by sending the individual correlograms to a computer where they can be processed and a direct readout given of velocity and phase. This currently being implemented and, although the technique will perhaps always be somewhat slower than using, say, constant volume velocity techniques, it is absolute and accurate, not relying on any assumptions about the sound field (except periodicity) or on any external calibrations. We feel it may provide a useful tool in a number of areas of acoustics ranging from the design of sound systems to the study of musical instrument mouthpieces.

Acknowledgements

This work is funded by the Science and Engineering Research Council and British Telecom. John Sharpe is also in receipt of a grant from the Department of Education for N. Ireland.

(Received September 14th, 1987.)

References

[1] Kinsler et al., Fundamentals of acoustics. John Wiley and Sons. New York 1982.

[2] Fahy, F. J., Measurement of acoustic intensity using the cross-spectral density of two microphone signals. J. Acoust. Soc. Amer. 62 [1977], 1057–1059.

[3] Chung, J. Y., Cross-spectral method of measuring acoustic intensity without error caused by instrument phase mismatch. J. Acoust. Soc. Amer. 64 [1978], 1613–1616.

[4] Bruel & Kjaer Technical Review No. 4 [1982], Sound Intensity (Instrumentation & Applications).

[5] Bruel & Kjaer Technical Review No. 4 [1985], Validity of Intensity Measurements.

[6] Pratt, R. L. Elliott, S. J., and Bowsher, J. M., The measurement of the acoustic impedance of brass instruments. Acustica 38 [1977], 236–246.

[7] Backus, J., Input impedance curves for the reed woodwind instruments. J. Acoust. Soc. Amer. 56 [1974], 1266–1279.

[8] Taylor, K. J., Absolute measurement of acoustic particle velocity. J. Acoust Soc. Amer. 59 [1976], 691–694.

[9] Taylor, K. J., Absolute calibration of microphones by a laser Doppler technique. J. Acoust. Soc. Amer. 70 [1981], 939–945.

[10] Davis, M. R. and Hews-Taylor, K. J., Laser Doppler measurement of complex acoustic impedance. J. Sound Vib. 107 [1986], 451–470.

[11] Sharpe, J. P. and Greated, C. A., The measurement of periodic acoustic fields using photon correlation spectroscopy. J. Phys. D. 20 [1987], 418–423.

[12] Sharpe, J. P. and Greated, C. A., Laser measurement of random and periodic sound fields. Proc. Institute Acoustics 9 [1987], 183–191.

[13] Brandt, O. et al. Z. Phys. 104 [1937], 511–533.

[14] Durrani, T. S. and Greated, C. A., Laser systems in flow measurement. Plenum Press, New York 1977.

[15] Easson, W. J., Griffiths, M., Sharpe, J. P., and Greated, C. A., Measurement of fluid velocity and acceleration using pulsed correlation techniques. Proceedings Electro-Optics and Laser U.K. '86, 1986.

[16] Morse, P. M., Vibration and sound. McGraw-Hill, New York 1948.

[17] King, R., Transmission line theory and its applications. J. Appl. Phys. 14 [1943], 577–600.

[18] Benade, A. H., On the propagation of sound waves in a cylindrical conduit. J. Acoust. Soc. Amr. 44 [1968], 616–623.

[19] Bruel & Kjaer, Condenser microphones and microphone preamplifiers for acoustic measurement. B & K Data Handbook, 1982.

[20] Sharpe, J. P. and Greated, C. A., Acoustic measurement using photon correlation spectroscopy. Proc. S.P.I.E., Vol. 808 (Inverse Problems in Optics), 1987.

Fig. 1. Typical correlogram indicating velocity amplitude of 24 mm/s. Sample time (τ) = 5.5 μs.

Fig. 2. Schematic diagram of apparatus.

Fig. 3. Close up of measuring section.

Fig. 4. Theoretical impedance curve and experimental points.

Fig. 5. Pressure signal and pulses. Frequency = 170 Hz, pulse width = 500 μs, delay time = 1000 μs.

Fig. 6. Typical velocity vs. delay time points. (o) 155 Hz, (o) 175 Hz.

Fig. 7. Theoretical phase curve and experimental points.

Proceedings of The Institute of Acoustics

LASER MEASUREMENT OF RANDOM AND PERIODIC SOUND FIELDS

J.P. Sharpe and C.A. Greated

Physics Department, Edinburgh University, Edinburgh.

ABSTRACT

In this paper the application of Laser Doppler Anemometry (L.D.A.), which is both absolute and non-instrusive, to the measurement of acoustic particle velocities is described. Reasons for the photon correlation method of signal analysis are outlined and a gating technique, which allows the relative phase of the velocity and pressure to be deduced is described.

INTRODUCTION

To obtain a full description of a sound field at any point the pressure, velocity and phase relationship between the two must be determined. The pressure is quite easily measured using microphones but velocity measurements are considerably more difficult. Several methods have been proposed of which one of the more recent is the pressure gradient microphone [1,2]. Such methods suffer however from the need for calibration, the application of empirical correction factors depending on distance from the sound source etc. and the fact that they intrude into and hence distort the field.

The technique of L.D.A. though can overcome these difficulties [3,4]. It provides an absolute measurement of the velocity and, since it relies on the scattering of light from very small particles suspended in the medium under investigation, it is essentially non-intrusive. The actual experimental arrangements of L.D.A. systems are numerous, as are the methods for analysing the intensity fluctuations of the scattered light [5]. In this work the Gaussian crossed beam setup employing the photon correlation method of signal analysis is used. The photon correlation method is best suited to the low density of scattering particles generally available in air flows and also seems to be more robust and versatile than say frequency tracking systems.

In this paper we present results for the form of the correlation function due to periodic, and band limited noise fields and discuss the form of the correlation function when the Doppler signal is gated.

Measurements made in a travelling wave tube are presented and compared to those made with a microphone. Further extensions of the work are proposed and limitations of the technique discussed.

Proceedings of The Institute of Acoustics

LASER MEASUREMENT OF RANDOM AND PERIODIC SOUND FIELDS

REVIEW OF L.D.A. TECHNIQUE

L.D.A. relies on the scattering of light from small particles suspended in, and faithfully following the motions of the fluid under investigation.

In the Guassian crossed beam setup light from a laser is split into two beams which are then focussed down to a point in the fluid (see Fig. 1). At he intersection of these two beams a fringe pattern is set up, as shown.

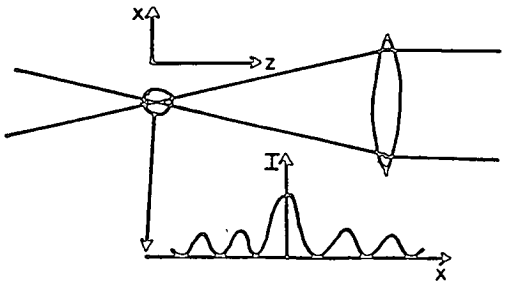

Figure 1. Production of L.D.A. fringe pattern. I is light intensity.

Particles passing through this pattern will scatter light in a manner depending on their velocities and the geometrical form of the fringe pattern. Thus it is possible to deduce the fluid velocity by collecting the scattered light and analysing it. The method of analysis is dictated by the density of seeding particles in the fluid, parameters of the flow to be measured and various other factors. Photon correlation (which analyses signals in the time domain) is found to be easy to use though other workers have made measurements using frequency analysis systems [3].

THEORY

In this section is it stated how the velocity and average velocity amplitude of the sound field can be deduced from the observed characteristics of the correlation function. The effect of gating (to determine the phase relationship between the pressure and velocity fluctuations) on the correlation function is also described.

Periodic Sound Fields

It has already been shown [4] that the correlation function due to a sinusoidal oscillation with no mean flow takes the form

$$R(\tau) = A + B\, J_o(a_m D\tau) \qquad (1)$$

where A and B are constants, J_o is the zero order Bessel function a_m is the velocity amplitude of the vibration, D is the frequency to velocity conversion factor and τ is the lag time on the correlator. D depends only on the wavelength of the laser light used and the geometry of the L.D.A. system so it is possible to deduce the velocity amplitude of the sound field at any point by measuring some parameter of the autocorrelation function (we use the first minimum) and using the tabulated values of the Bessel function.

Another approach is to use the autocorrelation function for frequency modulation which is essentially what is happening here - the sinusoidal intensity distribution of the fringe pattern due to the laser beams is being modulated by the sinusoidal oscillations of the sound field. This yields [6]

$$R(\tau) = \frac{A_o}{2} J_o\left(2\mu \sin \frac{\omega_m \tau}{2}\right) \cos \omega_o \tau \qquad (2)$$

Where A_o is the amplitude of the frequency modulated signal, μ is the modulation index, ω_m is the frequency of the modulating signal and ω_o is the carrier frequency. For no mean flow ($\omega_o = 0$) and for

$\frac{\omega_m \tau}{2} \ll 1$ equation (2) reduces to equation (1). However the latter

condition does not always obtain in practice and affects the correlation function in the regimes of low intensity and high frequency. Discussion of this and possible remedies will be deferred until the conclusion.

Noise Fields.

The effect of narrow band noise on the autocorrelation function was studied because of the occurrence of this type of noise in many situations (e.g. resonance set up in ducts by noise). The correlation function was deduced by integrating the correlation function for a single tone sound field over the probability density function for the amplitude distribution of band limited white noise [7]. This gave the form of the autocorrelation function as a Gaussian and the average velocity amplitude of the sound field to be deduced as

$$\bar{a}_m = \sqrt{\frac{\pi}{2(D\sigma_n)^2}} \qquad (3)$$

where σ_n is the standard deviation of the correlogram.

LASER MEASUREMENT OF RANDOM AND PERIODIC SOUND FIELDS

The gating technique

To implement the gating technique the signal from a microphone in the sound field is fed to a microcomputer which supplies a pulse of preset width at a preset delay time from the zero upcrossings of the signal. These pulses are then fed to the photomultiplier and only for their duration is the Doppler signal analysed. Thus, by varying the delay time, the velocity at different portions of the acoustic cycle is sampled. Furthermore, by incorporating a frequency or phase shifting device into the optics the sign of the velocity can be deduced. This would then allow the phase relationship between the velocity and pressure to be determined.

The gating however affects the correlogram by causing it to be damped and ride on a sloping base line [°]. The degree of damping is increased as the pulse width is decreased and generally some compromise must be reached between damping of the correlogram and velocities to be sampled.

APPARATUS

A schematic diagram of the apparatus is shown in figure 2.

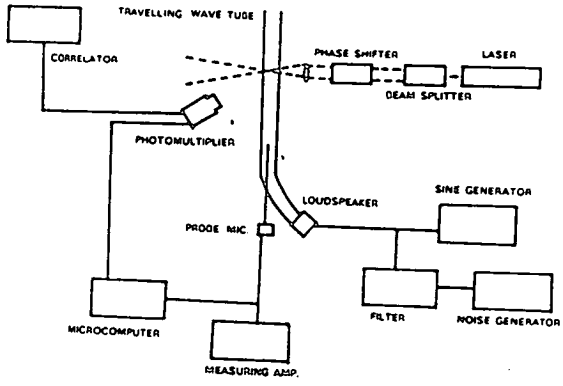

Figure 2. Diagram of apparatus.

The sound field is fed into a tube of length 1.5 m, diameter 2 cm, the final metre of the tube being filled with absorbing material to prevent the reflection of sound and hence the production of standing waves. A probe microphone could be inserted into the tube to monitor the sound field and thus make comparisons with the laser measurements. This arrangment was chosen because of the particularly simple relationship between the pressure and velocity fluctuations. The sound field could be chosen as either single tone

or band limited white noise.

On the optical side a 32 mW He-Ne laser was used. After splitting and passing through a phase shifter the beams were focussed down into the tube from a separation of 2 cm using a 200 mm focal length lens. A small quantity of tobacco smoke was generally introduced into the tube for seeding purposes.

MEASUREMENTS AND RESULTS

Periodic Sound Fields

To measure the velocity amplitude of a single tone sound field the microcomputer gating system and the phase shifter were made inactive. A sound frequency of 1260 Hz was used, the probe microphone having been calibrated at this frequency to an accuracy of about 0.5 dB. Figure 3 shows a typical correlogram and compares its estimate of the velocity amplitude to that of the probe microphone. It was found that over the range of sound intensity from about 95 dB to 120 dB the L.D.A. system and probe microphone agreed with each other to within about 5%.

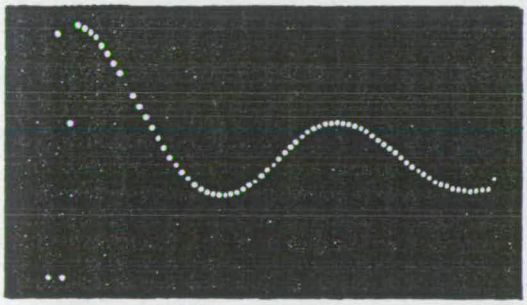

Figure 3. Correlogram due to 1260 Hz sound field.
Velocity amp from correlogram = 80.4 mm/sec.
From probe mic. = 80.6 ± 2 mm/sec. τ = 2μs.

Band limited noise field

For these measurements white noise was filtered about 1260 Hz and passed into the tube. A typical correlogram is shown in figure 4. These measurements showed rather more deviation than those for the single tone case, but this would have been expected considering the difficulty of estimating the standard deviation of the correlogram, the irregular pressure fluctuations in the tube and the fact that the microphone response is non-linear over frequency. All measurements however agreed to well within 10%.

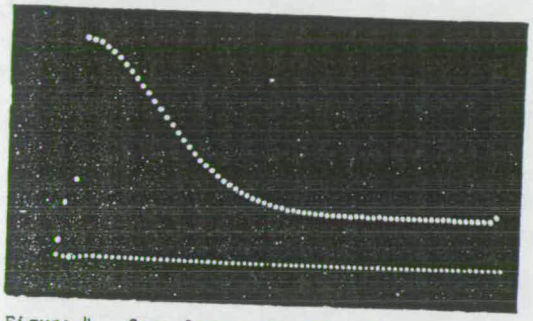

Figure 4. Correlogram due to noise filtered about 1260 Hz.
Average velocity amp. from correlogram = 51.2 mm/sec.
From probe mic. = 49.1 mm/sec. τ = 2μs.

Gating the sound field

These measurments followed the procedure outlined in the theory section. The sound frequency was again 1260 Hz and the phase shifter was set at 50 kHz. This later provided a velocity pedestal of 0.317 m/sec against which to measure the velocity at any particular position in the acoustic cycle. Figure 5 shows an oscillogram of the pressure and gating pulses while figures 6(a) and (b) show correlograms obtained using different delay times. Measurments such as these allowed the velocity time history to be plotted as in Figure 7. As can been seen the graph indicates a velocity ampliutde of about 85 mm/sec while measurements with ungated correlograms and the probe microphone indicated velocity amplitudes of 86 mm/sec and 85 mm/sec respectively. It is encouraging that the three procedures show such close agreement.

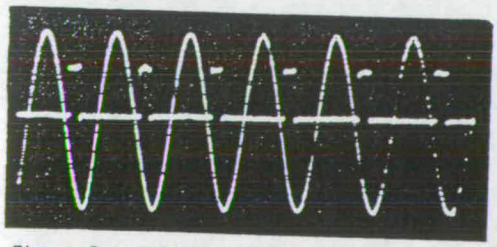

Figure 5. Gating pulses and sinusoidal pressure fluctuation.
Delay time = 400 μs. Pulse width = 100 μs.

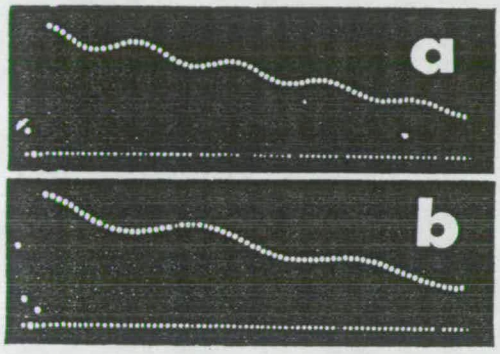

Figure 6. Gated correlograms for different delay times in 1260 Hz cycle. Frequency shift = 50 Hz. τ = 1μs. Pulse width = 100 μs. (a) Delay = 300 μs. (b) Delay = 700 μs.

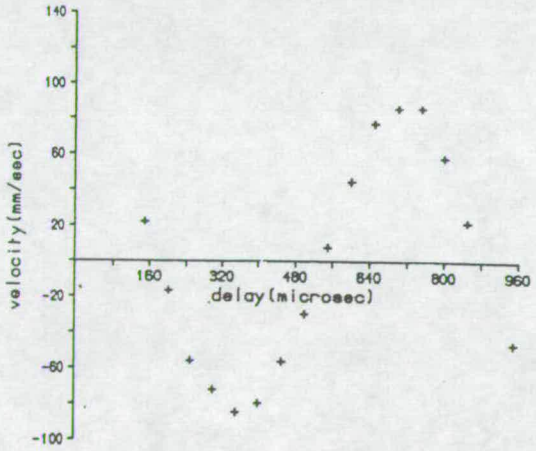

Figure 7. Velocity vs. delay time using gating technique.

LASER MEASUREMENT OF RANDOM AND PERIODIC SOUND FIELDS

DISCUSSION

It has been seen that L.D.A. can provide accurate measurement of acoustic velocity flutuations in the regime of intensities from about 90 dB to 120 dB. In itself this is quite useful but, as mentioned earlier, the method begins to fail at lower intensities and higher frequencies (~ 3 kHz). This is due to the $\omega_m\tau/2$ term in equation 2. For example, if intensity is low then the correlator lag time must be increased so that the first minimum of the Bessel function can be measured. This causes the correlogram to become modulated by the sin function (see fig. 8) and hence makes it difficult or impossible to estimate the velocity amplitude. This effect can be reduced to some extent

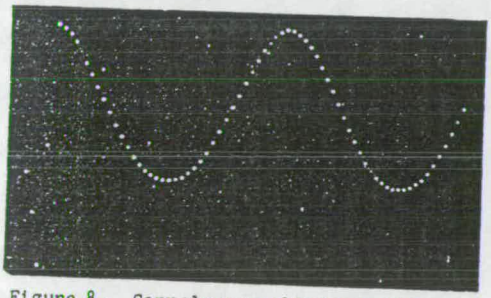

Figure 8. Correlogram obtained with τ = 20 μs.

by altering the optical arrangement (increasing the angle of intersecton of the beams) which would decrease the lower limits to about 80 dB. Higher frequencies have a similar effect on the correlogram. A possible solution to these problems may be tranformation of the correlogram into the frequency domain, a facility which is not at present available on our correlator.

It is imagined however that the technique will be of interest to laboratory acousticians and present research is directed towards measuring complex acoustic impedances using the gating technique. Further extensions of the work include the investigation of superimposed flow fields on the correlogram.

REFERENCES

[1] Fahy, F.J., "Measurement of Acoustic Intensity using the Cross Spectral Density of Two Microphone Signals". J.A.S.A. 62 (4) 1057-1059 (1977).

[2] Bruel and Kjaer Technical Review: No. 4, "Sound Intensity (Instrumentation and Application)", (1982).

[3] Davis, M.R., Hews-Taylor, K.J., "Laser Doppler Measurement of Complex Acoustic Impedance". Journal of Sound and Vibration, 107, (3) 451-470, (1986) and references.

[4] Sharpe, J.P., Greated, C.A. "The Measurement of Periodic Acoustic Fields using Photon Correlation Spectroscopy". Journal of Physics D (Applied Physics) 20.

[5] Durrani, T.S., Greated, C.A. "Laser Systems in Flow Measurement". Plenum Press (1977).

[6] Middleton, D. "An Introduction to Statistical Communication Theory". McGraw-Hill (1960).

[7] Sharpe, J.P., Greated, C.A. "Acoustic Measurement using Photon Correlation Spectroscopy". Proceedings S.P.I.E. Vol. 808 (1987).

[8] Easson, W.J., Griffiths, M., Sharpe, J.P. and Greated, C.A. "Measurement of Fluid Velocity and Acceleration using Pulsed Correlation Techniques". Proceedings Electro-Optics and Laser U.K. '86 (1986).

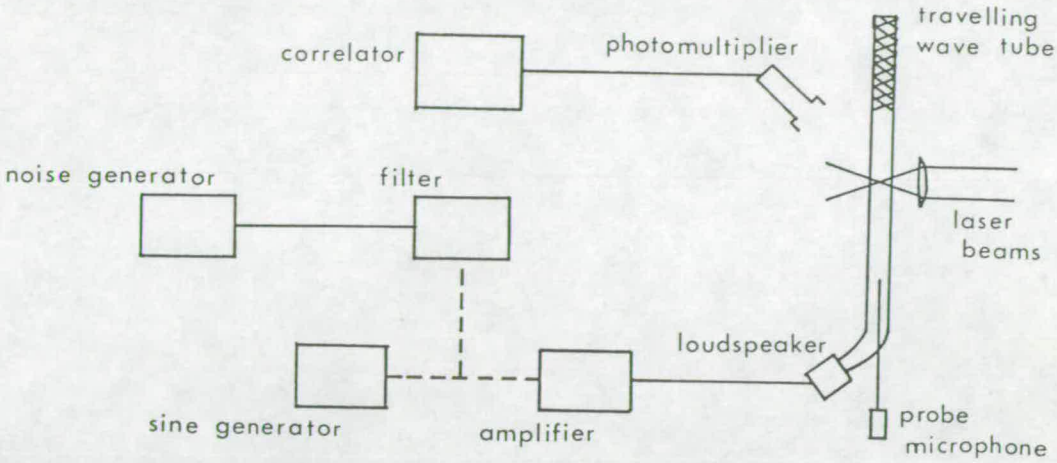

Figure 1. Schematic diagram of apparatus.

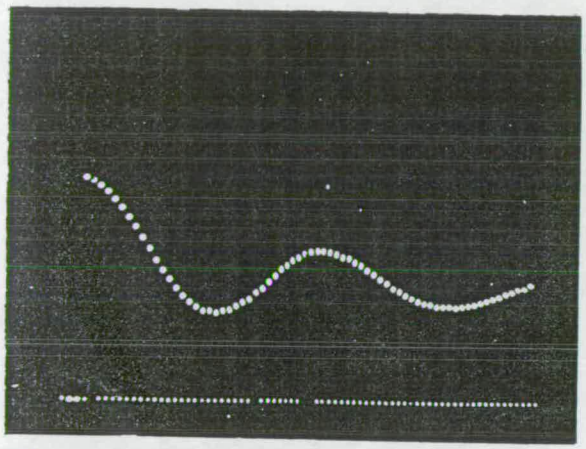

Figure 2. Correlogram obtained with 1260 Hz sound field. τ = 3μs.
Velocity amplitude deduced using correlogram = 64.3 mm/sec.
Velocity amplitude deduced using microphone = 63.3 mm/sec.

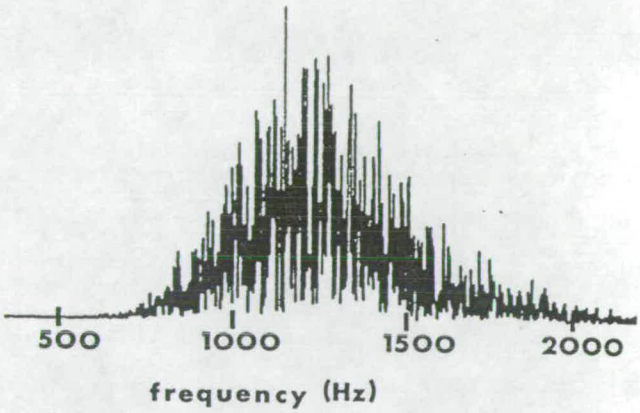

Figure 3. Spectrum of filtered noise.

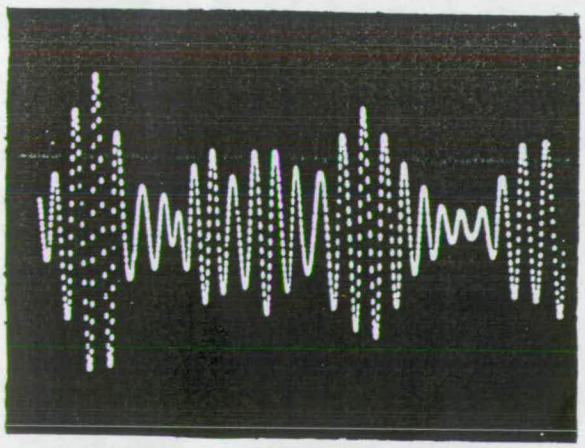

Figure 4. Time history of filtered noise.

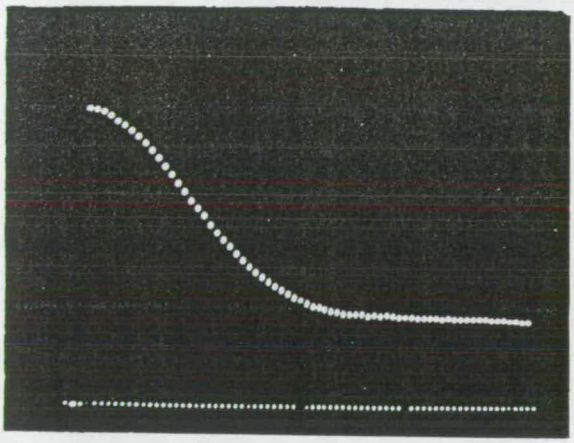

Figure 5. Correlogram obtained with noise field filtered about 1260 Hz. τ = 2μs.
Average velocity amplitude deduced using correlogram = 43.0 mm/sec.
Average velocity amplitude deduced using microphone = 44.8 mm/sec.

The velocity amplitude was deduced using, in the case of the correlogram, equation 2 and, in the case of the microphone, by measuring the pressure in the tube and converting to velocity amplitude using the assumption that the sound in the tube has a plane wave form.

Noise fields.

For the noise measurements white noise was band filtered about 1260 Hz and fed into the travelling wave tube. The spectrum of the filtered noise is shown in Fig. 3 while Figure 4 shows the time history of the filtered noise. A typical correlogram is shown in Figure 5 and in this case the velocity amplitude was estimated by estimating the standard deviation of the Gaussian. The velocity was determined from the probe microphone by measuring the average sound pressure and converting to velocity amplitude by assuming the major proportion of the sound excitation occured at 1260 Hz. It was found that the laser technique seemed to consistently under estimate the average velocity by a factor of about 5-10%. This is probably due to several factors including the effect of small amounts of turbulence in the tube which causes excess damping and the fact that the analysis assumes a perfect Rayleigh distribution for the velocity amplitudes.

Phase measurements.

In order to deduce the phase relationship between the pressure and velocity a gating technique was used. This involved programming a microcomputer to detect the zero up-crossing of the pressure fluctuations from the microphone and provide a pulse of predetermined width at a preset delay time after this event. This pulse was fed to the photomultiplier and only for the duration of the pulse was the Doppler signal processed. A phase modulating device, incorporated into the optics, provided a velocity pedestal allowing the sign of the acoustic fluctuation to be deduced. The technique has already been described[7,10] and at present is being used in attempting to measure complex acoustic impedances, an area of considerable practical importance.

Conclusion

It has been seen that photon correlation spectroscopy can provide an accurate measure o acoustic velocity amplitudes both for single tone and narrow band noise fields. The range of applicability and limitations of the technique are still being investigated especially with regard to very high and low intensity fields and in the regime of very high frequencie (~10 kHz) where slippage of the seeding particles will undoubtedly become a dominant effec

The measurement of acoustic impedances is also being investigated at the present time b utilizing the gating technique described elsewhere[7,10]. This allows the phase relationshi between velocity and pressure to be deduced.

It is forseen that the technique will be of considerable use to, for example, laborator acousticians since it provides direct, accurate and absolute measurement of acoustic veloc ity. Another area of possible use could be in environmental monitoring of noise though in this case a careful investigation of the effect of superimposed flows will have to be made

References

1. Fahy, F.J., "Measurement of Acoustic Intensity using the Cross Spectral Density of Two Microphone Signals". Journal of the Acoustical Society of America, 62, (4), 1057-1059 (1977).
2. Chung, J.Y., "Cross Spectral Method of Measuring Acoustic Intensity Without Error Caused by Instrument Phase Mismatch". Journal of the Acoustical Society of America, 64, 1613-1616, (1978).
3. Bruel and Kjaer Technical Review: No.4, "Sound Intensity (Instrumentation and Applications)", (1982).
4. Taylor, K.J., "Absolute Measurement of Acoustic Particle Velocity". Journal of the Acoustical Society of America, 51, 691-694, (1976).
5. Taylor, K.J., "Absolute Calibration of Microphones by a Laser Doppler Technique". Journal of the Acoustical Society of America, 70, 939-945, (1981).
6. Davis, M.R., Hews-Taylor, K.J., "Laser Doppler Measurement of Complex Acoustic Impedance". Journal of Sound and Vibration, 107, (3), 451-470, (1986).
7. Sharpe, J.P., Greated, C.A., "The Measurement of Periodic Acoustic Fields Using Photon Correlation Spectroscopy". Journal of Physics D. In press.
8. Middleton, D., "An Introduction to Statistical Communication Theory". McGraw-Hill (1960).
9. Tranter, C.J., "Bessel Functions with Some Physical Applications". The English Universities Press Ltd., (1968).
10. Easson, W.J., Griffiths, M., Sharpe, J.P. and Greated, C.A., "Measurement of Fluid Velocity and Acceleration using Pulsed Correlation Techniques". Proceedings Electro-Optics and Laser U.K. '86, (1986).

ω_m the frequency of the modulating signal and ω_o the carrier frequency. For zero carrier frequency (no mean flow) and small lag times

$$\left(\frac{\omega_m \tau}{2} \ll 1\right)$$

expression (3) reduces to the form of (1).

For the case of a noise field we consider band limited white noise. The velocity distribution will have a Gaussian form and, in the case of narrow band noise, the velocity amplitudes will have a Rayleigh probability density.

$$p(a_m) = \frac{a_m}{\sigma^2} \exp\left[\frac{-a_m^2}{2\sigma^2}\right] \tag{4}$$

where σ is the standard deviation of the velocity distribution. To obtain the autocorrelation function of the noise we integrate the autocorrelation function for a single tone field over this density.

$$R_{noise}(\tau) = \frac{B}{\sigma^2} \int_0^\infty a_m \exp\left[\frac{-a_m^2}{2\sigma^2}\right] J_o(a_m D \tau) da_m. \tag{5}$$

which evaluates to[9]

$$R_{noise}(\tau) = B \exp\left[\frac{-(D \tau \sigma)^2}{2}\right] \tag{6}$$

It is known that for Rayleigh distribution the mean value is equal to $\sigma\sqrt{\pi/2}$. Therefore we can write the average velocity amplitude $\bar{a}_m$ as

$$\bar{a}_m = \sigma \sqrt{\pi/2} \tag{7}$$

$$R_{noise}(\tau) = B \exp\left[\frac{-(D \tau \bar{a}_m)^2}{\pi}\right] \tag{8}$$

This has a Gaussian form in τ with standard deviation of say σ_n. Hence we can write

$$\bar{a}_m = \sqrt{\frac{\pi}{2(D\sigma_n)^2}} \tag{9}$$

The average velocity amplitude can thus be deduced by measuring the standard deviation of the correlogram.

Apparatus

A schematic diagram of the apparatus used is shown in figure 1. The measurements were carried out in a travelling wave tube of diameter 2 cm and length approximately 1.5 m. The sound field was introduced at one end using a loudspeaker and the tube was terminated throughout the last meter with absorbing material. This absorber prevented reflection of sound and the formation of standing waves. The termination was of course not perfect but for the case of the 1260 Hz sound wave used, the ratio of maximum to minimum sound pressures was less than 0.8 dB indicating a maximum phase difference between the velocity and pressure of around 5^0.

The laser used was a 32 mW He-Ne (λ = 633 nm) and the beams were focussed down from 2 cm apart using a 200 mm focal length lens. A small amount of tobacco smoke was usually introduced into the tube for seeding purposes. The probe microphone, which could be moved along the tube, had been calibrated to about 0.5 dB.

Measurements and results

Periodic sound fields.

In this case the sound field was derived directly from the sine generator, the noise generator and filter being made inactive. In Figure 2 a typical correlogram is shown.

Acoustic measurement using photon correlation spectroscopy

J.P. Sharpe, C.A. Greated,

Department of Physics, Edinburgh University, J.C.M.B., King's Buildings, Mayfield Road, Edinburgh, Scotland.

Abstract

An investigation of Laser Doppler Anemometry (L.D.A.) for the measurement of acoustic velocity fields using the photon correlation method of signal analysis has been made. It is shown how estimates of velocity amplitudes can be obtained for the cases of single tone and band limited noise fields. Measurements made in a travelling wave tube are presented and are shown to compare well with microphone measurements.

A discussion is also made of the measurement of complex impedances and possible industrial uses of the technique are mentioned.

Introduction

In order to obtain a complete description of a sound field the acoustic velocity, acoustic pressure and the phase relationship between the two must be determined. It is relatively easy to measure pressure using microphones but considerably more difficult to measure acoustic velocity. Methods in the past have included hot wire anemometers, Rayleigh Discs and, more recently, calculations from the pressure gradients between two closely spaced microphones[1,2]. All of these methods however intrude into the field and require the application of empirical correction factors depending on the frequency of the acoustic field, distance from the sound source etc.[3].

L.D.A. though can surmount these difficulties[4,5,6,7] and combining it with the photon correlation method of signal analysis makes the technique generally more suitable for the low density of scattering particles available in air flows.

Presented here are measurements made on both single tone and band limited noise fields in a travelling wave tube. This setup was chosen because the pressure and velocity fluctuations are both in phase and hence facilitate comparison of microphone and laser measurements. Results previously published were carried out in standing wave tubes[7]. The measurement of noise fields was investigated because of the widespread occurrence of this type of sound in industry. For example, sound fields set up due to resonance in ducts by noise will have the spectral characteristics of filtered white noise or the sound from an engine in any particular frequency range may be thought of as a dominant tone with a considerable amount of noise pollution around it. A gating technique which can be used to elucidate the phase relationship between the pressure and velocity is also discussed.

Theory

It has already been shown[7] that, using the Gaussian crossed beam setup for L.D.A., the autocorrelation function due to sinusoidal oscillation in the case of no mean flow is well approximated by

$$R(\tau) = A + B\, J_o(a_m D\tau) \tag{1}$$

where A and B are constants, J_o is the zero order Bessel function, a_m is the velocity amplitude of the vibration, D is the radial frequency to velocity conversion factor and τ is the lag time. Thus the velocity amplitude of the fluctuation can be deduced by counting up the lag time to the first minimum of the Bessel function and applying the formula

$$a_m = \frac{3.832}{D\,\tau} \tag{2}$$

Expression (1) was originally derived by integrating the correlation over the velocity probability density function for a sine wave. A more general expression however for frequency modulation by a sine wave is given by Middleton[8]

$$R(\tau) = \frac{A_o}{2}\, J_o\left(2\mu \operatorname{Sin} \frac{\omega_m \tau}{2}\right) \operatorname{Cos}\omega_o \tau \tag{3}$$

Where A_o is the amplitude of the frequency modulated signal, μ is the modulation index,

J. Phys. D: Appl. Phys. 20 (1987) 418–423. Printed in the UK

The measurement of periodic acoustic fields using photon correlation spectroscopy

John P Sharpe and Clive A Greated
Department of Physics, Edinburgh University, UK

Received 18 June 1986, in final form 29 August 1986

Abstract. A method of measuring the velocity amplitudes of acoustic vibrations using the laser Doppler photon counting technique (photon correlation spectroscopy) is described. The results are compared with measurements made using a pressure microphone and close agreement is found. A gating technique is also described which allows time histories of the fluctuation to be obtained if periodicity is assumed.

1. Introduction

Sound waves are normally measured with microphones which respond either to the pressure or the pressure gradient at a point, whereas the acoustic field is only fully defined if the pressure plus all three velocity components are known. Values of instantaneous velocity and pressure are required for an evaluation of both sound intensity and acoustic impedance, the two quantities which are most frequently required in industrial acoustics. Sound intensity is a vector quantity which describes the magnitude and direction of acoustic energy flow and is the standard parameter used in analysing the sound power emitted by machinery and other industrial and environmental sources. Unlike sound pressure levels, intensity measurements are only sensitive to the active component in the sound field, ignoring the reactive part. They can thus be used to study sound sources in their natural environment, without recourse to an anechoic chamber. This is a most important consideration in many practical investigations. Acoustic impedance is also a vector quantity, being the ratio of pressure to the associated particle velocity. This parameter is of particular importance in the analysis of standing wave patterns, e.g. in musical instruments, or ducts used for transmitting sound waves e.g. telephone headsets and loudspeaker horns.

Particle velocities can be inferred by measuring the pressure gradient at a point either using a pressure-gradient microphone (e.g. a ribbon microphone) or, more commonly, two pressure microphones placed a short distance apart. The equations of motion for the sound waves are then used to transform pressure gradients to velocities (Fahy 1975, Chung 1978). This method, however, requires calibration and the application of correction factors depending on the proximity of the microphones in relation to the source and the frequency of the acoustic disturbance (Bruel and Kjaer 1982a, b). More important still, the introduction of microphones disturbs the acoustic field which necessitates the application of further factors which can only be derived empirically. Other intrusive techniques, such as the Rayleigh disc, are beset with similar difficulties which combine to make them either inaccurate or impractical for many applications.

It is however possible to measure acoustic velocities absolutely and non-intrusively using the laser Doppler technique. This has been done by Taylor (1976, 1981); the principle is described in Durrani and Greated (1977). Application of the technique in acoustics is made difficult by the fact that the frequencies of the velocity fluctuations are high; up to 15 kHz. For a typical acoustic frequency of 1 kHz, light scattered from the laser beam must be sampled over time periods of 100 μs or less if velocities are to be recorded over a complete wave cycle. Since with a lower power laser the photon count rate is only one or two per microsecond for the light scattered from dust particles naturally present in the air, this rules out the frequency tracking and pulse counting techniques commonly used in flow measurement. To apply these either a very high power laser is required or heavy seeding needs to be added to the air. Also these techniques are only directly applicable when scattering particles pass completely through the fringe pattern formed within the measuring volume. In an acoustic field particle excursions are frequently less than a single fringe spacing, so this condition is not fulfilled.

0022-3727/87/040418 + 06 $02.50

These difficulties have been overcome by employing the photon correlation method of signal analysis (Greated 1986). The method has been applied in two ways. Either time-averaged correlograms over the full acoustic cycle are used to compute velocity amplitudes, or a gating technique is applied so that the photon counts are only recorded at a predetermined phase position in the cycle. The velocity variation as a function of time is then obtained by computing the correlogram at a number of different phase positions thus yielding directly the relationship between the pressure and velocity fluctuations.

In the original experiments of Greated (1986) a phase shifting device was used in the optical system when constructing the correlograms averaged over the complete cycle. This effectively introduced a pedestal velocity onto the fluctuations which were to be measured so that the form of the correlogram was essentially the same as that produced by a steady flow on which sinusoidal fluctuations had been superimposed. Experiments have now shown that the phase shifter is unnecessary if only velocity amplitudes are required. This greatly simplifies the optical system and makes the estimation of the velocity amplitude much more accurate. In this paper we give the theory for the formation of the correlogram in a sinusoidally varying acoustic field and also show that the results give close quantitative agreement with pressure microphone measurements. In addition, we describe the gating technique which can be used to determine temporal variations, which are necessary for the measurement of acoustic impedance and sound intensity or in the mapping of three-dimensional fields. In order to validate the technique the standing wave in a closed tube at resonance has been studied. This particular situation has been chosen because the relationship between the pressure and velocity fluctuations is well known (Morse 1948). The field is essentially one-dimensional with velocity nodes and pressure anti-nodes at the ends.

2. Theory

2.1. Form of the time-averaged correlogram

In the analysis to follow it is assumed that the gaussian beam difference Doppler optical arrangement is used, this being by far the most common.

The form of the correlation function for a steady flow perturbed by a sinusoidal fluctuation has been derived by Durrani and Greated (1977). In this case each scattering particle traverses the complete measuring volume, whereas in the acoustic situation under study the particles may oscillate within distances of less than one fringe spacing. Despite this a similar method of derivation can be applied since the signal is derived from the light scattered by many particles randomly distributed within the measuring volume, but moving coherently at any instant of time. Since the averaging times of the correlograms are many oscillation periods (typically 10000) this ensures that particles will have sufficient time to redistribute themselves (due to diffusion etc) and hence eliminate excessive weighting to any given part of the fringe pattern.

The instantaneous velocity of the particles is

$$u(t) = a_m \sin(\omega_m t) \tag{1}$$

where a_m and ω_m are the amplitude and frequency of the velocity fluctuation respectively.

The velocity probability density is then given by

$$\begin{aligned} p(u) &= \frac{1}{\pi}(a_m^2 - u^2)^{-1/2} && |u| < a_m \\ p(u) &= 0 && |u| > a_m. \end{aligned} \tag{2}$$

We can thus write the autocorrelation function as

$$R_a(sT) = E[R_a(sT, u)] = \int_{-a_m}^{+a_m} p(u) R_a(sT, u)\, du \tag{3}$$

where s is the address number on the correlator, T is the sample time and $E[\ldots]$ denotes the expectation operator.

Applying now the weighting function for a gaussian beam system and the form for the intensity distribution of the fringes we obtain

$$R_a(sT) = \frac{1}{3\pi}\int_{-a_m}^{+a_m} \frac{1}{(a_m^2 - u^2)^{1/2}} \times \exp\left(\frac{-(sT)^2u^2}{4r_x^2}\right)(2 + \cos DusT)\, du \tag{4}$$

where r_x is the distance across the observation volume and D is the (radial) frequency to velocity conversion factor i.e.

$$D = \omega_0/u = 4\pi \sin\theta/\lambda. \tag{5}$$

Here θ is the half-angle between the beams and λ the wavelength of the light.

Separating the integral in (4) into two parts such that

$$R_a(sT) = F_1 + F_2 \tag{6}$$

where

$$F_1 = \frac{1}{3\pi}\int_{-a_m}^{a_m} \frac{2}{(a_m^2 - u^2)^{1/2}} \exp\left(\frac{-(sT)^2u^2}{4r_x^2}\right) du \tag{7}$$

and

$$F_2 = \frac{1}{3\pi}\int_{-a_m}^{a_m} \frac{1}{(a_m^2 - u^2)^{1/2}} \times \exp\left(\frac{-(sT)^2u^2}{4r_x^2}\right)\cos DsTu\, du \tag{8}$$

we proceed to evaluate these by substituting $u =$

$a_m \sin \omega_m t$. Thus

$$F_1 = \frac{2\omega_m}{3\pi} \int_{-\pi/2\omega_m}^{+\pi/2\omega_m} \exp\left(\frac{-(sT)^2 a_m^2 \sin^2 \omega_m t}{4r_x^2}\right) dt \quad (9)$$

and by expanding the exponential term and integrating we obtain

$$F_1 \simeq \frac{2}{3} - \frac{(sT)^2 a_m^2}{12 r_x^2} + \frac{(sT)^4 a_m^4}{64 r_x^4} - \ldots \quad (10)$$

to a good approximation.

For F_2 we find

$$F_2 = \frac{\omega_m}{3\pi} \int_{-\pi/2\omega_m}^{\pi/2\omega_m} \exp\left(\frac{-(sT)^2 a_m^2 \sin^2 \omega_m t}{4r_x^2}\right) \times \cos[DsTa_m \sin(\omega_m t)]\, dt \quad (11)$$

$$= \frac{\omega_m}{3\pi} \int_{-\pi/2\omega_m}^{\pi/2\omega_m} \exp\left(\frac{-(sT)^2 a_m^2 \sin^2 \omega_m t}{4r_x^2}\right) \left(J_0(DsTa_m) + 2\sum_{n=1}^{\infty} J_{2n}(DsTa_m) \cos 2n\omega_m t\right) dt \quad (12)$$

(12) being obtained by using the identity

$$\cos(\beta \sin \omega_m t) = J_0(\beta) + 2\sum_{n=1}^{\infty} J_{2n}(\beta) \cos(2n\omega_m t) \quad (13)$$

where J_n is the Bessel function of order n.

Expanding the exponential term as before and carrying out the integration we find

$$F_2 \simeq J_0(DsTa_m)\left(\frac{1}{3} - \frac{(sT)^2 a_m^2}{24 r_x^2} + \frac{(sT)^4 a_m^4}{128 r_x^4} - \ldots\right). \quad (14)$$

Since in most cases $(sT)^2 a_m^2 \ll r_x^2$ we can write the autocorrelation function as

$$R_a(sT) = F_1 + F_2 = \tfrac{2}{3} + \tfrac{1}{3}[J_0(a_m DsT)]. \quad (15)$$

Since the first minimum of the zero-order Bessel function occurs at 3.832 we can immediately deduce the velocity amplitude by counting the number of points on the correlogram up to the first minimum and applying the formula

$$a_m = 3.832/DsT. \quad (16)$$

2.2. Form of the gated autocorrelation function

By using a gating technique we can sample specific portions in time of the acoustic fluctuation. This allows us to deduce the temporal variation of the velocity fluctuation. For these measurements a phase shifter must be used in order to obtain the direction of the velocity at any given phase position in the cycle.

The effect of gating on the form of the correlogram has already been discussed (Grant and Greated 1980, Easson *et al* 1986). The photodetector current due to a continuous Doppler signal $c(t)$ riding on a pedestal DC current p and sampled by a square gating pulse is

$$I(t) = (c(t) + p)\varphi(t) \quad (17)$$

where $\varphi(t)$ is a pulse taking the value 1 between times t_1, t_2 and 0 elsewhere. For $c(t)$ a stationary process, the autocorrelation function takes the form

$$R_I(\tau) = R_c(\tau)R_\varphi(\tau) + p^2 R_\varphi(\tau). \quad (18)$$

Since the autocorrelation of a square pulse is a triangular pulse, $R_I(\tau)$ is a linearly damped correlogram (the damping becoming complete at $\tau = t_2 - t_1$ the pulse width) and rides on a sloping base line. In the case of the multiple gating of a harmonic signal it may be shown that the sum of the autocorrelations of all the observed pulses is contained in the first triangular pulse and represent an average Doppler signal for that phase in the cycle.

3. Apparatus

Figure 1 is a schematic representation of the arrangement used for the experiments. Standing waves were set up in a glass tube of length 46.5 cm and diameter 2 cm using a probe loudspeaker. The tube was terminated at each end by rubber stoppers and a probe microphone was used for measuring the pressure fluctuations.

For the optical measuring system an 8 mW He–Ne laser ($\lambda = 633$ nm) was used as a light source. Parallel beams of light were produced using a beam splitter and these were passed through a phase shifter and then focused down to a point on the axis of the tube. This is essentially the gaussian crossed beam system described in the literature e.g. in Durrani and Greated (1977) which utilises the scattering of light by small particles as they pass through the fringe system set up at the intersection of the two beams. The light scattered from the observation volume was collected using a photomultiplier angled at about 35° to the straight-through axis, this rather large angle being required to reduce noise caused by flare from the tube walls.

For the time-averaged correlograms the signal from the photomultiplier was fed directly to the correlator and analysed, the microcomputer being made inactive. In this case the phase shifter was not used.

The probe microphone, which had been calibrated to an accuracy of about 1 dB using an acoustic coupler, could be moved along the axis of the tube to monitor the pressure fluctuations at any point.

In the case of gated correlograms the microcomputer was programmed to detect the zero upcrossing of the waveform from the probe microphone and provide pulses at a predetermined delay time after this point. The pulse length and the delay time could be varied independently. Only for the duration of the pulse width was the signal from the photomultiplier analysed. The waveform and pulses were generally

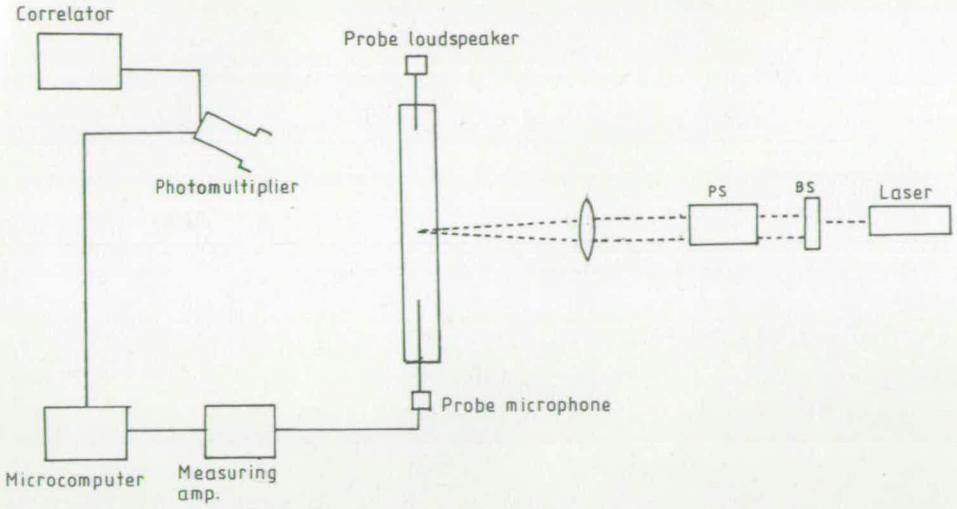

Figure 1. A schematic layout of the apparatus: BS, Beam splitter; PS, Phase shifter.

monitored on an oscilloscope and their form is seen in figure 2.

4. Method and results

4.1. Time-averaged correlograms

A small quantity of tobacco smoke was introduced into the tube for seeding purposes and the tube terminated at both ends. The air column was excited to its 4th harmonic (frequency = 1470 Hz) with the probe loudspeaker. The intersection of the laser beams was then scanned along the axis of the tube (by moving the tube-loudspeaker assembly) to a distance of 18 cm from the end, with correlograms being recorded at 2 cm intervals. At these positions the pressure was also recorded using the probe microphone.

The velocity amplitudes were then derived using, in the case of the correlograms, the method described in § 2.1 and in the case of the probe microphone the formula (Greated 1986)

$$a_m = 0.0694 \times 10^{(0.05I-6)} \tag{19}$$

where I is the intensity in decibels.

Figure 3 shows the form of the correlograms obtained at various intensities and sample times. (*a*), (*b*) and (*c*) were taken at 'moderate' intensity values and show how the position of the first minimum of the Bessel function changes as the intensity changes, in accordance with equation (15). (*d*) demonstrates the effect of the

$$(sT)^2 a_m^2/24r_x^2$$

term in equation (14) due to very high intensities and larger sample times.

The velocity amplitudes as deduced from the correlograms and from the probe microphone were then plotted as a function of distance along the tube (see figure 4). The velocity amplitudes measured from the correlograms represent the actual velocities in the tube whereas the values deduced from the probe microphone output are pressures converted to the same velocity scale. The two curves should be 90° out of phase but have the same amplitude (Morse 1948). As can be seen there is good agreement between both sets of results, validating the theory presented earlier and the assumptions about the physical characteristics of the system.

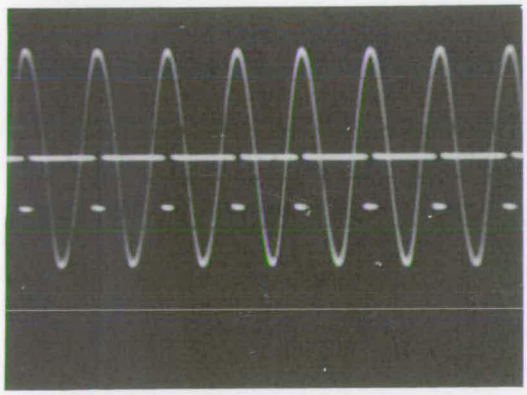

Figure 2. The waveform and pulses as monitored during the gating experiments. The delay and pulse times are 100 μs and 80 μs respectively.

4.2. Gated correlograms

For these measurements the intersection of the laser beams was positioned at a velocity node to ensure large fluctuations and the tip of the probe microphone were kept well away from this observation volume to avoid distortion of the acoustic field. A phase shift of 47.62 kHz was used, corresponding

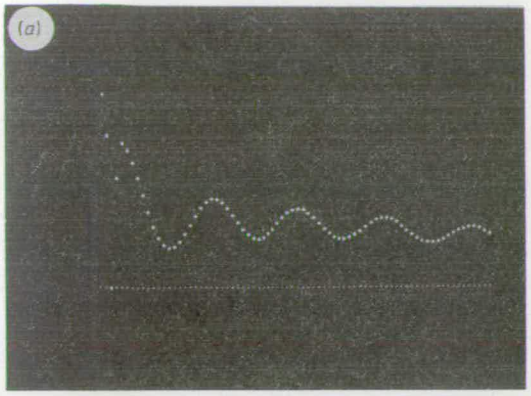

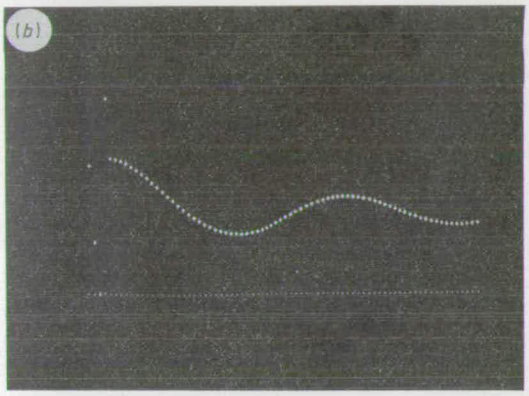

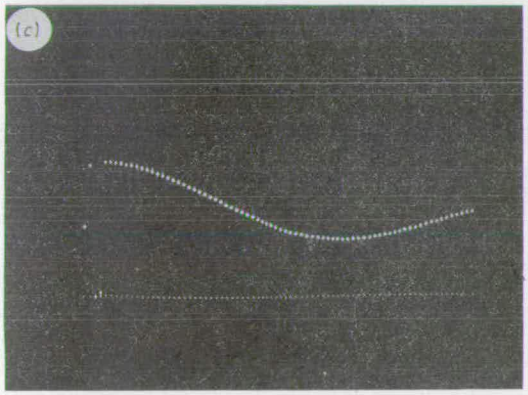

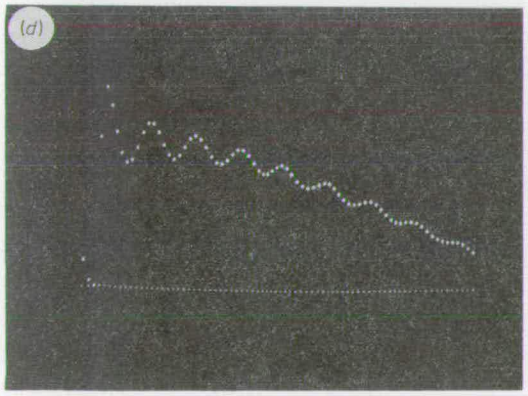

Figure 3. The time-averaged correlograms obtained with no phase shift. (*a*) Velocity amplitude = 257 mm s^{-1}, sample time = 1.5 μs. (*b*) Velocity amplitude = 103 mm s^{-1}, sample time = 1.5 μs. (*c*) Velocity amplitude = 8 mm s^{-1}, sample time = 1.5 μs. (*d*) Very large velocity amplitude and large sample time.

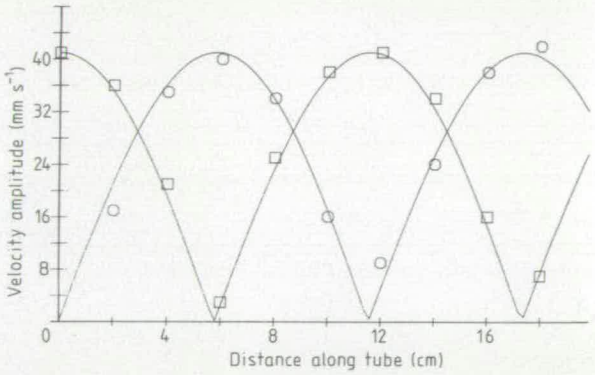

Figure 4. The velocity amplitude as a function of distance along the tube: ○, velocities deduced from the correlograms; □, velocities deduced from the probe microphone.

to an apparent velocity of 0.3 m s^{-1}. The pulse width was 70 μs and the delay time increased in intervals of 50 μs, using a sample time of 1.5 μs. A typical correlogram obtained is shown in figure 5.

The velocities were deduced by the standard method of counting the number of points per cycle and the phase shift allowed the velocity direction to be obtained. The velocity was plotted as a function of delay time and is shown in figure 6. The full curve's amplitude was obtained from the maximum velocity deduced using the pressure microphone and equation (19). As can be seen the points deduced from the correlograms fit the sinusoidal curve very well, as expected from theory.

5. Conclusions

It has been shown that the photon correlation technique can be used to measure sinusoidal velocity fluctuations in an acoustic field and that the values obtained are in close agreement with those deduced from calibrated probe-microphone readings. The measurements presented in this paper are for essentially one-dimensional standing wave patterns, it

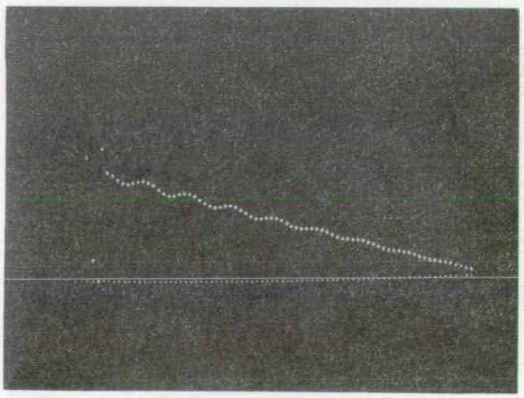

Figure 5. Form of gated correlogram.

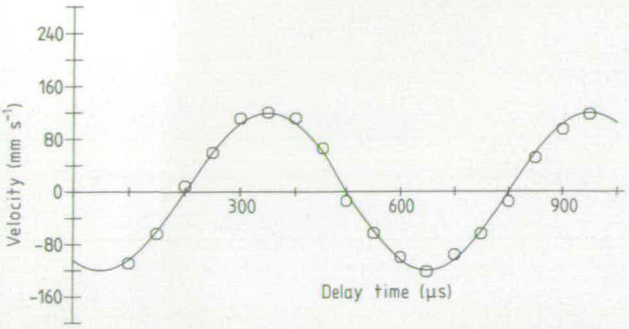

Figure 6. The velocity fluctuation as a function of delay time.

being recognised that the system we have set up only measures velocity components rather than the full velocity vector. For more complex flow fields, which show dominant two- or three-dimensional characteristics, further measurements would have to be made to determine all three velocity components, thus allowing a complete description of the field. When used in conjunction with a probe microphone the instrument allows both acoustic impedance and intensity to be measured directly.

The measurement of random noise fields has not been considered in this paper but it has been demonstrated earlier (Greated 1986) that the instrument does respond to changing noise intensity levels. It should not be difficult to extend the theory presented here to derive the shape of the time-averaged correlogram as a function of intensity but there appears to be no simple way in which temporal characteristics could be obtained, due to the absence of periodicity in this situation.

A detailed study is now in progress to evaluate the intensity and frequency ranges over which the method is applicable. At very high frequencies and intensities it is expected that the scattering particles will not be able to follow the acoustic field, whereas at low intensities Brownian motion may become important. The effect of superimposed flow fields is also being considered.

Acknowledgments

This work is funded from the Science and Engineering Research Council and British Telecom. John Sharpe is also in receipt of a studentship from The Department of Education for Northern Ireland.

References

Bruel and Kjaer 1982a *Bruel and Kjaer Tech. Rev. No 3: Sound Intensity (Theory)*

—— 1982b *Bruel and Kjaer Tech. Rev. No 4: Sound Intensity (Instrumentation and Applications)*

Chung J Y 1978 *J. Acoust. Soc. Am.* **64** 1613–6

Durrani T S and Greated C A 1977 *Laser Systems in Flow Measurement* (New York: Plenum)

Easson W J, Griffiths M, Sharpe J P and Greated C A 1986 *Proc. Electro-Optics and Lasers UK 1986*

Fahy F J 1975 *J. Acoust. Soc. Am.* **62** 1057–9

Grant I and Greated C A 1980 *J. Phys. E: Sci. Instrum.* **13** 571–4

Greated C A 1986 *Strain* 21–4

Morse P M 1948 *Vibration and Sound* (New York: McGraw-Hill)

Taylor K J 1976 *J. Acoust. Soc. Am.* **51** 691–4

—— 1981 *J. Acoust. Soc. Am.* **70** 939–45

A PennWell Publication

December 1987

LASER FOCUS

THE MAGAZINE OF ELECTRO-OPTICS TECHNOLOGY

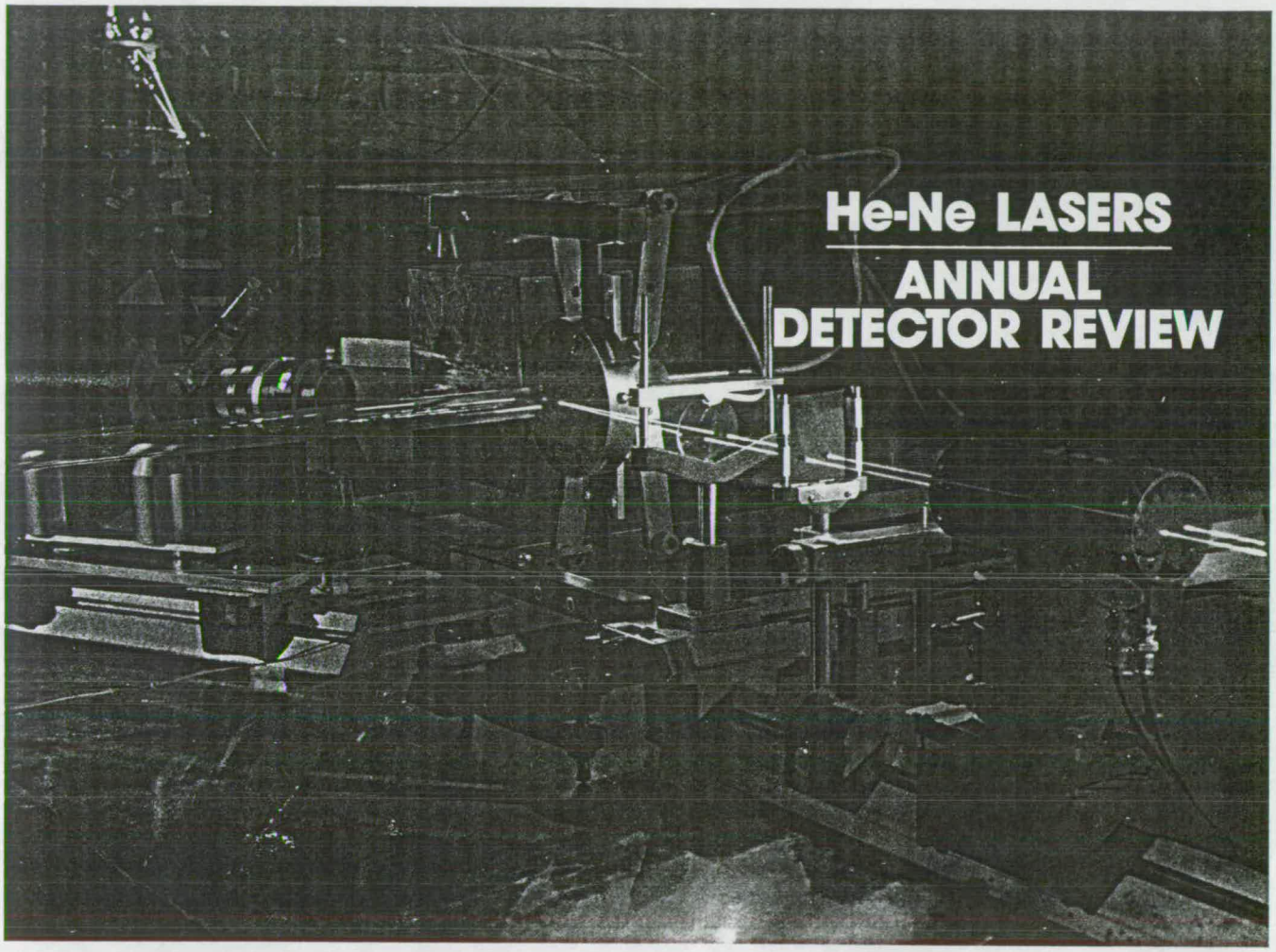

He-Ne LASERS

ANNUAL DETECTOR REVIEW

FIBEROPTICS: LONG-WAVELENGTH PHOTODIODES

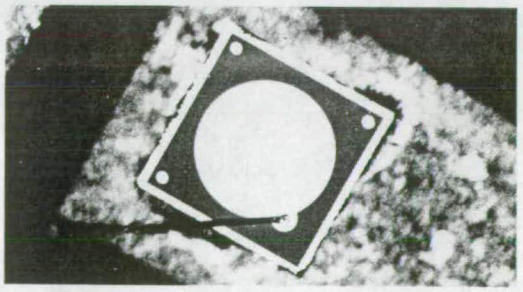

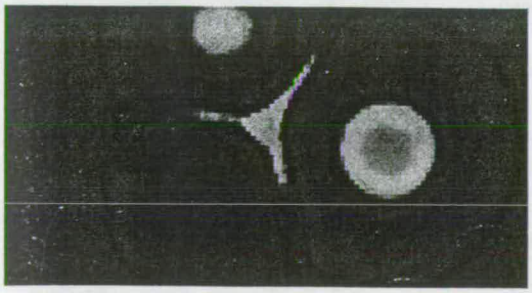

ELECTRONIC IMAGING:
ANNUAL REVIEW OF MARKETS & TECHNOLOGY

He-Ne LASER MEASURES ACOUSTIC FIELDS

A nonintrusive laser Doppler anemometry technique for directly measuring acoustic particle velocities can provide more detailed information than is obtained by using conventional microphones. It can be employed to give direct records of acoustic impedance. The method is now being extended to three-dimensional sound patterns. Applications of the technique are expected to be in telecommunications and in noise measurement in industrial environments. The work has been carried out by the Fluid Dynamics Unit in the Physics Department of the University of Edinburgh, Edinburgh, U.K., under the direction of Dr. Clive A. Greated.

To obtain a full description of an acoustic field at any point, the pressure, the velocity, and the phase relationship between these two quantities must be determined. The pressure is easily measured with a microphone, but velocity measurements are much more difficult. Laser Doppler anemometry provides an absolute measurement of velocity and is essentially nonintrusive because it relies on the scattering of light from small particles.

The Edinburgh work used a Gaussian crossed-beam system in which the light from a laser was split into two beams, which were then focused to a point where a fringe pattern was produced. Particles passing through this pattern scattered light in a manner depending on their velocities and on the geometrical form of the fringe pattern. The scattered light could be collected and analyzed to determine the fluid velocity.

The analytical method is determined by the density of the particles, the flow parameters, and such. A photon correlation technique was used for signal analysis. This technique is most suitable for the low density of the scattering particles normally available in air flows. It also seemed to be more versatile than other techniques, such as frequency tracking systems.

High-power laser

In the experimental arrangement of Fig. 1, the sound field was fed into a tube 1.5-m long with a diameter of 20 mm. The last two-thirds of the tube were filled with absorbing material to prevent the production of standing waves by reflection. This arrangement was selected because it provides a very simple relationship between pressure and velocity fluçtuations. The sound field could be either a single tone or band-limited white noise.

The light from a He-Ne laser passed through a beam splitter and through a phase shifter. The beams were focused into the tube from a

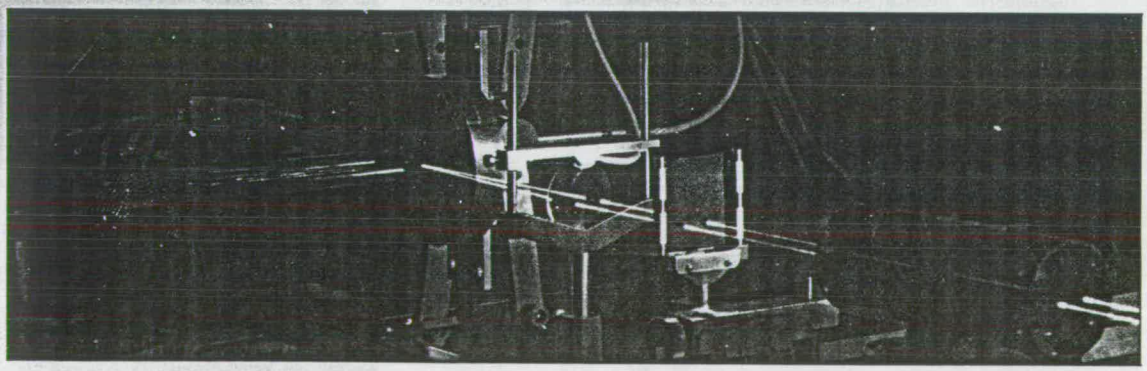

FIGURE 1. Photomultiplier behind clear gas tube surveys fringe pattern produced by dual He-Ne laser beams (see Fig. 2). Smoke seeded into the gas varies the detected signal, providing information on acoustic particle velocities. (Photo courtesy of J. Sharpe, Edinburgh University. Photographer: Peter Tuffy.)

Because of the importance of large-volume manufacture, the recent announcement that Uniphase will take over Spectra-Physics's low-power He-Ne line has attracted a great deal of industry attention. According to Uniphase Vice President of Marketing Dave Osborne, Uniphase production capacity will increase 50% to 150,000 annually, as a result of the deal with Spectra-Physics. The newly acquired production capacity will move from Eugene, Oreg., to the Uniphase plant in Mantika, Calif.

Osborne claims that Uniphase now will have "50% of the total market." At Melles Griot, previously the largest U.S. manufacturer, Marketing Director John Post Wheeler provides a similar assessment. According to Wheeler, the

separation of 20 mm using a 200-mm focal length lens. Tobacco smoke was used for seeding purposes.

The He-Ne laser was a 32-mW device from Spectra-Physics. Edinburgh researcher John Sharpe explained: "We chose a laser of this power since the light scattering from air flows is generally of quite a low level. Actually, a less powerful laser would probably have done the job, but we also wish to apply the laser to particle-image velocimetry, in an attempt to make accurate measurements of acoustic streaming effects. This work, which is now under way, needs high light intensity."

Gated signals

A gating technique was incorporated into the system to allow the relative phase of the velocity and the pressure to be deduced. A signal from a microphone in the sound field was fed to a microcomputer; the latter supplied a pulse of preset width at a preset delay time from the zero up-crossings of the signal. These pulses were fed to a photomultiplier and the Doppler signal was analyzed only during the pulse duration. The delay time was varied so as to sample the velocity at different portions of the acoustic cycle.

Gated sound measurements used a 1260-Hz frequency with the phase shifter set at 50 kHz. This provided a velocity pedestal of 0.317 m/s against which the velocity could be measured. The correlogram indicated a velocity amplitude of 85 mm/s, in close agreeement with measurements using ungated correlograms (86 mm/s) and those using the probe microphone (85 mm/s).

The laser technique was shown to provide accurate measurements of acoustic velocity fluctuations over intensities in the approximate range 90 to 120 dB, but it tended to fail at low intensities and at higher frequencies. Increasing the angle of intersection of the beams can decrease the lower limit to about 80 dB. It is suggested that the transformation of the correlogram into the frequency domain may offer a solution to the problem, but this was not possible with the correlator available.

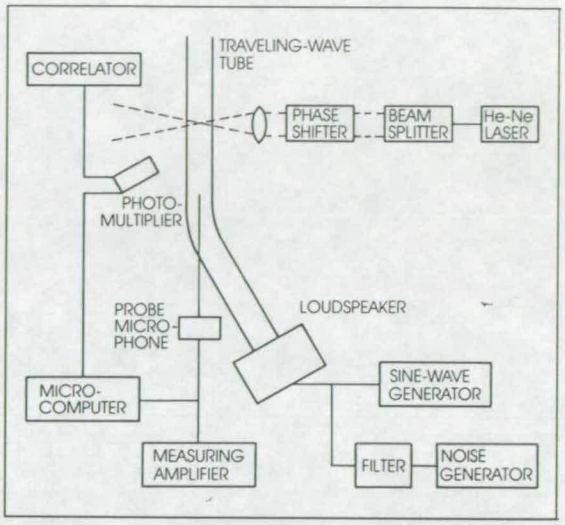

FIGURE 2. Dual beams derived from a single He-Ne laser form a fringe pattern within a gas tube as the basis for studies of acoustic impedance.

Complex impedances

Current work is directed toward the measurement of complex acoustic impedances using the gating technique. It is intended to investigate the effect of superimposed flow fields on the correlogram.

John Sharpe, of Edinburgh University, told us: "Estimates can also be made of the average velocity amplitude in a noisy field and, in the periodic case, the gating technique allows the phase relationship between the pressure and velocity to be deduced. The work has important implications for acousticians, since the measurement of acoustic velocities (a hitherto rather difficult task) would allow easier measurement of acoustic impedances."

The work has been funded by the British Science and Engineering Research Council (SERC) and British Telecom.

Brian Dance

deal makes Uniphase the same size as Melles Griot, and the two companies will now run neck and neck in annual production. He says, "Each will have around 35 to 40% of the market."

At Aerotech, Product Marketing Manager Dan Smyers suggests that his company will experience no net negative or positive effects from the Uniphase/Spectra-Physics deal. "It helps that Spectra sold its line," says Smyers, "but then, another company gets bigger as a result."

High-power devices

At Spectra-Physics, Steve Anderson, who is marketing manager for gas lasers, says that his company now will concentrate on a small range of scientific and high-power He-Ne lasers. These

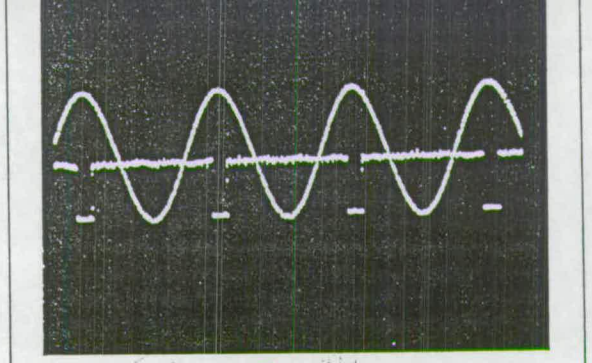

Fig 5.

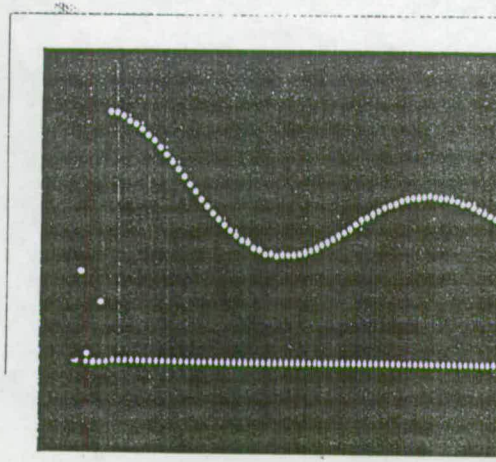

Fig. 1

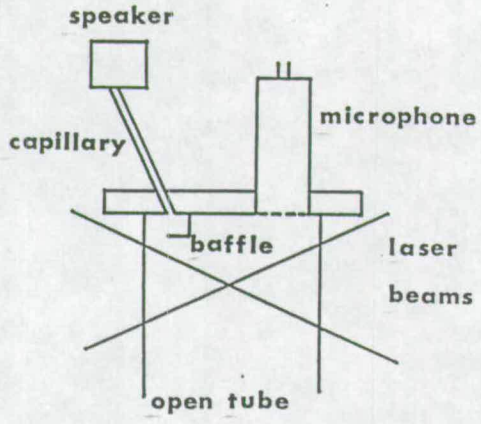

Fig 3.

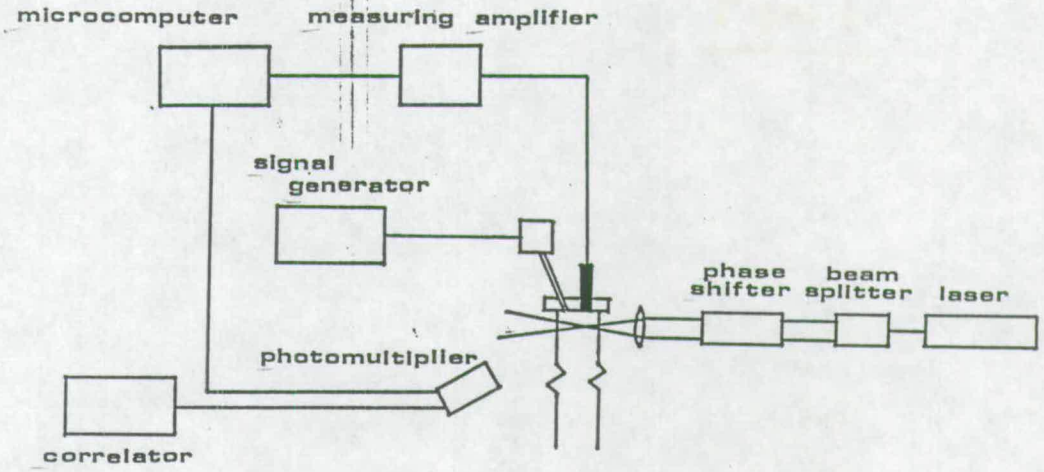

Fig 2.

1/2

Acu 406

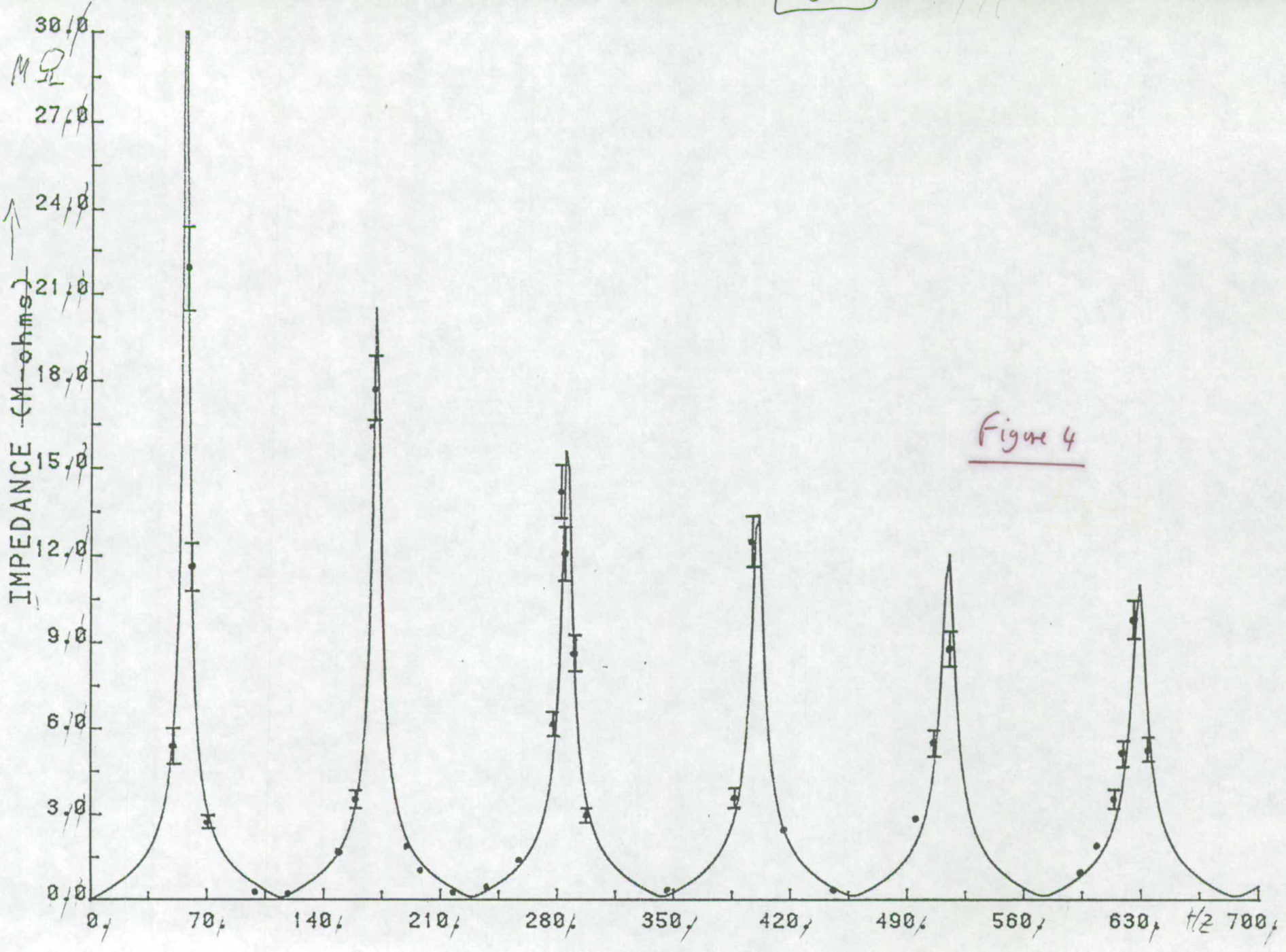
30,0
MΩ
27,0
24,0
21,0
18,0
15,0
12,0
9,0
6,0
3,0
0,0
IMPEDANCE (M ohms)
0
70
140
210
280
350
420
490
560
630
f/2 700
FREQUENCY (Hz) →

Figure 4

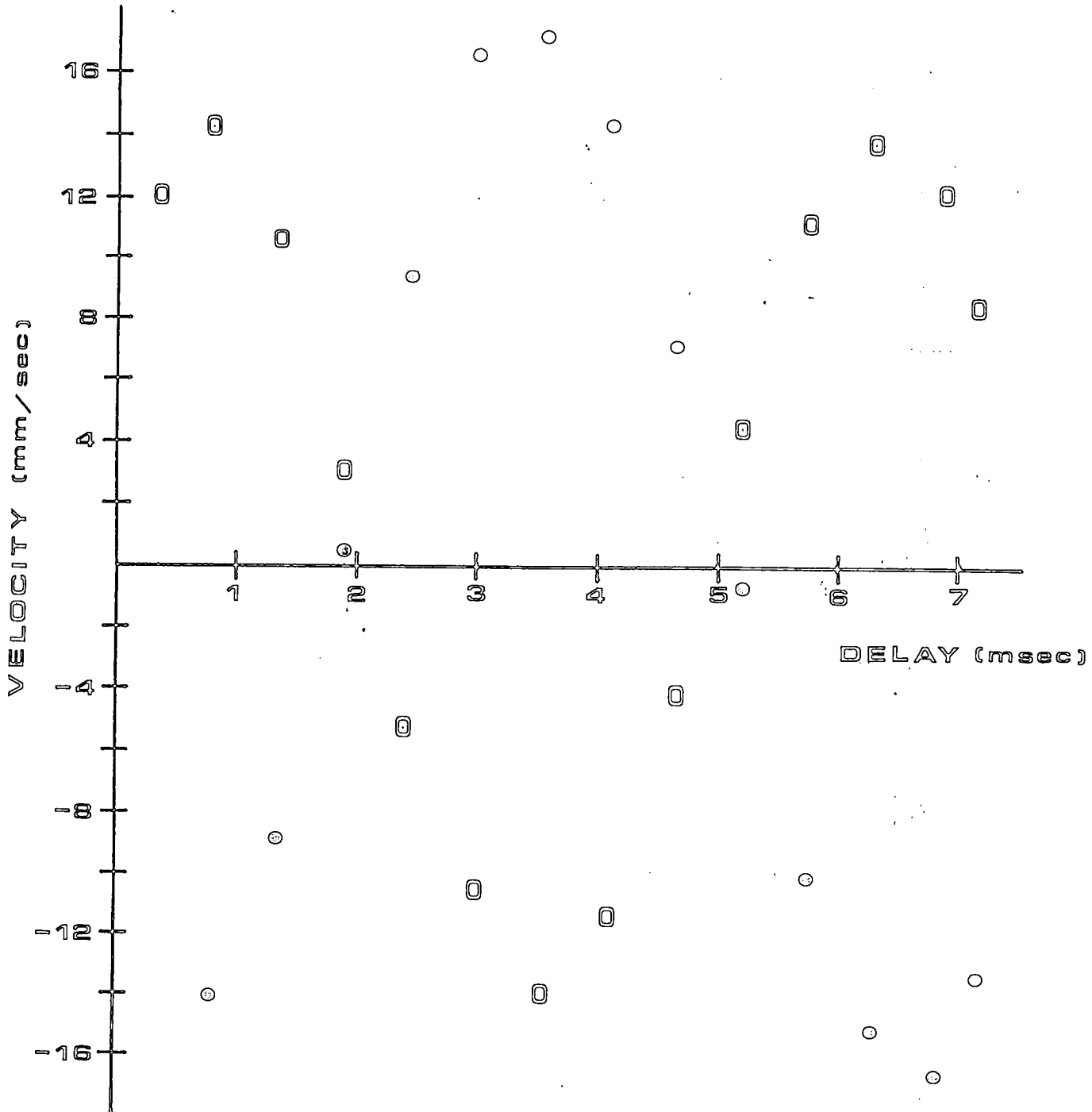

Figure 6

Figure 7.
SHARPE, GREATED &

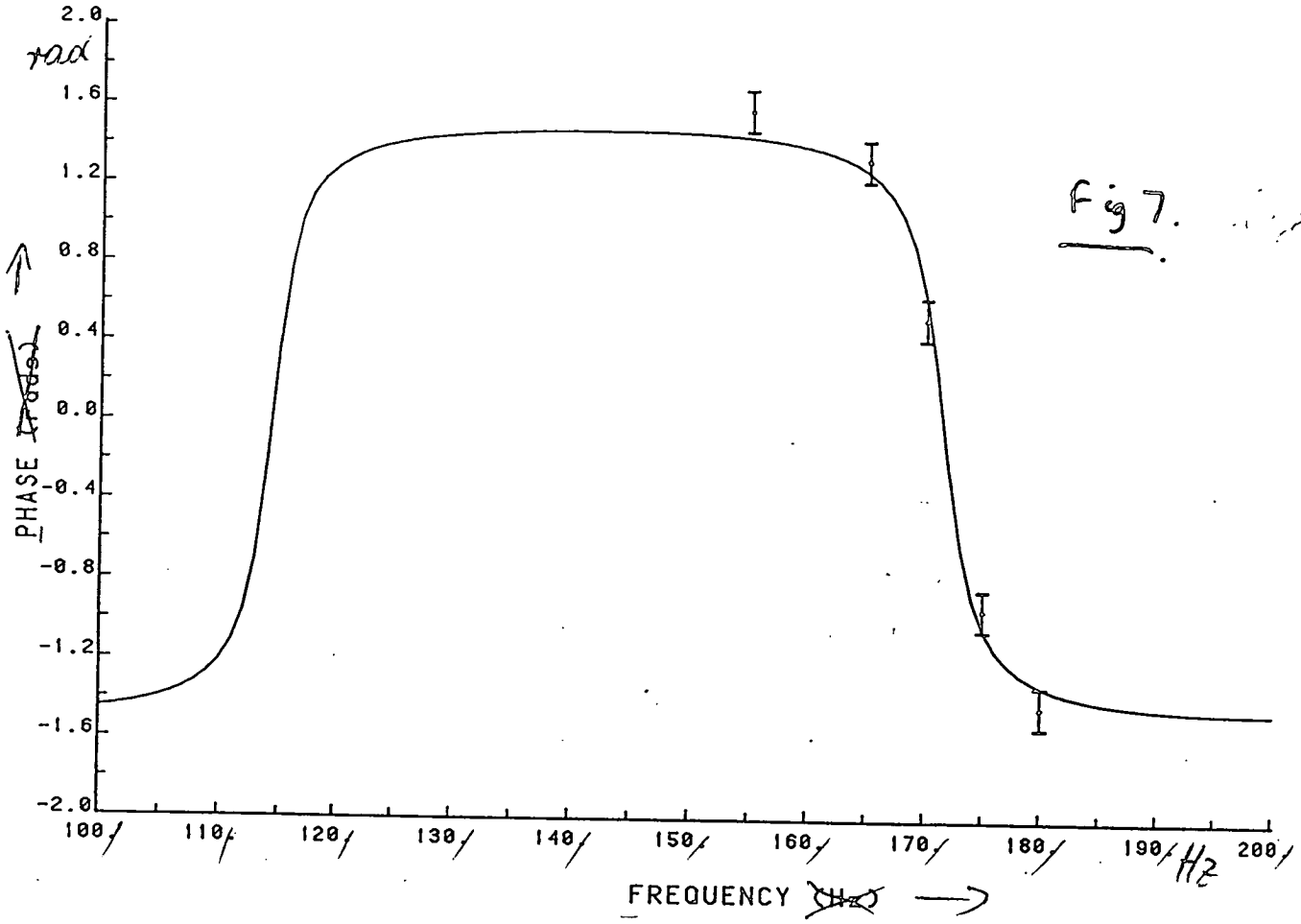

Fig 7.

Jun 4068

The Measurement of Acoustic Streaming using Particle Image Velocimetry

MANUSCRIPT ACCEPTED BY "ACUSTICA"

J. P. Sharpe, C. A. Greated, C. Gray & D. M. Campbell.

Physics Dept., Edinburgh University, Edinburgh, Scotland.

ABSTRACT.

In this paper the application of a whole field optical velocity measuring technique (Particle Image Velocimetry) to the measurement of acoustic streaming is described. Results are presented for measurements near a velocity node in the case of Rayleigh Streaming and comparisons with theory and pressure measurements show good agreement. The technique is shown to be useful in an area where conventional material or optical probes are impossible or impractical to use. Limitations of the technique are also discussed.

1. INTRODUCTION.

Acoustic Streaming, which may be described here as the generation of non-zero mean motions by a sound field, has been a subject of investigation since the time of Rayleigh [1]. Although, as Lighthill points out in his excellent review article [2], the topic has been somewhat neglected of late, it is still of considerable interest to acousticians [3] and to fluid dynamicists interested in Lagrangian mean flows [4].

The phenomenon typically arises when a sound field is attenuated or dissipated due to its interaction with the medium of propagation or with the boundary layer when a solid wall is present. Quite a body of theoretical work has been produced on the subject [see above references] but experimental work is rather scarce. Reasons for this lack of measurement are not difficult to appreciate when one considers that in the regimes where acoustic streaming takes place there can be considerable interaction between the sound field and any measuring device introduced to measure the flow e.g. [5]. Consequently one sees in the literature qualitative statements about "strong" or "weak" streaming and comparisons with theory made on the basis of flow visualisation [3] [4].

We present here the application of an optical technique (Particle Image Velocimetry) to the measurement of Rayleigh Streaming. This form of streaming was chosen since it is reasonably easy to generate, it is well understood and its magnitude can be independently estimated from pressure measurements of the sound field causing it.

Sections 2 and 3 outline Rayleigh Streaming and the optical technique while 4 and 5 describe the experimental setup, measurements and results. Section 6 discusses the advantages, limitations and accuracy of the technique.

2. RAYLEIGH STREAMING.

Rayleigh Streaming occurs when an acoustic standing wave suffers dissipation in the boundary layer generated by a solid wall. The most common configuration in which to observe the phenomenon occurs when a standing wave is set up in a circular tube. The

form that the streaming takes was calculated by Rayleigh himself [1] and is illustrated in figure 1.

The velocity of the streaming at the wall of the tube (or rather just beyond the boundary layer) is given by Rayleigh's Law,

$$u_s = \frac{-3}{4\omega} V(x) \frac{dV(x)}{dx} \qquad (1)$$

where V(x) is the acoustic particle velocity outside the boundary layer at any point x along the tube and ω is the radial frequency of the sound field. This velocity u_s (sometimes called the slip velocity) is directed towards the velocity nodes and is matched by a return flow up the centre of the tube and away from the velocity nodes such that on any section through the axis of the tube the velocity is given by

$$u = u_s \left(1 - \frac{2r^2}{a^2}\right) \qquad (2)$$

where r is the distance from the tube axis and a is the tube radius.

If the acoustic particle velocity of the sound field is given by

$$V(x) = a_m \sin\left(\frac{2\pi x}{\lambda}\right)$$

where a_m is the velocity amplitude then, inserting this into (1) yields

$$u_s = \frac{-3a_m^2}{8c} \sin\left(\frac{4\pi x}{\lambda}\right) \qquad (3)$$

where c is the speed of sound. It may be noted that, interestingly, (3) does not depend on the viscosity of the medium. Thus, using the relationship between the velocity and pressure in a standing wave , it is possible to estimate the magnitude of the slip velocity at any point in the tube outside the boundary layer.

3. PARTICLE IMAGE VELOCIMETRY.

Particle Image Velocimetry (P.I.V.) is a velocity measuring technique which can "instantaneously" record velocities over a whole field [6]. The technique relies on photographing small particles contained in and faithfully following the flow under

investigation.

Light from a laser is expanded into a two-dimensional sheet and projected into the flow (see figure 2). The laser beam is then pulsed (by either Q-switching or chopping the beam from a continuous laser) so that successive particle images are recorded on the film plane of a camera placed at right angles to the expanded sheet of laser light. Actually the light does not need to be coherent (flash lamps have been used for P.I.V. measurements [7]) but a laser provides very high light density in an easily controlled form.

The velocity information on the film can then be recovered by ascertaining the separation of the particle images. This can be done by either observing the film directly using a microscope or, more commonly, interrogating each point on the film using a low power laser beam. This method produces, in the far field diffraction zone, a series of fringes analagous to those produced in the Young's double slit experiment (figure 3). The distance between the fringes is inversely proportional to the particle image separation at that point on the film and their orientation is perpendicular to the flow direction. Knowing the magnification of the camera and the time between the light pulses it is then an easy matter to deduce the flow velocity.

As may be appreciated, if the particle images are too close then the fringes are so far apart that only one may be visible, or, if the images are too far apart, it may be impossible to resolve the individual fringes. Such limitations on the dynamic range of the technique have been discussed previously [8] though a convenient rule of thumb is that, on the film plane, the particle images should be separated by approximately 0.1 mm. It is necessary therefore (if one wants to avoid much tedious work) to be able to estimate roughly the range of velocities in the flow under investigation.

Since a typical region needing analysis can contain from say fifty to several hundred points it is necessary in practice to analyse the fringes automatically. This is most commonly done by capturing the fringe pattern with a video camera and frame grabber and using a computer to extract the velocity information. Such a system has been developed at our

institution [9] and there are many other publications e.g.[10], [11] describing the accuracy, speed etc. of various implementations of the technique. In our implementation the slide is automatically scanned using a computer controlled micropositioner, the fringes at each point captured with a video camera and the velocity information extracted using a two dimensional Fast Fourier transform.

4. EXPERIMENTAL APPARATUS.

A diagram of the experimental setup is shown in figure 4. Light from a 32mW He-Ne laser (λ=633nm) was expanded into a two dimensional sheet using the lens l and the two cylindrical lenses c1 and c2. When the sheet entered the tube, cutting the axis, it was approximately 2cm high and 1/2 mm thick. It was noticed while conducting the experiments that the streaming motions could be greatly affected by small temperature gradients. To minimise this the tube was lagged with polyurethane foam at all points except the working section and baffles were placed around the apparatus to reduce air movements. Positioned between l and the laser was the shutter while the chopper was placed at the focus of l.. The chopper, which was a rotating disc with a slot cut in it, formed the pulses of light while the shutter could be adjusted to let a preset number of pulses through. This use of an external shutter (rather than the camera's own shutter) was employed to reduce camera vibration to a minimum. Although the chopper (Scitec Model 300CD) came with it's own electronic display to indicate the frequency of rotation, this was found to be unreliable at the low chopping speeds we were to use. Consequently a photodiode and storage oscilloscope were used to give a more precise frequency reading.

The camera used was a 35 mm Nikon with a 50 mm flat focus lens at a magnification of 0.773. This type of lens was found to be essential if one wanted to avoid distortion of the image in the off axis region. The film used was Kodak T-Max 400 which provided good sensitivity (400 ASA) and adequate resolution ($\sim$100 lines/mm depending on contrast). During actual experimental runs the laboratory was always illuminated with extremely subdued light and the photograph taken against a black background to increase contrast.

The amount of distortion in the image plane due to the curvature of the glass tube was estimated by putting a piece of graph paper in the tube, photographing it, and examining the developed film with a travelling microscope. A negligible amount of distortion was found except at approximately 1 mm or so from the tube wall. Since, as it turned out, the amount of flare from the wall tended to make any measurements in this region impossible anyway it was not necessary to calculate correction factors for this effect.

5. MEASUREMENTS AND RESULTS.

The apparatus was set up as indicated in figure 4. Sound of frequency 2460 Hz was introduced into the tube (length 450 mm, internal diameter 23.3 mm) using a horn loudspeaker with the horn removed. The tube was sealed at the other end with a rubber bung which had a tightly fitting metal plate attached to its inside face to ensure a rigid termination. The sound field thus corresponded to the 7th normal mode of the air column. A probe microphone, (Bruel & Kjaer type 4166 with 2 mm i.d. probe attachment) inserted through the rigid end monitored the pressure. The probe microphone had previously been calibrated to within 0.5 dB using an acoustic coupler. Although the intensities required to produce streaming were near the limits of the microphone's range [12] they were still within the 10% distortion limit - leading to an extra possible error of around 1 dB. So, although the pressure measurements were not highly accurate they did provide a useful independent check on the streaming velocities.

Tobacco smoke was introduced into the tube to render the flow visible and streaming was set up, the field having a pressure at the rigid end of 151 dB (re 20μPa). Because of the limited dynamic range of the P.I.V. technique (see section 3) the streaming velocity was first estimated by eye and the chopper then set to provide pulses with a separation of 0.114 second and duration 0.0057. It is necessary to have the ratio of pulse separation to duration so large because one only wants information about particle separations and, if the particle displacements and separations are of a similar order, they will give rise to similarly sized contributions in the spatial frequency domain which will lead to a loss of velocity

information. Such details of the technique are well discussed in [8]. The shutter, set to 0.5 second, allowed 4 pulses through.

Photographs were taken near a velocity node and a print of the film used to provide the measurements quoted here is shown in figure 5. The individual particle images can be clearly seen. In fact, measurements could not be made far from the velocity nodes because, at the frequencies and intensities used here, the vibrational displacement amplitudes became of the same order as the particle displacements required to give fringes. This is quite an important point and will be returned to and discussed at some length in section 6.

The film was analysed in the fashion indicated in section 3. It is clear from figure 5 that not all areas of film yielded a velocity measurement, due either to flare from the tube walls or uneven seeding. The latter is a problem in all P.I.V. measurements and seems to be more difficult to overcome in air than in water. Perhaps this is due to the larger convective currents found in air coupled with its lower viscoscity.

The measurements were transferred to a computer which, after interpolating missing points and smoothing the velocities using a third order Chebyshev interpolation routine, drew a velocity map (see figure 6). As can be seen, the measurements look slightly asymmetric with the velocities in the upper left vortex seeming to sweep over too much to the right. This was probably due to outside air currents. As a check on the accuracy of the measurements it is noticed from equation 2 that the axial velocity should be parabolic across any section of the tube with maximum velocity given by equation 1 and zeroes at distances r=0.707a from the axis of the tube. Axial velocities were therefore computed from the original unsmoothed data for three separate lines across the tube (figure 7.). The solid parabolae were fitted using the measured velocity maxima and the theoretical zero points. The fits are quite good though the velocities do show some deviation near the left crossover point, reflecting the assymmetry mentioned earlier. A calculation using (3) and a value of 151 dB for the maximum pressure indicates a maximum slip velocity of $\sim$6.5 mm/s, giving the corresponding maximum axial velocity a few millimeters from the

velocity node to be of the order of 3-4 mm/s - in agreement with figure 7. The cross sectional velocity measurements agree with the theoretical curves to within about 10% in the region of the central return velocity but deteriorate in the outer regions. This is due not only to extraneous air currents but to the fact that small positional errors in the interrogating laser beam lead to large velocity errors because of the large velocity gradient in these regions. Inaccuracies also occur due to the finite area of the interrogating laser beam. That is, in regions where the seeding is quite sparse the particle images which produce the fringe pattern may not lie on average at the centre of the laser beam which is where the velocity is taken to be measured. The measured velocities in figure 7 also show quite a bit of scatter about the theoretical lines and this reflects a basic problem in P.I.V.: because the measurement is taken effectively instantaneously effects such as particle diffusion and random particle distributions which can upset an individual velocity measurement are not averaged out. It is impossible thus to assign a statistical measure (in terms of these effects) to each separate velocity. It is however possible to assign a measure in terms of the point's nearest neighbours because we know that the flow is continuous. This is our justification for using the velocity smoothing routine mentioned earlier.

6. DISCUSSION AND CONCLUSIONS.

It has been demonstrated that P.I.V. can accurately measure acoustic streaming effects; an area that cannot be tackled using conventional probe devices. Also, in contrast to the more common optical technique of Laser Doppler Anemometry (L.D.A.), it can measure "instantaneously" over a whole field. To make the type of measurements described in this paper using L.D.A. would require a two component L.D.A. system, a carefully controlled environment to prevent changing ambient conditions from upsetting the streaming over the time (many hours) that would be required to make the measurements and some method of traversing the L.D.A. measuring volume accurately to each point in the flow.

There are however several limitations to the P.I.V. technique. Firstly, any flows measured must be essentially two dimensional: if there is too much out of plane motion then the

particle images will become decorrelated and no velocity information can be extracted. Secondly, and just as importantly for acoustic streaming, if the vibrational displacement of the sound field becomes too large then it can effectively swamp the velocity displacement images (the particle images become streaked and overlap). Such an effect was noticed in this work (Section 3.) Furthermore, in regions not too far from the velocity node the streaking of the particles causes the circular halo in which the fringes are confined to become elongated and outer lobes to become visible. (see figure 8.) This can have serious implications for the fringe analysis system since, in our implementation, an average circular halo is subtracted from each fringe pattern in order to remove low frequencies which could otherwise swamp the fringe frequency [9]. Clearly it is impossible to define such a halo if it changes for different portions of the film. We get round this problem by instructing the computer to make measurements on successive lines perpendicular to the tube axis across which the vibrational amplitudes are constant. The computer can then gather an average halo from from each of these lines and use it to remove the low frequencies for that line.

In fact the particle streaks are dumbell shaped due to the particles moving more rapidly at the centre than at the extremities of their displacements. The halo (in the direction parallel to the particle displacements) then takes the profile of a squared zero order Bessel function from which it would be possible to estimate the magnitude of the particle displacements [15]. Such estimates would probably however be of quite low accuracy and such measurements would perhaps be of little practical use anyway. It may however be of interest to note that, knowing the sound field and the particle's density, it would be possible in principle to deduce the particle sizes from their displacement amplitudes.

A way round the above problem would be to pulse the laser fast enough to "freeze" the particle images, the pulse former being triggered from the sound field to capture the images at the same phase positions. To illuminate the particle for say 1/10 of its period would require, for frequencies of the order we have here, laser pulses lasting only small fractions of a millisecond. This would then require (if we scale up the intensities used here) laser powers of the order of several watts. Such lasers are not uncommon though their use

does entail certain difficulties and hazards. It may be noted however that more effective use can be made of available laser light by employing scanning beam technology [13] or by using more sensitive films and sacrificing resolution.

However, despite these limitations the technique should be of considerable interest both to acousticians and fluid dynamicists. It may also be noted that in other areas the technique would perhaps not suffer from the aforementioned difficulties. For example, in the regions of much higher frequencies, say 20 kHz upwards, the vibrational amplitudes can become quite small though the streaming effects are very large [2], [14]. The authors feel that the P.I.V. technique begins to complement their earlier work on the optical measurement of acoustic velocities [16] and hope to go on to apply both techniques to the measurement of practical acoustic situations (e.g. the acoustics of musical instruments).

ACKNOWLEDGEMENTS.

This work is supported by the SERC and British Telecom. JPS and C. Gray are grateful to the Dept. of Education for N. Ireland and the SERC respectively for studentships.

References

1. Lord Rayleigh (1896) "Theory of Sound." Vol.2, Art.352. Dover Publications, 1945 reissue.

2. Lighthill, M. J. (1978) "Acoustic Streaming." Journal of Sound and Vibration 61(3), 391-418.

3. Keefe, D. H. (1983) "Acoustic Streaming, Dimensional Analysis of Nonlinearities and Tone Hole Mutual Interaction in Woodwinds." Journal of the Acoustical Society of America. 73(5), 1804-1820.

4. Andrews, D. G. & McIntyre, M. E. (1978) "An Exact Theory of Nonlinear Waves on Lagrangian-Mean Flow." Journal of Fluid Mechanics 89(4), 609-646.

5. Merkli, P. & Thomann, H. (1975) "Transition to Turbulence in Oscillating Pipe Flow." Journal of Fluid Mechanics 68(3), 567-575.

6. Dudderar & Simpkins (1978) "Laser Speckle Measurements of Transient Benard Convection." Journal of Fluid Mechanics 89(4), 665-671.

7. Bernabeau, E., Amare, J. C. & Arroyo, M. P. (1982) "White light Speckle Method of Measurement of Flow Velocity Distribution." Applied Optics 21(4), 2583-2586.

8. Meynert, R. & Lourenco, V. K. I. (1984) "Digital Image Processing in Fluid Dynamics." Von Karmen Institute for Fluid Dynamics Lecture Series 1984-03.

9. Gray, C. & Greated, C. A. (1988) "Application of P.I.V. to Measurement Under Water Waves." Optics & Lasers in Engineering (In Press).

10. Robinson, D. W. (1983) "Role for Automatic Fringe Analysis in Optical Metrology." SPIE Vol. 376.

11. Huntly, J. M. (1986) "An Image Processing System for the Analysis of Speckle Photographs." Journal of Physics E., 19, 43-49.

12. Bruel & Kjaer (1982) "Condenser Microphones and Microphone Preamplifiers for Acoustic Measurement." B & K Data Handbook.

13. Gray, C. & Greated, C. A. (1988) "A Scanning Laser Beam System for Two- Dimensional Illumination of Flow Fields." Proceedings of Particle Image Displacement Velocimetry Conference. Von Karmen Institute for Fluid Dynamics, Belgium, March 1988.

14. Bergmann, L. (1938) "Ultrasonics." G. Bell & Sons Ltd., London.

15. Tiziani, H. J.(1971) "Application of Speckling for in-plane Vibration Analysis." Optica Acta 18 (12), 891-902.

16. Sharpe, J. P. & Greated, C. A. (1987) "The Measurement of Periodic Acoustic Fields using Photon Correlation Spectroscopy." Journal of Physics D. (Applied Physics) 20,418-423.

Figure Captions.

Figure 1. Rayleigh Streaming in a circular tube of radius a. vn = velocity node, va = velocity antinode.

Figure 2. Schematic diagram of P.I.V. setup.

Figure 3. Production of P.I.V. fringes.

Figure 4. Apparatus for acquisition of P.I.V. photographs.

Figure 5. Print of P.I.V. transparency used to provide measurements.

Figure 6. Smoothed velocity map (1 cm = 4.37 mm/s).

Figure 7. Axial velocities in tube (symbols) and theoretical values (solid lines).

Figure 8. P.I.V. fringe patterns. (a) acquired near velocity node and (b) a few millimeters away from velocity node.

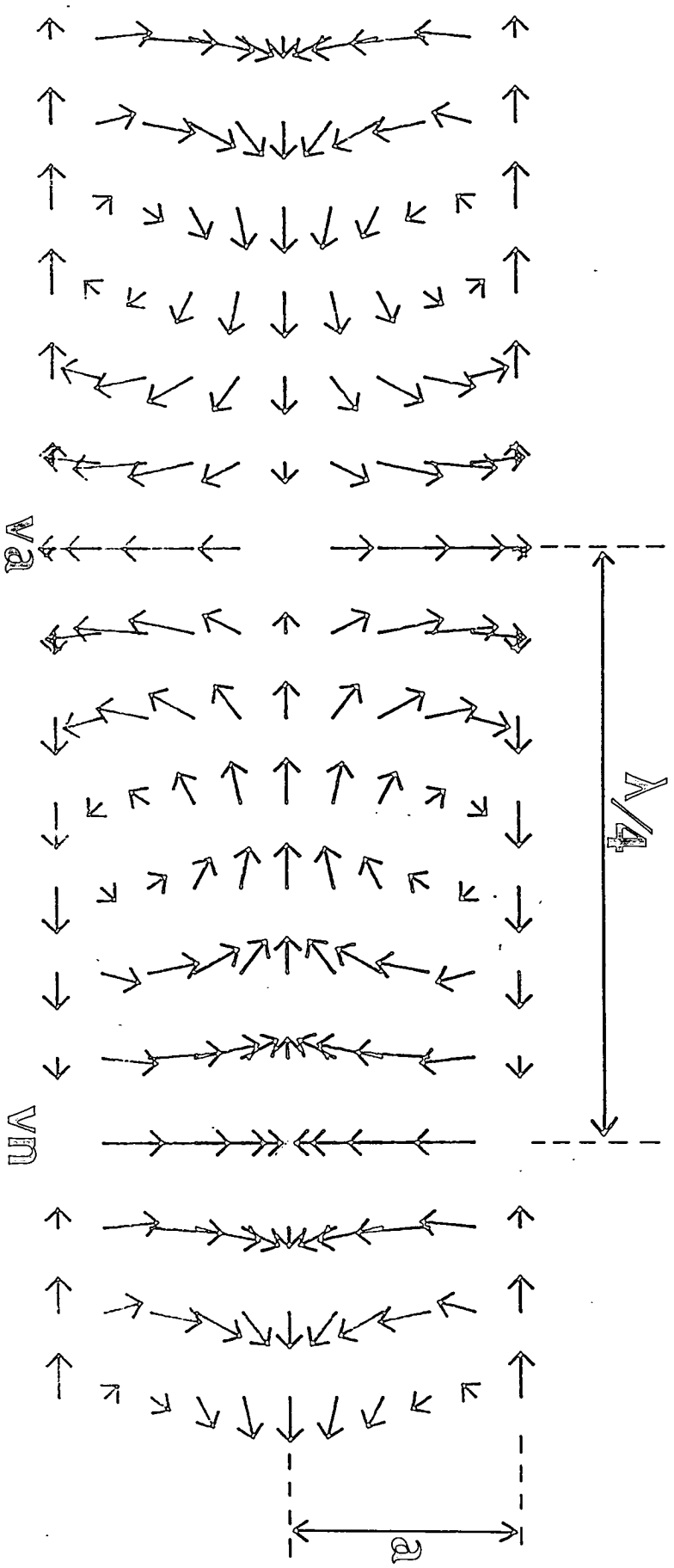

Fig 1.

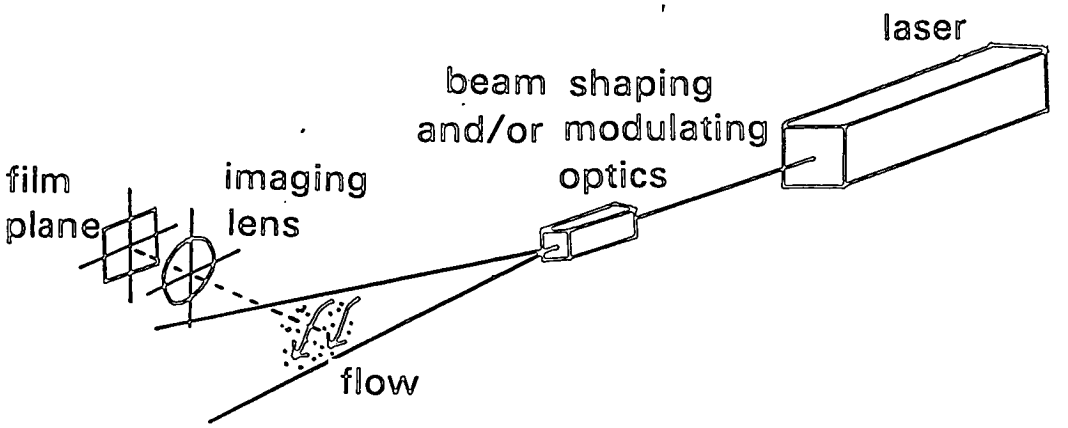
laser
beam shaping
and/or modulating
optics
film
plane
imaging
lens
flow

Fig 2.

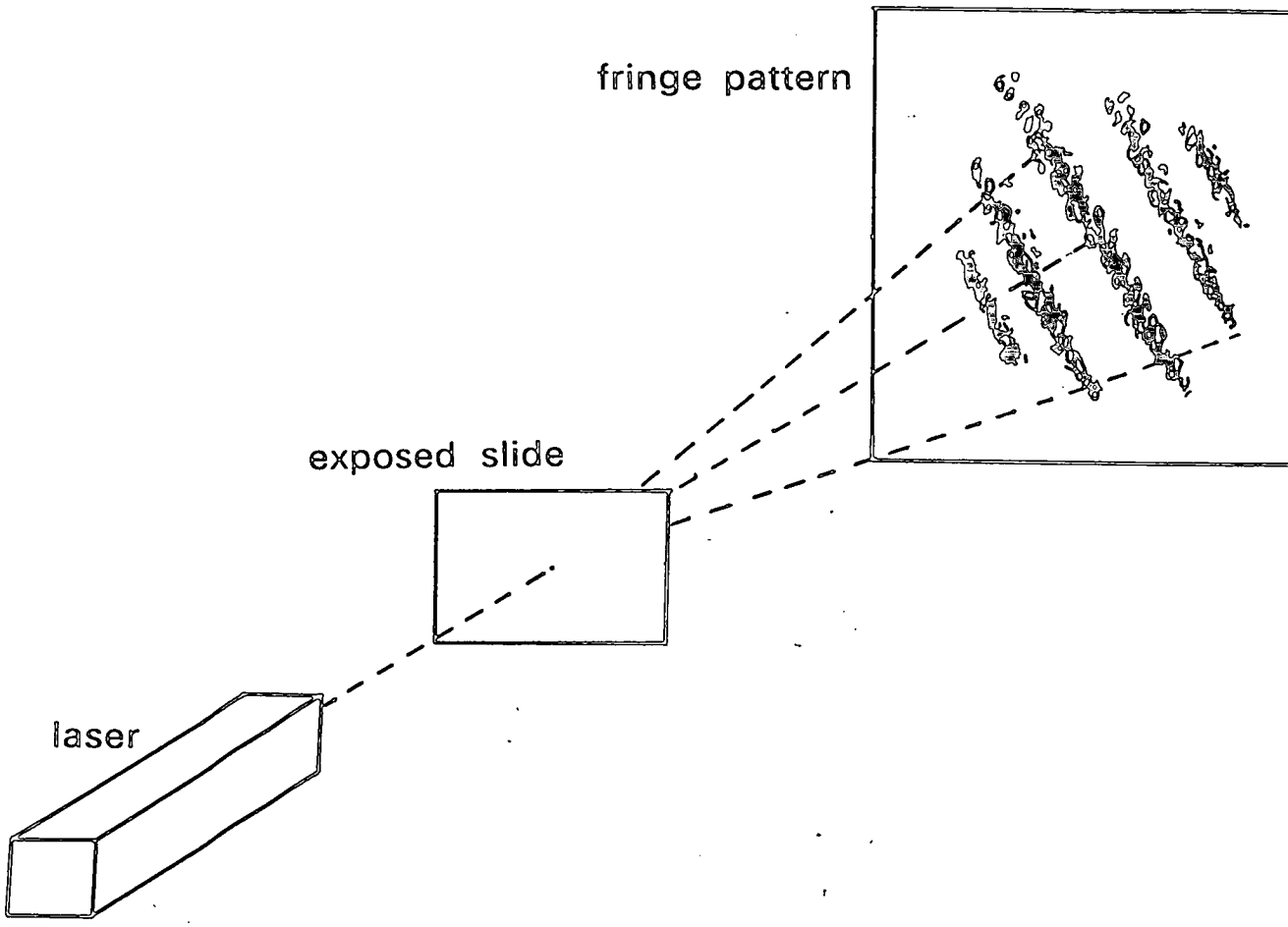

Fig 3

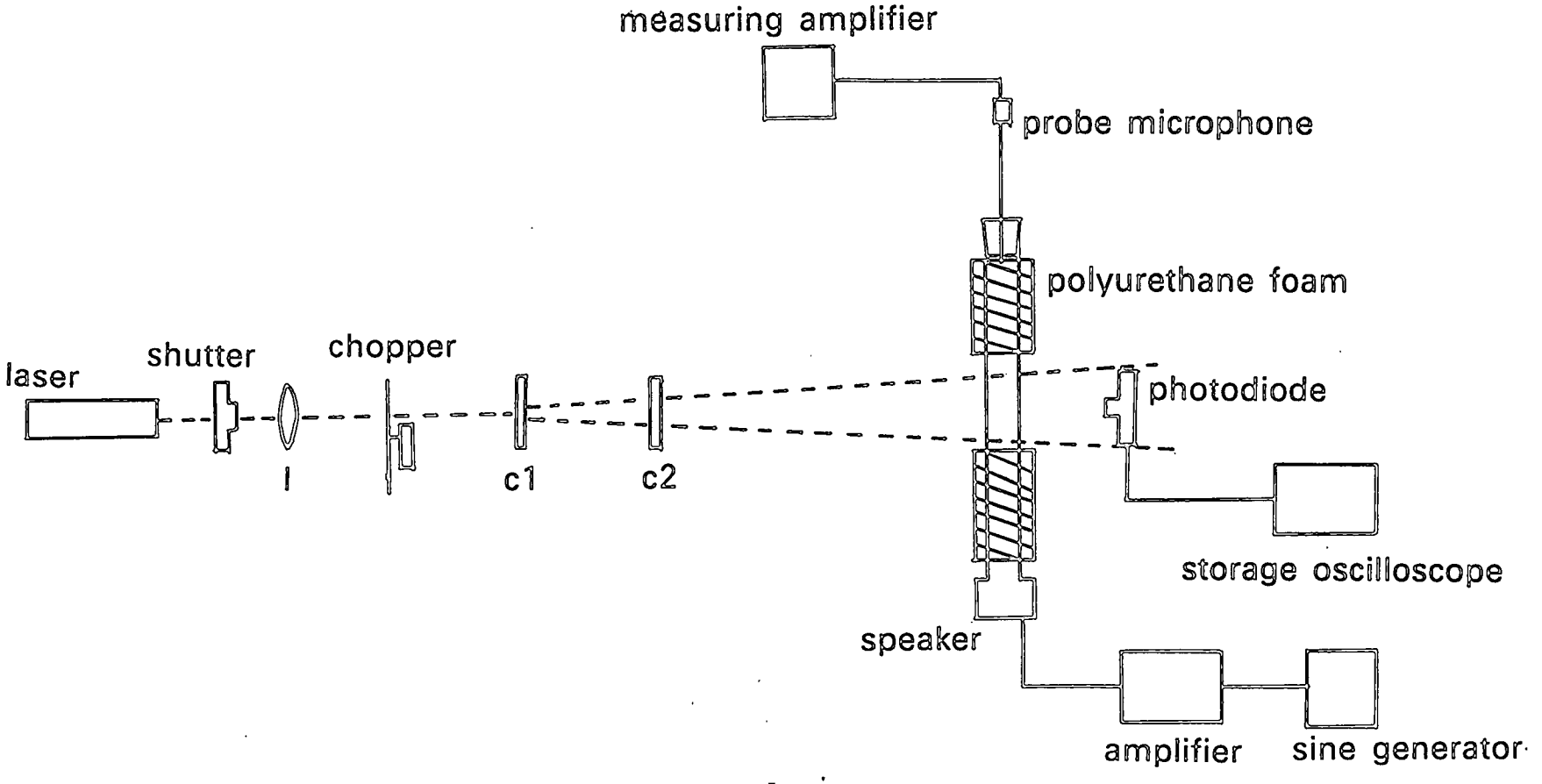
measuring amplifier
probe microphone
polyurethane foam
laser
shutter
chopper
photodiode
l
c1
c2
storage oscilloscope
speaker
amplifier
sine generator

Fig4.

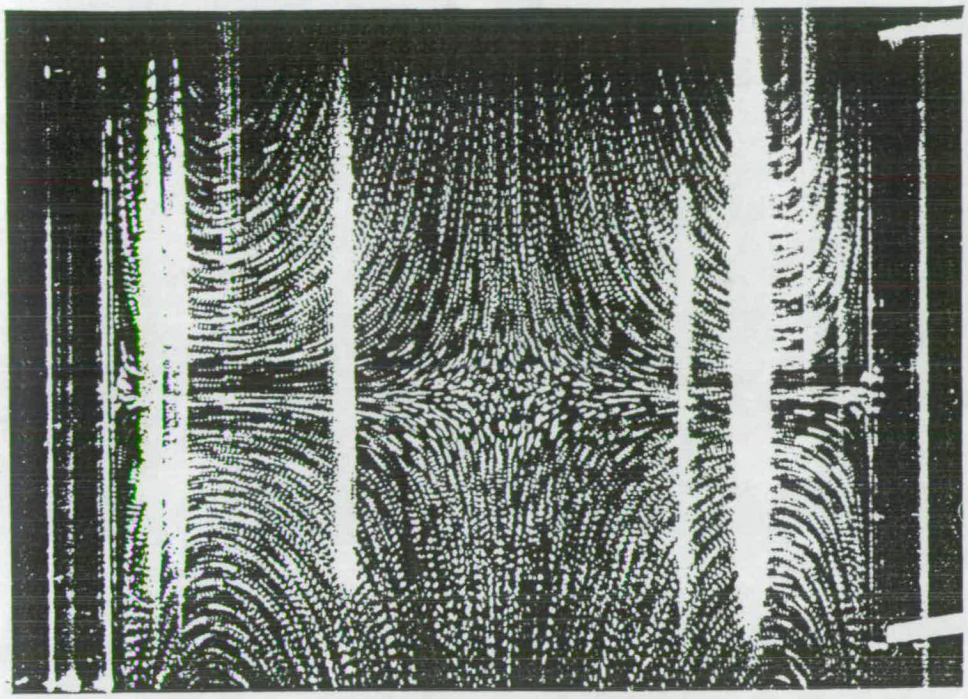

Fig 5.

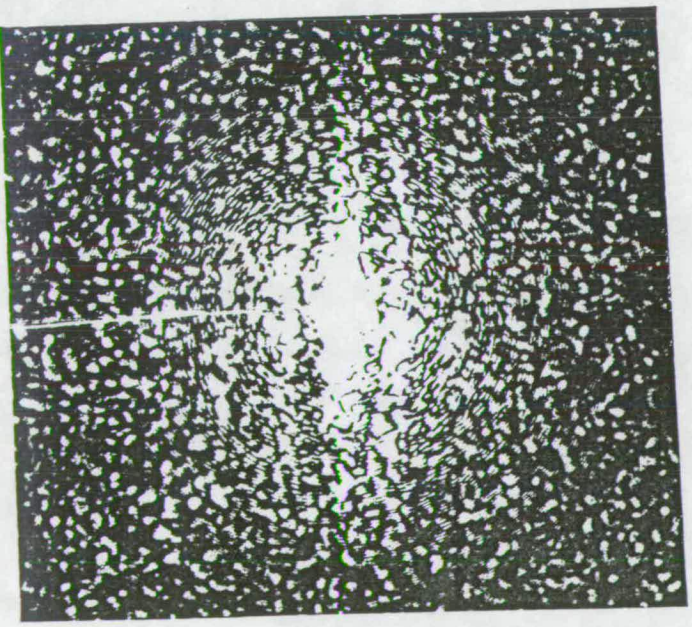

Fig 8(a)

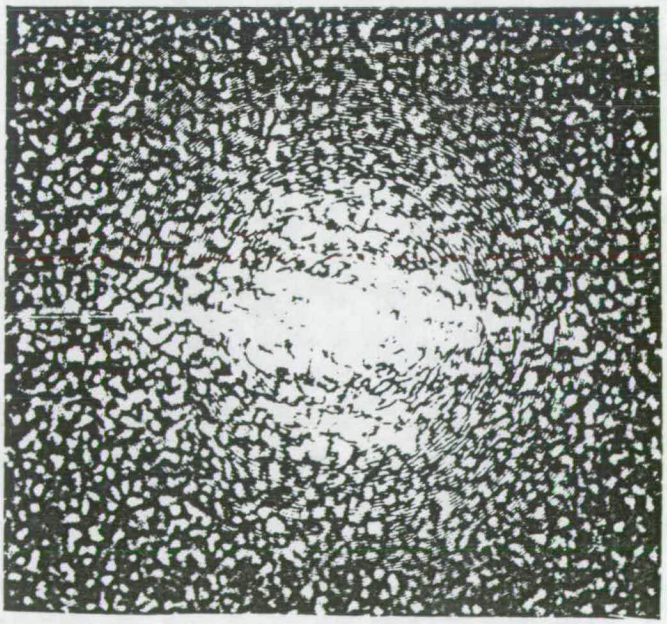

Fig 8(b)

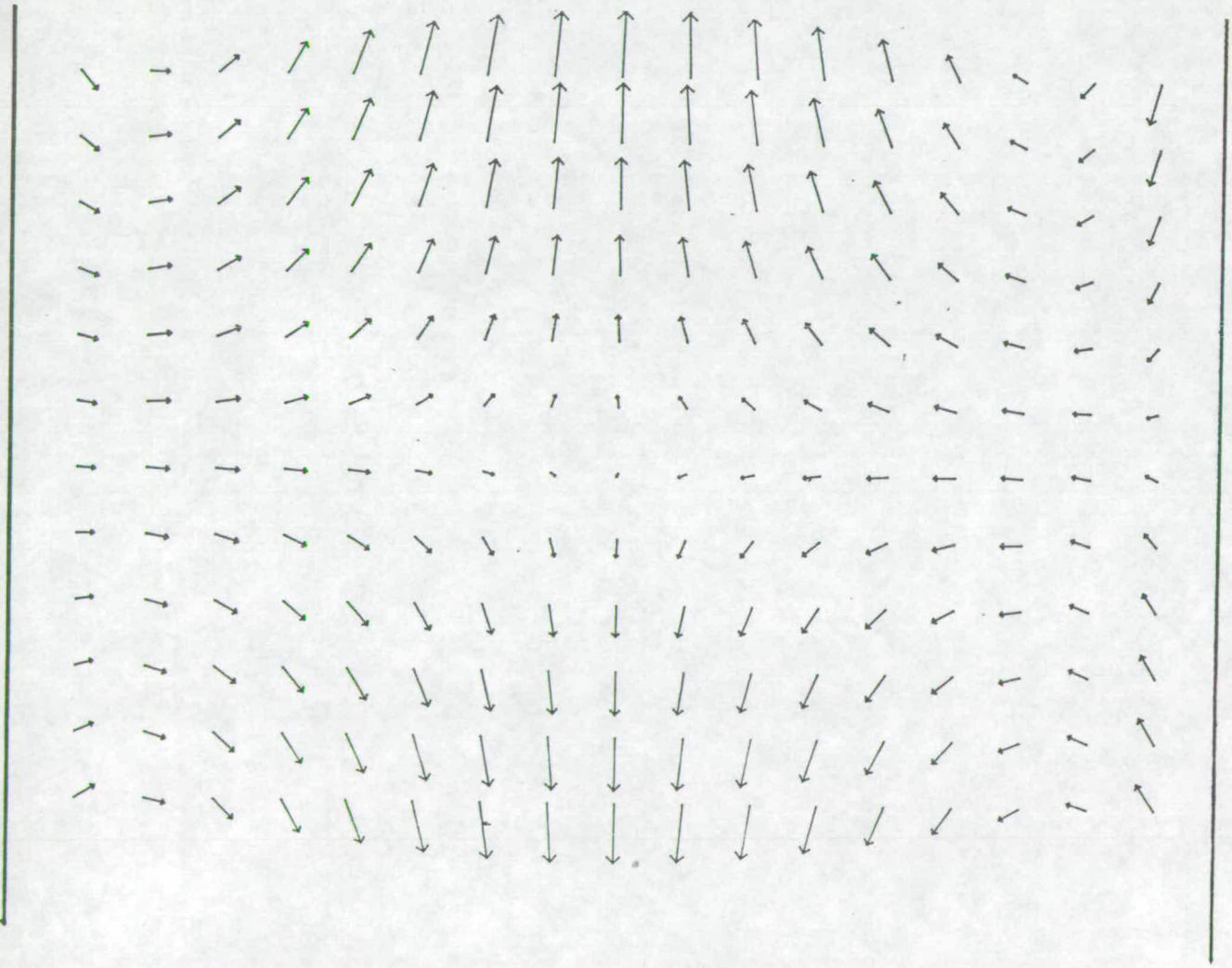

Fig 6.

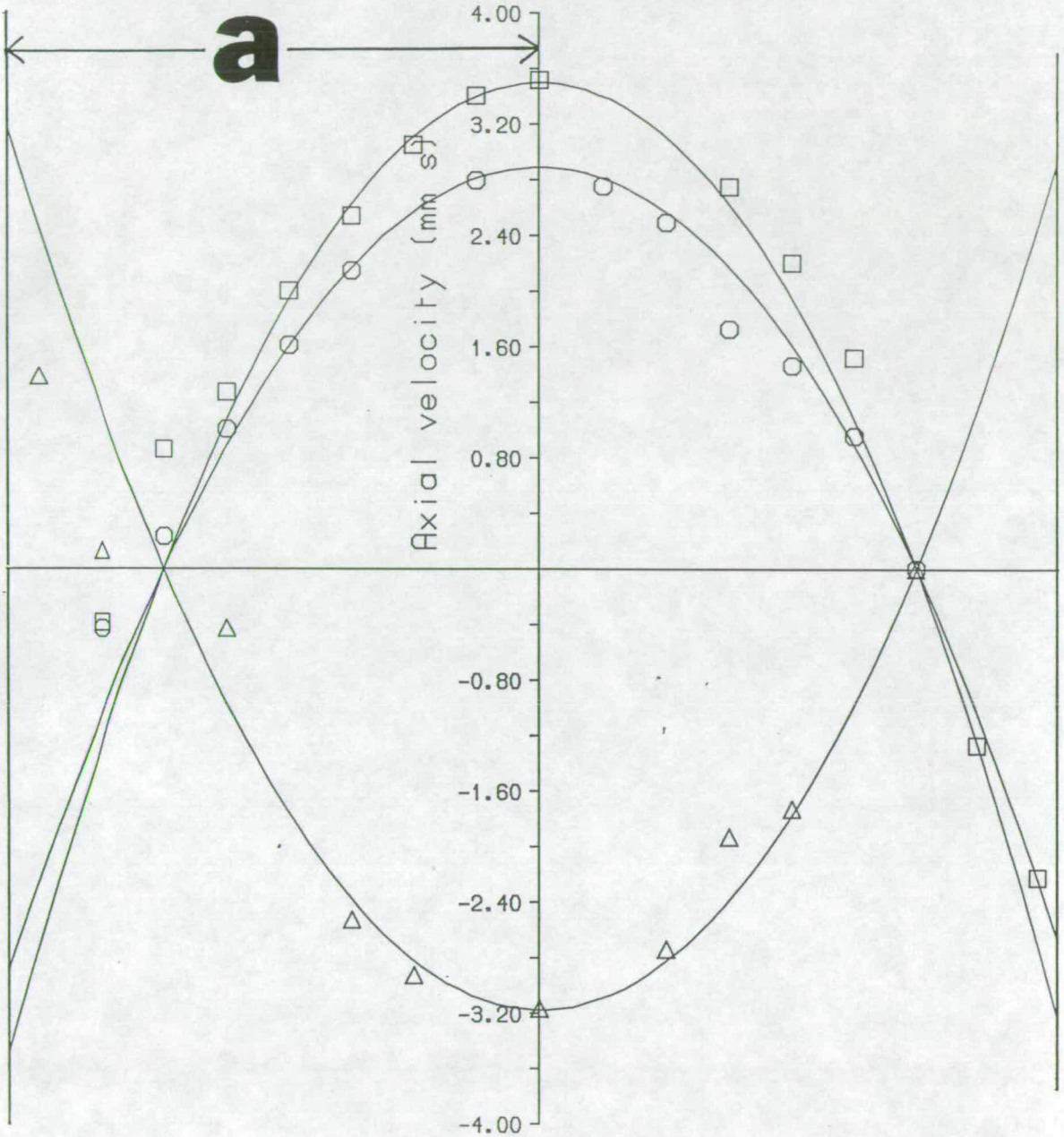

Fig 7.

BIBLIOGRAPHY

Andrews, D. G. and McIntyre, M. E., "An exact theory of nonlinear waves on a Lagrangian-mean flow.," **J. Fluid Mech.**, vol. 89, pp. 609-646, 1978.

Backus, J., "Input impedance curves for the reed woodwind instruments.," **J. Acoust. Soc. Am.**, vol. 56, pp. 1266-1279, 1974.

Batchelor, G. K., **An introduction to fluid dynamics.**, Cambridge Univ. Press., London., 1970.

Benade, A. H., "On the propagation of sound waves in a cylindrical conduit.," **J. Acoust. Soc. Am.**, vol. 44, pp. 616-623, 1968.

Bendat, J. S. and Piersol, A.G., **Measurement and analysis of random data.**, John Wiley & Sons., New York., 1966.

Bergmann, L., **Ultrasonics.**, G. Bell & Sons., London., 1938.

Bernabeau, E., Amare, J., and Arroyo, M. P., "White light speckle method of measurement of flow velocity distribution.," **App. Opt.**, vol. 21, pp. 2583-2586, 1982.

Betts, J. A., **Signal processing, modulation and noise.**, The English Universities Press., London., 1970.

Beyer, R. T., **Nonlinear acoustics**, U. S. Navy, 1974.

Bracewell, R. N., **The Fourier transform and it's applications.**, McGraw-Hill Book Co., New York., 1986.

Brandt, O., Freund, H., and Heidemann, E., "Schwebstoffe in schallfeld.," **Z. Phys.**, vol. 104, pp. 511-533, 1937.

Brown, R. G. W. and Gill, M. E., "Comparison of photon correlation laser Doppler anemometry data processing techniques.," **Proc. S.P.I.E.**, vol. 369 , 1982.

Bruel & Kjaer, "Condenser microphones and microphone preamplifiers for acoustic measurement.," **Bruel & Kjaer Data Handbook**, 1982.

Bruel & Kjaer, "Sound Intensity (Instrumentation and Applications).," **Bruel & Kjaer Technical Review (No.4).**, 1982.

Bruel & Kjaer, "Validity of Intensity Measurements.," **Bruel & Kjaer Technical Review (No.4).**, 1985.

Campbell, D. M., "Input impedance measurements on historic brass instruments.," **Proc. Institute Acoustics.**, vol. 9, pp. 111-118, 1987.

Campbell, M. and Greated, C. A., **The musicians guide to acoustics.**, J. M. Dent & Sons., London., 1987.

Chung, J. Y., "Cross-spectral method of measuring acoustic intensity without error caused by instrument phase mismatch.," **J. Acoust. Soc. Am.**, vol. 64, pp. 1613-1616, 1978.

Dainty, J. C. (Editor), **Laser speckle and related phenomena.**, Springer-Verlag, Berlin., 1975.

Davis, M. R. and Hews-Taylor, K. J., "Laser Doppler measurement of complex acoustic impedance.," **J. Sound Vib.**, vol. 107, pp. 451-470, 1986.

Drain, L. E., **The laser Doppler technique.**, John Wiley & Sons., New York., 1980.

Durrani, T. S. and Greated, C. A., **Laser systems in flow measurement.**, Plenum Press., New York., 1977.

Durst, F., Melling, A., and Whitelaw, J. H., **Principles and practice of laser Doppler anemometry.**, Academic Press., New York., 1976.

Edwards, R. V., Angus, J. C., French, M. J., and Dunning, J. W., "Spectral analysis of the signal from the laser Doppler flowmeter: time independent systems.," **J. Appl. Phys.**, vol. 42, pp. 837-850, 1971.

Elliot, S., Bowsher, J., and Watkinson, P., "Input and transfer response of brass wind instruments.," **J. Acoust. Soc. Am.**, vol. 72, pp. 1747-1760, 1982.

Erbeck, R., "Fast image processing with a microcomputer applied to speckle photography.," **App. Opt.**, vol. 24, pp. 3838-3841, 1985.

Fahy, F. J., "Measurement of acoustic intensity using the cross-spectral density of two microphone signals.," **J. Acoust. Soc. Am.**, vol. 62, pp. 1057-1059, 1977.

Gauthier, V. and Riethmuller, M. L., "Application of PIDV to complex flows: Measurements of the third component.," **Von Karmen Institute for Fluid Dynamics Lecture Series (1988-06).**, 1988.

Gradshteyn, I. S. and Ryzhik, I. M., **Table of integrals, series and products.**, Academic Press., New York., 1965.

Gray, C. and Greated, C. A., "Application of P.I.V. to measurement under water waves.," **Optics and Lasers in Engineering (in press).**, 1988.(a)

Gray, C. and Greated, C. A., "A scanning laser beam system for two-dimensional illumination of flow fields.," **Proc. P.I.D.V. Conference Von Karmen Inst.**, Von Karmen Institute for Fluid Dynamics., Brussels., 1988. (b)

Greated, C. A., "Measurement of acoustic velocity fields.," **Strain.**, vol. 22, pp. 21-24, 1986.

Hanson, S., "Broadening of the measured frequency spectrum in a differential laser anemometer due to interference plane gradients.," **J. Phys. D. (Applied Physics).**, vol. 6, pp. 164-171, 1973.

Hinze, J. O., **Turbulence,** McGraw-Hill Book Co., New York., 1959.

Huntley, J. M., "An image processing system for the analysis of speckle photographs.," **J. Phys. E. (Sci. Instrum.)**, vol. 19, pp. 43-49, 1986.

Jensen, H. H. and Saermark, K., "On the theory of the Rayleigh-Disk and the sound pressure radiometer.," **Acustica.**, vol. 8, pp. 79-86, 1958.

Keefe, D. H. and Benade, A. H., "Impedance measurement source and microphone proximity effects.," **J. Acoust. Soc. Am.**, vol. 69, pp. 1489-1495, 1981.

Keefe, D. H., "Acoustic streaming, dimensional analysis of nonlinearities and tone hole mutual interaction in woodwinds.," **J. Acoust. Soc. Am.**, vol. 73, pp. 1804-1820, 1983.

Keith, C. H. and Derrick, J. C., "Measurement of particle size distribution and concentration of cigarette smoke by the "conifuge".," **J. Coll. Sci.**, vol. 15, pp. 340-356, 1960.

Kergomard, J. and Causse, R., "Measurement of acoustic impedance using a capillary: An attempt to achieve optimization.," **J. Acoust. Soc. Am.**, vol. 79, pp. 1129-1140, 1986.

King, R., "Transmission line theory and it's applications.," **J. Appl. Phys.**, vol. 14, pp. 577-600, 1943.

Kinsler, L. E., Frey, A. R., Coppens, A. B., and Sanders, J. V., **Fundamentals of acoustics.,** John Wiley & Sons., New York., 1982..

Lighthill, M. J., **Waves in fluids.,** Cambridge Univ. Press., London., 1978.(b)

Lighthill, M. J., "Acoustic Streaming.," **J. Sound Vib.**, vol. 61, pp. 391-418, 1978.(a)

McLachlan, N. W., **Bessel functions for engineers.,** Oxford University Press., London., 1934.

Merkli, P. and Thomann, H., "Transition to turbulence in oscillating pipe flow.," **J. Fluid Mech.**, vol. 68, pp. 567-575, 1975.

Meynert, R. and Lourenco, V. K. I., "Digital image processing in fluid dynamics.," **Von Karmen Institute for Fluid Dynamics Lecture Series (1984-03).**, 1984.

Middleton, D., **An introduction to statistical communication theory.,** McGraw-Hill Book Co., New York., 1960.

Minten, M., Cops, A., and Lauriks, W., "Absorption characteristics of an acoustic material at oblique incidence measured with the two-microphone technique.," **J. Sound Vib.**, vol. 120, pp. 499-510, 1988.

Morse, P.M., **Vibration and sound.,** McGraw-Hill Book Co., New York., 1948.

Mullin, T. and Greated, C. A., "Measurement of pulsating flows by photon correlation.," **J. Phys. E. (Sci. Instrum.).**, vol. 11, pp. 643-646, 1978.

Nyborg, W. L., "Acoustic streaming due to attenuated plane waves.," **J. Acoust. Soc. Am.**, vol. 25, pp. 68-75, 1953.

Papoulis, A., **Systems and transforms with applications in optics.**, Mc Graw-Hill Book Co., New York., 1968.

Pickering, C. and Halliwell, N. A., "Speckle photography in fluid flows: signal recovery with two step processing.," **App. Opt.**, vol. 23, pp. 1128-1129, 1984.

Pratt, R. L., Elliott, S. J., and Bowsher, J. M., "The measurement of the acoustic impedance of brass instruments.," **Acustica**, vol. 38, pp. 236-246, 1977.

Rasmussen, C. G., "An experimental investigation of the diffraction correction for a Rayleigh-Disc.," **Acustica.**, vol. 14, pp. 148-156, 1964.

Rayleigh, Lord, **Theory of sound,** Dover Publications (1945 reissue), New York., 1945.

Robinson, D. W., "Role for automatic fringe analysis in optical metrology.," **Proc. S.P.I.E.**, vol. 376, 1983.

Royer, H., "Particle image displacement velocimetry. Full 3D measurements: The holographic approach.," **Von Karmen Institute for Fluid Dynamics Lecture Series (1988-06).**, 1988.

Salava, T., "Acoustic impedance measurement using constant volume velocity.," **J. Acoust. Soc. Am.**, vol. 67, pp. 1831-1833, 1980.

Sharpe, J. P. and Greated, C. A., "The measurement of periodic acoustic fields using photon correlation spectroscopy.," **J. Phys. D. (Applied Physics).**, vol. 20, pp. 418-423, 1987.(a)

Sharpe, J. P. and Greated, C. A., "Laser measurement of random and periodic sound fields.," **Proc. Institute Acoustics.**, vol. 9, pp. 183-191, 1987.(b)

She, C. Y. and Wall, L. S., "Analytical evaluation of techniques for use of a laser Doppler velocimeter to measure flow and turbulence.," **J. Opt. Soc. Am.**, vol. 65, pp. 69-77, 1975.

Simpkins, P. G. and Dudderar, T. D., "Laser speckle measurements of transient Benard convection.," **J. Fluid Mech.**, vol. 89, pp. 665-671, 1978.

Taylor, K. J., "Absolute measurement of acoustic particle velocity.," **J. Acoust. Soc. Am.**, vol. 59, pp. 691-694, 1976.

Taylor, K. J., "Absolute calibration of microphones by a laser Doppler technique.," **J. Acoust. Soc. Am.**, vol. 70, pp. 939-945, 1981.

Tiziani, H. J., "Application of speckling for in-plane vibration analysis.," **Optica Acta.**, vol. 18, pp. 891-902, 1971.

Tranter, C. J., **Bessel functions with some physical applications.,** The English Universities Press., London, 1968.

Watrasiewicz, B. M. and Rudd, M. J., **Laser Doppler measurements.,** Butterworths., London., 1976.

Westervelt, P. J., ''The theory of steady rotational flow generated by a sound field.,'' **J. Acoust. Soc. Am.**, vol. 25, pp. 60-67, 1953.

Yeh, H. and Cummins, H. Z., ''Localised fluid flow measurements with a He-Ne laser spectrometer.,'' **Appl. Phys. Lett.**, vol. 4, pp. 176-178, 1964.